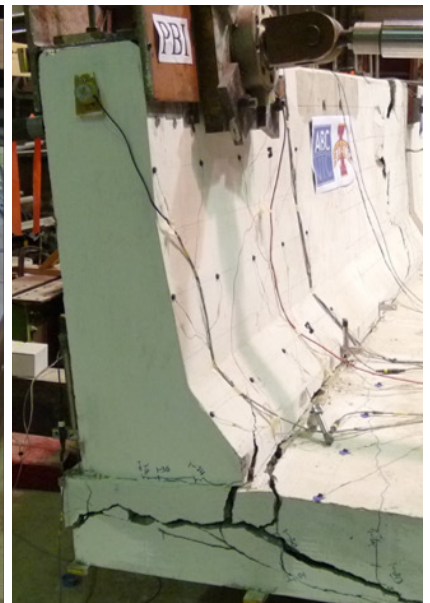
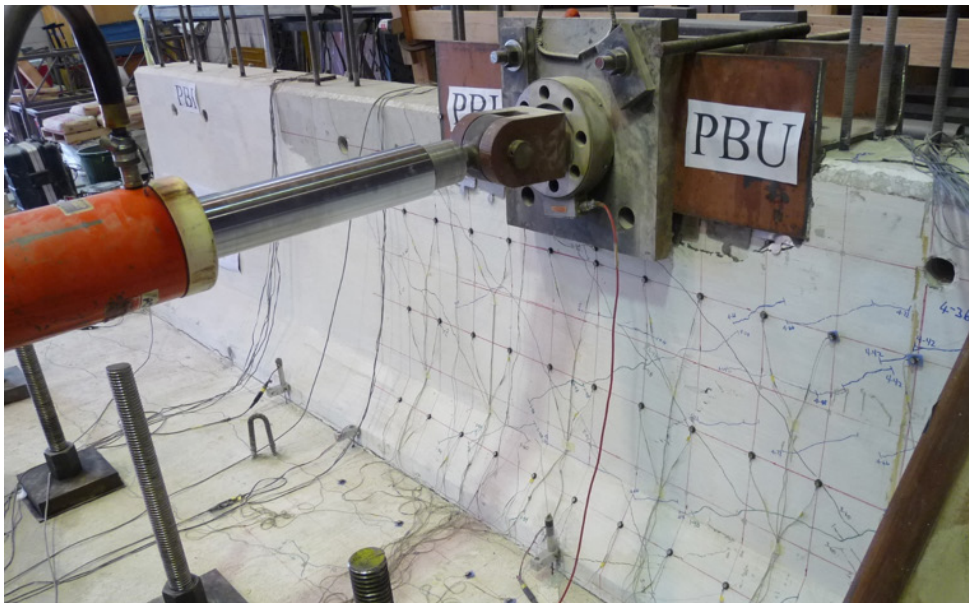


# Precast Concrete Bridge Barriers for Accelerated Bridge Construction

**Final Report**  
**October 2018**



**Sponsored by**  
Accelerated Bridge Construction  
University Transportation Center



IOWA STATE UNIVERSITY  
Institute for Transportation

## **About the ABC-UTC**

The Accelerated Bridge Construction University Transportation Center (ABC-UTC) is a Tier 1 UTC sponsored by the U.S. Department of Transportation Office of the Assistant Secretary for Research and Technology (USDOT/OST-R). The mission of ABC-UTC is to reduce the societal costs of bridge construction by reducing the duration of work zones, focusing special attention on preservation, service life, construction costs, education of the profession, and development of a next-generation workforce fully equipped with ABC knowledge.

## **About the BEC**

The mission of the Bridge Engineering Center (BEC), which is part of the Institute for Transportation (InTrans) at Iowa State University, is to conduct research on bridge technologies to help bridge designers/owners design, build, and maintain long-lasting bridges. The mission of InTrans is to develop and implement innovative methods, materials, and technologies for improving transportation efficiency, safety, reliability, and sustainability while improving the learning environment of students, faculty, and staff in transportation-related fields.

## **ISU Non-Discrimination Statement**

Iowa State University does not discriminate on the basis of race, color, age, ethnicity, religion, national origin, pregnancy, sexual orientation, gender identity, genetic information, sex, marital status, disability, or status as a U.S. veteran. Inquiries regarding non-discrimination policies may be directed to Office of Equal Opportunity, 3410 Beardshear Hall, 515 Morrill Road, Ames, Iowa 50011, Tel. 515-294-7612, Hotline: 515-294-1222, email [eooffice@iastate.edu](mailto:eooffice@iastate.edu).

## **Notice**

The contents of this report reflect the views of the authors, who are responsible for the facts and the accuracy of the information presented herein. The opinions, findings and conclusions expressed in this publication are those of the authors and not necessarily those of the sponsors.

This document is disseminated under the sponsorship of the U.S. DOT UTC program in the interest of information exchange. The U.S. Government assumes no liability for the use of the information contained in this document. This report does not constitute a standard, specification, or regulation.

The U.S. Government does not endorse products or manufacturers. If trademarks or manufacturers' names appear in this report, it is only because they are considered essential to the objective of the document.

## **Quality Assurance Statement**

The Federal Highway Administration (FHWA) provides high-quality information to serve Government, industry, and the public in a manner that promotes public understanding. Standards and policies are used to ensure and maximize the quality, objectivity, utility, and integrity of its information. The FHWA periodically reviews quality issues and adjusts its programs and processes to ensure continuous quality improvement.

## Technical Report Documentation Page

<b>1. Report No.</b>	<b>2. Government Accession No.</b>	<b>3. Recipient's Catalog No.</b>	
<b>4. Title and Subtitle</b> Precast Concrete Bridge Barriers for Accelerated Bridge Construction		<b>5. Report Date</b> October 2018	
		<b>6. Performing Organization Code</b>	
<b>7. Authors</b> Ashley Ecklund and Sri Sritharan		<b>8. Performing Organization Report No.</b>	
<b>9. Performing Organization Name and Address</b> Bridge Engineering Center Iowa State University 2711 South Loop Drive, Suite 4700 Ames, IA 50010-8664		<b>10. Work Unit No. (TRAIS)</b>	
		<b>11. Contract or Grant No.</b>	
<b>12. Sponsoring Organization Name and Address</b> <div style="display: flex; justify-content: space-between;"> <div> Accelerated Bridge Construction University Transportation Center Florida International University 10555 W. Flagler Street, EC 3680 Miami, FL 33174 </div> <div> U.S. Department of Transportation Office of the Assistant Secretary for Research and Technology 1200 New Jersey Avenue, SE Washington, DC 20590 </div> </div>		<b>13. Type of Report and Period Covered</b> Final Report	
		<b>14. Sponsoring Agency Code</b>	
<b>15. Supplementary Notes</b> Visit <a href="http://www.intrans.iastate.edu">www.intrans.iastate.edu</a> for color pdfs of this and other research reports from the Bridge Engineering Center at Iowa State University.			
<b>16. Abstract</b> <p>Many transportation organizations have embraced Accelerated Bridge Construction (ABC) to reduce both the traffic impacts and societal costs. One of the most common means to achieve ABC is to utilize prefabricated elements that are connected on site to construct a bridge. ABC will not be effective if the barrier requires cast-in-place construction. The purpose of this report is to present details of a precast barrier and two connection alternatives between the deck and precast barriers. In addition, a new connection between two adjacent prefabricated barriers was presented. All three connections were tested using full-scale precast barriers and a video summarizing the test can be found at <a href="https://youtu.be/up6sMEeqfaU">https://youtu.be/up6sMEeqfaU</a>.</p> <p>One barrier-to-deck connection used inclined reinforcing bars with threaded ends that were connected to bar splicers embedded in the bridge deck. The other barrier-to-deck connection used U-shaped bars that were inserted into the barrier from the underside of the bridge deck overhang. Factors that were considered when designing the connections were minimal damage to deck, easy replacement of barrier, constructability, durability, and cost.</p> <p>The barrier-to-barrier connection utilized headed reinforcement in the longitudinal and transverse directions. The connections were designed to meet TL-4 loads as per the Manual for Assessing Safety Hardware (MASH) and Load and Resistance Factor Design (LRFD) Bridge Design Specifications.</p> <p>This report presents results from various tests and shows that all proposed connections are viable for accelerated construction of concrete barriers, although some refinement to the tested details will be needed.</p>			
<b>17. Key Words</b> ABC—accelerated bridge construction—barrier-to- barrier connections— barrier-to-deck connections—concrete bridge barriers—precast concrete barriers		<b>18. Distribution Statement</b> No restrictions.	
<b>19. Security Classification (of this report)</b> Unclassified.	<b>20. Security Classification (of this page)</b> Unclassified.	<b>21. No. of Pages</b> 101	<b>22. Price</b> NA



# **PRECAST CONCRETE BRIDGE BARRIERS FOR ACCELERATED BRIDGE CONSTRUCTION**

**Final Report  
October 2018**

**Principal Investigator**

Terry Wipf, Professor  
Civil, Construction, and Environmental Engineering, Iowa State University

**Co-Principal Investigator**

Sri Sritharan, Professor  
Civil, Construction, and Environmental Engineering, Iowa State University

**Graduate Research Assistant**

Ashley Ecklund

**Authors**

Ashley Ecklund and Sri Sritharan

**Sponsored by**

Accelerated Bridge Construction University Transportation Center and  
U.S. Department of Transportation  
Office of the Assistant Secretary for Research and Technology

A report from

**Bridge Engineering Center**

**Institute for Transportation**

**Iowa State University**

2711 South Loop Drive, Suite 4700

Ames, IA 50010-8664

Phone: 515-294-8103 / Fax: 515-294-0467

[www.intrans.iastate.edu](http://www.intrans.iastate.edu)



## TABLE OF CONTENTS

ACKNOWLEDGMENTS .....	xi
INTRODUCTION .....	1
Overview .....	1
Accelerated Bridge Construction .....	1
Current Practices .....	2
Scope of Research .....	5
Research Objectives .....	5
Report Layout .....	6
LITERATURE REVIEW .....	7
Introduction .....	7
Design of Barriers .....	7
Experimental Evaluation .....	11
Practice of State DOTs .....	11
Precast Barriers .....	12
EXPERIMENTAL PLAN .....	26
Introduction .....	26
Guiding Parameters .....	26
Barrier-to-Deck Connections .....	26
Barrier-to-Barrier Connections .....	28
Deck Design .....	29
CONSTRUCTION OF TEST UNIT .....	31
Introduction .....	31
Precast Barrier Construction .....	31
Bridge Deck Construction .....	33
Assembly and Grouting .....	38
Instrumentation .....	43
Load Application .....	46
Material Properties .....	48
TESTING AND RESULTS .....	50
Introduction .....	50
Test 1 Observations: PBI Middle .....	52
Test 1 Results: PBI Middle .....	54
Test 2 Observations: PBU Middle .....	58
Test 2 Results: PBU Middle .....	59
Test 3 Observations: At Barrier-to-Barrier Connection .....	64
Test 3 Results: At Barrier-to-Barrier Connection .....	65
Test 4 Observations: Off-Center, PBI Side .....	69
Test 4 Results: Off-Center, PBI Side .....	71
Test 5 Observations: End of PBI .....	75
Test 5 Results: End of PBI .....	79

Test 6 Observations: End of PBU .....	81
Test 6 Results: End of PBU .....	83
SUMMARY AND CONCLUSIONS .....	86
Summary .....	86
Conclusions.....	86
REFERENCES .....	89



## LIST OF FIGURES

Figure 1.1. Cast-in-place barrier requiring maintenance .....	1
Figure 1.2. Prefabricated bridge element.....	2
Figure 1.3. F-shaped concrete barrier and reinforcement details.....	3
Figure 1.4. Rockridge Road bridge with exposed barrier connection reinforcement.....	4
Figure 1.5. Rockridge Road barrier after adding additional reinforcing .....	4
Figure 2.1. Bridge barrier design force locations as suggested in AASHTO LRFD specifications.....	9
Figure 2.2. Yield line pattern used for designing concrete barrier under load, $F_t$ .....	9
Figure 2.3. Commonly used concrete bridge barrier profile shapes .....	13
Figure 2.4. Through-deck bolting detail developed by Florida DOT .....	14
Figure 2.5. Adhesive-bonded anchor detail .....	14
Figure 2.6. Ryerson barrier-to-deck slab connection details .....	15
Figure 2.7. Proposed barrier-to-barrier connection details by Ryerson University .....	16
Figure 2.8. Barrier load application .....	16
Figure 2.9. Clampcrete barrier system.....	17
Figure 2.10. X-bolt connection concept.....	17
Figure 2.11. X-bolt test specimen .....	18
Figure 2.12. Damage to 10-ft long prefabricated barrier with X-bolt connections .....	18
Figure 2.13. Damage to 30-ft long precast barrier with X-bolt connections .....	19
Figure 2.14. Impact bogie vehicle.....	19
Figure 2.15. Plan view and elevation view of I-shaped rail connection between barriers .....	20
Figure 2.16. A plan view of MWRSF I-shaped rail connection .....	20
Figure 2.17. Failed MWRSF I-shaped rail connection .....	21
Figure 2.18. Side bolts and shear tube connection prior to testing .....	21
Figure 2.19. Side bolt and shear tube connection failure.....	22
Figure 2.20. Plan view and elevation view of I-shaped rail connection improvements .....	22
Figure 2.21. Redesign I-shaped rail connection after bogie testing.....	23
Figure 2.22. Plan view and elevation view of alternate modifications to the I-shaped rail connection .....	23
Figure 2.23. Alternate redesign I-shaped rail connection failure.....	24
Figure 2.24. Side bolts and shear tube connection improvements.....	24
Figure 2.25. Side bolt and shear tube connection after testing .....	25
Figure 3.1. Inclined bar connection between precast barrier and deck.....	27
Figure 3.2. U-bar connection between precast barrier and deck.....	28
Figure 3.3. Plan view of the barrier-to-barrier connection .....	29
Figure 3.4. End of bridge deck reinforcement (7-ft segment analysis) .....	30
Figure 3.5. Bridge deck reinforcement (10.5-ft segment analysis).....	30
Figure 3.6. Moment curvature responses of different deck segments .....	30
Figure 4.1. PBI and PBU at the CoreSlab facility prior to the concrete pour.....	31
Figure 4.2. Longitudinal double-headed ties used for barrier-to-barrier connection.....	32
Figure 4.3. Transverse double-headed ties used for barrier-to-barrier connection.....	32
Figure 4.4. End of precast barriers with longitudinal double-headed ties and receiving pocket .....	33
Figure 4.5. Bridge deck supporting beams with formwork .....	34

Figure 4.6. Inclined bar connection in deck.....	34
Figure 4.7. Connected inclined receiving end piece to the deck formwork .....	35
Figure 4.8. Deck block outs to facilitate U-bar installation.....	35
Figure 4.9. Bridge deck reinforcement .....	36
Figure 4.10. Installed PBI connection sleeve with deck reinforcement .....	36
Figure 4.11. U-bar access blocks outs with terminated bottom deck steel and top deck steel positioned to be within a U-bar connection .....	37
Figure 4.12. Bridge deck concrete pour.....	37
Figure 4.13. Threaded end of inclined reinforcement.....	38
Figure 4.14. Inclined reinforcing bars connected to bridge deck before placement of precast barrier.....	38
Figure 4.15. Barrier-to-barrier connection.....	39
Figure 4.16. Pockets used to install transverse barrier-to-barrier connection.....	39
Figure 4.17. Reinforcing steel bar chairs for #5 bars.....	40
Figure 4.18. Reinforcing steel bar chairs for #7 bars.....	40
Figure 4.19. Insertion of U-bars.....	40
Figure 4.20. Sealed U-bar pocket for grouting .....	41
Figure 4.21. Foam added to grout pad to minimize damage cover concrete .....	41
Figure 4.22. Grouting of U-bar pockets.....	42
Figure 4.23. Finished U-bar grout pocket.....	42
Figure 4.24. Completed barrier installation .....	42
Figure 4.25. Location of strain gauges in precast barrier reinforcement and bottom deck reinforcement .....	43
Figure 4.26. Location of strain gauges in barrier connection reinforcement and top deck reinforcement .....	44
Figure 4.27. Location of string pots and LVDTs on front side of testing unit .....	45
Figure 4.28. Location of string pots and LVDTs on backside of testing unit.....	46
Figure 4.29. 3D model of identifying the testing sequence and load application areas .....	46
Figure 4.30. Laboratory test set-up .....	47
Figure 4.31. Test set-up for Test 1 .....	48
Figure 5.1. Continuous test plot of top of barrier deflection for Tests 1–4 .....	50
Figure 5.2. Brace beam .....	51
Figure 5.3. Top of barrier deflection for Tests 5 and 6.....	51
Figure 5.4. Test 1: Formation of flexural cracks on the deck overhang .....	52
Figure 5.5. Test 1 (PBI middle) barrier cracks .....	53
Figure 5.6. Formation of crack on backside of test unit during Test 1 .....	53
Figure 5.7. Force displacement for Test 1 – PBI.....	54
Figure 5.8. Top barrier deflection profiles of PBI during Test 1 .....	55
Figure 5.9. Strain profiles of the inclined reinforcement barrier connection bars at the deck interface during Test 1 .....	56
Figure 5.10. Strain profiles of the deck reinforcement at the front barrier interface during Test 1 .....	57
Figure 5.11. Components of the measured PBI deflections.....	58
Figure 5.12. Crack at the barrier-to-deck interface in PBU during Test 2.....	59
Figure 5.13. Lateral versus force displacement obtained for Test 2 – PBU .....	60
Figure 5.14. Lateral top deflection of PBU during Test 2 .....	61

Figure 5.15. Strain in the U-bar at the deck to barrier interface during Test 2.....	62
Figure 5.16. Strain profiles of the deck reinforcement at the front barrier interface during Test 2.....	63
Figure 5.17. Deflection of components.....	64
Figure 5.18. Diagonal cracks developed on PBI during Test 3 .....	65
Figure 5.19. Force-displacement response obtained for Test 3 .....	66
Figure 5.20. Top barrier deflection profiles established from Test 3 data.....	66
Figure 5.21. Strain in barrier-to-deck connection interface during Test 3.....	67
Figure 5.22. Strain in the center of the longitudinal double-headed ties in barrier-to- barrier connection during Test 3 .....	68
Figure 5.23. Strain in transverse double-headed ties placed near the barrier-to-barrier connection during Test 3.....	69
Figure 5.24. Beam used to brace PBU with respect to the deck during Test 4.....	69
Figure 5.25. Cracking under the loading beam on PBI during Test 4 .....	70
Figure 5.26. Failure pattern of barrier-to-barrier connection at the end of Test 4.....	71
Figure 5.27. Force-displacement response obtained for Test 4 .....	71
Figure 5.28. Top lateral deflection of barrier during Test 4 .....	72
Figure 5.29. Difference in barrier movement at barrier-to-barrier connection at the maximum load during Test 4 .....	73
Figure 5.30. Strain in barrier connection reinforcement at the deck interface during Test 4 .....	73
Figure 5.31. Strain in longitudinal double-headed ties in barrier-to-barrier connection during Test 4 .....	74
Figure 5.32. Strain in transverse double-headed ties during Test 4.....	75
Figure 5.33. Final barrier deflection and cracking in bridge deck during push direction loading in Test 5.....	76
Figure 5.34. Damage to barrier and deck after Test 5 pull test.....	77
Figure 5.35. Damage to barrier-barrier interface after Test 5.....	78
Figure 5.36. Concrete spalling on front of PBI at deck interface and barrier-to-deck connection .....	78
Figure 5.37. Recorded force-displacement response during Test 5.....	79
Figure 5.38. Deflection at the top of the barrier during Test 5 .....	80
Figure 5.39. Strains in PBI at the barrier-to-deck connection interface during Test 5 .....	81
Figure 5.40. Final barrier deflection and the corresponding damage to the bridge deck during Test 5 .....	82
Figure 5.41. Top mat of the bridge deck reinforcement after the Test 6 pull test .....	82
Figure 5.42. Recorded force-displacement response for push direction loading in Test 6.....	83
Figure 5.43. Top barrier deflection during push direction loading of Test 6.....	84
Figure 5.44. Strain in barrier-to-deck connection interface in PBU during push direction loading in Test 6.....	85
Figure 6.1. Recommended spacing for inclined bar connection at a bridge end .....	88

## LIST OF TABLES

Table 2.1. Test levels .....	8
Table 2.2. Design forces for traffic barrier .....	8
Table 2.3. Test Level 4 design forces .....	10
Table 2.4. Summary of results obtained from eight states.....	12
Table 6.1. Summary of various tests conducted on the barrier.....	86

## ACKNOWLEDGMENTS

This project was sponsored by the Accelerated Bridge Construction University Transportation Center (ABC-UTC at [www.abc-utc.fiu.edu](http://www.abc-utc.fiu.edu)) at Florida International University (FIU), as the lead institution, and Iowa State University (ISU) as a partner institution, and the U.S. Department of Transportation (DOT) Office of the Assistant Secretary for Research and Technology.

The authors would like to thank the following:

- Headed Reinforcement Corporation for the development and supply of the specially designed inclined reinforcement connection
- CoreSlab for prefabricating the two barriers included in the full-scale testing
- Terry Wipf for serving as the principal investigator
- Ahmad Abu-Hawash, Atorod Azizinamini, Michael Culmo, Kevin Goeden, and Timothy Fields for serving on the technical advisory committee and providing input and advice throughout the project

Finally, the authors would like to acknowledge staff of the Iowa State University Wallace W. and Julia B. Sanders Structural Laboratory, Doug Wood and Owen Steffens, for their assistance in the construction and testing of the precast barrier system.



# INTRODUCTION

## Overview

In bridge systems, one very important component of safety is the bridge barrier. The primary purpose of bridge barriers is to contain, redirect, and shield vehicles from off-road bridge accidents. Cast-in-place barriers are typically used and are proven to meet the structural requirements needed to achieve this purpose. However, in bridge construction, the use of prefabricated elements and systems has been gaining interest and momentum. Using prefabricated elements, bridges can be constructed or repaired faster with less disruption to traffic and with a safer work zone environment. Another benefit of prefabricated systems is the improved product quality due to the use of precast components in a controlled setting. Ensuring consistent quality during cast-in-place concrete barrier construction is a challenge, which increases the maintenance costs (Figure 1.1). However, the use of precast concrete barrier systems for bridge decks is still a relatively new development that needs more attention and research, which is the focus of this report.



T. Capuano

**Figure 1.1. Cast-in-place barrier requiring maintenance**

## Accelerated Bridge Construction

The Federal Highway Administration (FHWA) states that approximately one quarter of the nation's bridges need rehabilitation, repair, or total replacement (FHWA 2018). On-site bridge construction and repair can have significant impacts on mobility and safety. Accelerated Bridge Construction (ABC) techniques are used to reduce these bridge construction challenges. The purpose of ABC is to minimize mobility impacts that occur due to on-site construction. ABC improves the site constructability and the total project delivery time. The most common form of accelerated bridge construction uses prefabricated elements and systems that improve the material quality and product durability.

With ABC, the bridge components are built outside of the traffic area and transported to the bridge site where they can be installed quickly (Figure 1.2). This helps reduce the on-site construction time, weather-related delays, and impacts to traffic, while improving worker safety.



<https://www.fhwa.dot.gov/bridge/prefab/girder.cfm>

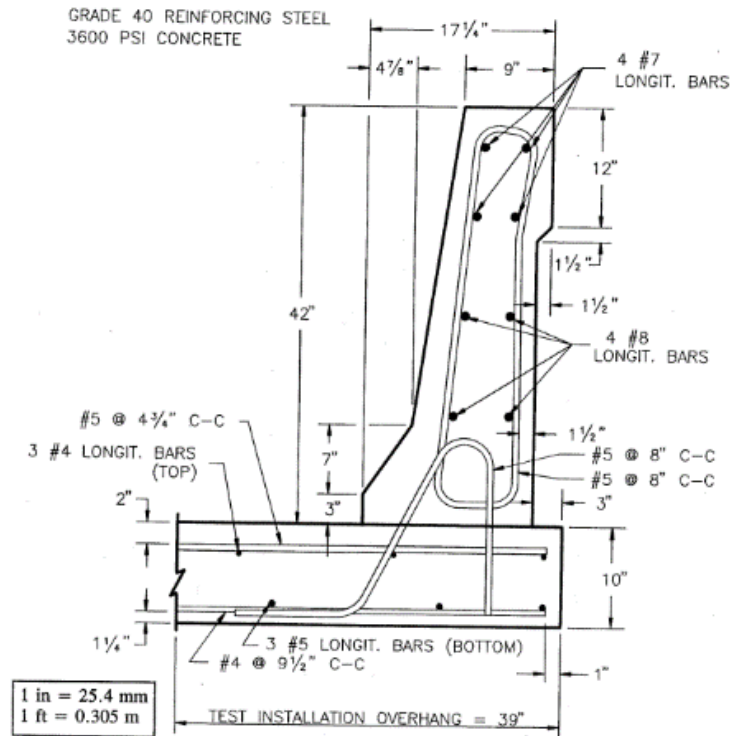
**Figure 1.2. Prefabricated bridge element**

Prefabricated elements and systems include decks, girders, piers, columns, and abutments. Prefabricated concrete bridge barriers are an emerging prefabricated element that will assist in reducing on-site construction time and traffic impacts. With more research and development, prefabricated bridge barriers may also improve bridge safety with appropriate anchorage details and construction quality while providing a viable alternative for easy repair of a damaged barrier.

### **Current Practices**

Currently, many concrete bridge barriers are installed using cast-in-place concrete. The barrier is connected to the bridge deck with vertical and inclined reinforcing steel from the bridge deck overhang. To achieve proper alignment of the steel and the barrier, the vertical reinforcing in the deck must be secured so that it prevents movement during bridge deck construction. Once the deck construction is complete, the barrier is then cast using slipform over the exposed vertical deck reinforcing steel connected with additional reinforcement. Figure 1.3 shows the steel reinforcement for a standard 42-in. tall F-shaped barrier.





Buth et al. 1997

**Figure 1.3. F-shaped concrete barrier and reinforcement details**

Common barrier profile shapes discussed in the following section include the New Jersey shape, the F-shape, and the single-slope barrier. The schematic in Figure 1.3 shows the vertical reinforcing steel extending from the bridge deck, which establishes the connection between the barrier and the bridge deck.

Completed ABC projects, such as the Rockridge Road bridge in Polk County, Florida, consisted of complete replacement of the substructure and superstructure. Per a presentation given in the 2014 Design Training Expo (Verrastro et al. 2014), the deck was reconstructed using precast, prestressed slab units. The new F-shaped barriers, however, were constructed as cast-in-place. A portion of the reinforcing steel bar was built into the deck slab unit (Figure 1.4), and bent to be integrated with the concrete barrier reinforcing as shown in Figure 1.5.



Verrastro et al. 2014

**Figure 1.4. Rockridge Road bridge with exposed barrier connection reinforcement**



Verrastro et al. 2014

**Figure 1.5. Rockridge Road barrier after adding additional reinforcing**

If a vehicle were to collide with a commonly constructed bridge barrier, a major repair project would take place. To install a new barrier, the construction would include a partial deck replacement. The construction of a bridge deck can be an intensive, costly project. With the new practice of accelerated bridge construction and the use of prefabricated concrete bridge barriers, the construction and repair of a bridge deck or barrier rail would generate more benefits, especially societal benefits, than current practices.

With the development of a precast bridge barrier system, there will be more benefits than the current practices with cast-in-place construction. The prefabricated barriers will result in a reduction in construction time. This also means that the bridge would be closed for a shorter period, minimizing the impact to the travelling public. Another benefit will be the ability to maintain and repair the barrier. With good connection details, precast barrier systems can be designed to be easier to replace with reduced construction time. This should also limit the damage to the bridge deck.

With the significant interest in ABC, there has been valuable research in many important and varied areas. However, one area that has not yet received notable research attention is in the area of prefabricated, crash-tested barrier rails. ABC projects to date have tended to rely upon systems that utilized crash-tested systems integrated into other, larger prefabricated elements. Although this has proved sufficient while ABC has been in its relative infancy, there is a critical need to develop prefabricated bridge concrete barriers with appropriate connection details together with validation tests.

## **Scope of Research**

Owners are moving to prefabricated bridge elements to facilitate rapid bridge construction and minimize the impact of construction on traffic. Development of prefabricated bridge barriers must be attached to a bridge superstructure with durable connections and be shown to satisfy the Manual for Assessing Safety Hardware (MASH) (AASHTO 2009, Ross et al. 1993). Anchorage systems needed will include robust details that connect the prefabricated bridge barrier to the bridge deck as well as that connect one prefabricated bridge barrier to an adjacent prefabricated bridge barrier. The long-term goal of this research effort was to establish crash-tested prefabricated concrete bridge barriers with recommended durable anchorage systems (between the barrier and the deck and between adjacent sections of barrier) and details that meet design test level TL-4 in accordance with the MASH and Load and Resistance Factor Design (LRFD) Bridge Design Specifications (AASHTO 2009 and 2012, Ross et al. 1993).

The scope of this research project is to establish a precast barrier with appropriate connections designed to test level TL-4 to be used in bridge construction. This was done by developing connection details for the use of a precast barrier system and by evaluating the developed details based on laboratory testing. Using quasi-static loading, the precast barrier and the deck system were evaluated to examine the load distribution and connection performance under different loading scenarios. Once satisfactory connections were established, the precast barrier needed to be crash tested in the next phase of the study.

## **Research Objectives**

This research project contained several components. To get a better understanding of precast barrier systems, a literature review was conducted to review all cast-in-place and prefabricated barrier designs and details, including anchorage systems that have been crash tested for use on the national highway system. The search also included a survey distributed to several state departments of transportation (DOTs) to determine their needs related to prefabricated concrete bridge barriers.

Based upon the results of the literature search, conceptual designs of prefabricated barriers with associated anchorage systems and details were developed. Although the ultimate goal was to develop a system that can be adopted for multiple barrier shapes, only one profile shape was selected in this experimental investigation. Two concepts for connecting the barrier to the bridge deck were designed for testing and one detail for connecting two adjacent barriers was conceptualized.

The laboratory testing was conducted on two full-scale test barriers with connections between the barrier as well as with a bridge deck using quasi-static loading. The barrier systems were evaluated for their connection performance, their individual strengths and force transfer, and corresponding distribution in the barrier and the bridge overhang. Although the research focused on barrier detail away from the end regions, suggestions to incorporate the details for end regions of the bridge were provided.

## **Report Layout**

Following this introduction, this report includes a literature review of cast-in-place and prefabricated barrier designs and details including anchorage systems that have been crash tested for use on the national highway system. The remainder of this report includes the following:

- The design criteria of the prefabricated barriers
- The conceptual designs of the developed anchorage systems and the experimental specimen design criteria and loading
- The laboratory results and evaluation of two barrier-to-deck connections and one barrier-to-barrier connection
- The conclusions of the study, recommendations to improve the precast barrier connection details, and suggestions for next the phase of the study

## **LITERATURE REVIEW**

### **Introduction**

In order to achieve a better understanding of the design and performance of prefabricated concrete bridge barriers, a literature review was performed. Accelerated bridge construction and the use of prefabricated elements and systems have received significant research attention in recent years. However, one area that has not yet received notable research consideration is prefabricated, crash-tested barrier rails. Nonetheless, a review was completed in order to gauge the state of knowledge at the beginning of the project.

### **Design of Barriers**

The primary function of a barrier system is to contain and redirect colliding vehicles. The American Association of State Highway and Transportation Officials (AASHTO) standards suggest that all vehicle traffic barriers must satisfy both geometric and strength requirements in order to have sufficient strength to survive the initial impact of the collision and to remain effective in redirecting the vehicle (AASHTO 2012). The barriers are designed so that if any failures occur, they happen within the barrier rather than to the bridge deck. The barrier can be readily repaired, whereas repairing a deck would cost more, take more time, and create more disruption.

#### *Concrete Barrier Strength*

According to MASH, barriers can be tested to six different test levels. The test level is defined by the impact conditions and the type of vehicle impacting the barrier. The first three test levels use passenger vehicles while the last three tests use a form of heavy truck. The test levels are summarized in Table 2.1.

**Table 2.1. Test levels**

Test level	Test Vehicle Designation and type	Weight of vehicle (lb)	Test conditions	
			Speed (mph)	Angle (degrees)
1	1100C (Passenger Car)	2,420	31	25
	2270P (Pickup Truck)	5,000	31	25
2	1100C (Passenger Car)	2,420	44	25
	2270P (Pickup Truck)	5,000	44	25
3	1100C (Passenger Car)	2,420	62	25
	2270P (Pickup Truck)	5,000	62	25
4	1100C (Passenger Car)	2,420	62	25
	2270P (Pickup Truck)	5,000	62	25
	10000S (Single-Unit Truck)	22,000	56	15
5	1100C (Passenger Car)	2,420	62	25
	2270P (Pickup Truck)	5,000	62	25
	36000V (Tractor-Van Trailer)	79,300	50	15
6	1100C (Passenger Car)	2,420	62	25
	2270P (Pickup Truck)	5,000	62	25
	36000T (Tractor-Van Trailer)	79,300	50	15

Source: AASHTO 2009

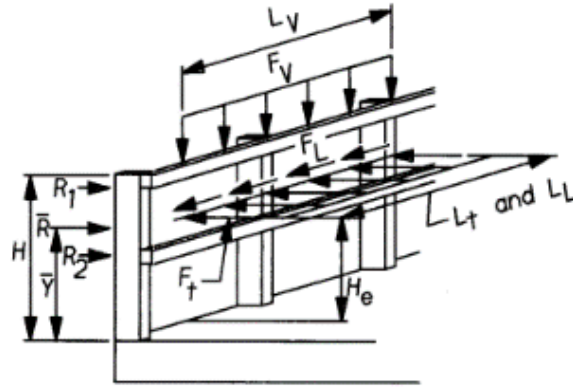
According to the AASHTO LRFD Bridge Design Specifications (2012), when designing barriers, the design forces and geometric criteria to be used in developing test specimens should be taken as specified in Table 2.2.

**Table 2.2. Design forces for traffic barrier**

Design Forces and Designations	Test levels					
	TL-1	TL-2	TL-3	TL-4	TL-5	TL-6
$F_t$ Transverse (kips)	13.5	27.0	54.0	54.0	124.0	175.0
$F_L$ Longitudinal (kips)	4.5	9.0	18.0	18.0	41.0	58.0
$F_v$ Vertical (kips) Down	4.5	4.5	4.5	18.0	80.0	80.0
$L_t$ and $L_L$ (ft)	4.0	4.0	4.0	3.5	8.0	8.0
$L_v$ (ft)	18.0	18.0	18.0	18.0	40.0	4.0
$H_e$ (min) (in.)	18.0	20.0	24.0	32.0	42.0	56.0
Minimum $H$ Height of Rail (in.)	27.0	27.0	27.0	32.0	42.0	90.0

Source: AASHTO 2012

Figure 2.1 shows the design force locations that must be applied to the barrier for each test level.



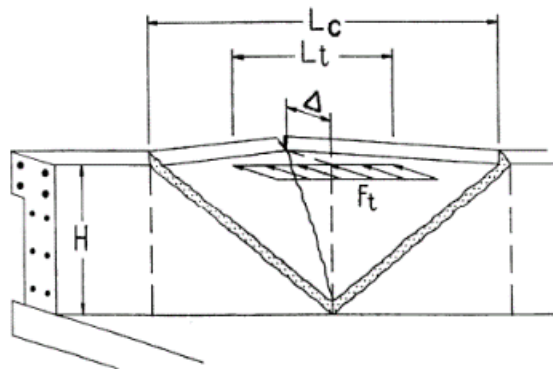
*AASHTO LRFD Bridge Design Specifications*, Copyright 2012 by the American Association of State Highway and Transportation Officials, Washington, DC. Used with permission.

**Figure 2.1. Bridge barrier design force locations as suggested in AASHTO LRFD specifications**

For this research project, as previously noted, the barriers were designed to sustain loads from test level TL-4, which is suitable for high-speed highways, freeways, expressways, and Interstate highways with a mixture of trucks and heavy vehicles. Accordingly, the barrier and its connection to the bridge deck must resist a transverse design force,  $F_t$ , of 54 kips, which is distributed over a length of 3.5 ft of the barrier (Table 2.2). This value represents the distributed impact force of a vehicle collision.

#### *Yield Line Analysis*

The strength of a barrier is based on the formation of yield lines at the limit state. The yield line approach can be used to check the strength of the concrete barrier away from an end or a joint and determine the distribution of the loads that must be transferred to the deck overhang. The variables used are illustrated in Figure 2.2. The nominal resistance of the barriers to transverse loads can be found using Equations 2.1 and 2.2.



*AASHTO LRFD Bridge Design Specifications*, Copyright 2018 by the American Association of State Highway and Transportation Officials, Washington, DC. Used with permission.

**Figure 2.2. Yield line pattern used for designing concrete barrier under load,  $F_t$**

$$L_c = \frac{L_t}{2} + \sqrt{\left(\frac{L_t}{2}\right)^2 + \frac{8H(M_b + M_w)}{M_c}} \quad (2.1)$$

$$R_w = \left(\frac{2}{2L_c - L_t}\right) \left(8M_b + 8M_w + \frac{M_c L_c^2}{H}\right) \quad (2.2)$$

where

$H$  = height of wall (ft)

$L_c$  = critical length of yield line failure pattern (ft)

$L_t$  = longitudinal distribution length of impact force (ft)

$M_b$  = additional flexural resistance of beam, if any, at top of wall (kip-ft)

$M_c$  = flexural resistance of wall about an axis parallel to the longitudinal axis of the bridge (kip-ft/ft)

$M_w$  = flexural resistance of wall about vertical axis (kip-ft)

$R_w$  = nominal barrier resistance to transverse load (kips)

The flexural resistance of the barrier wall about the vertical axis is based on the horizontal reinforcement within the wall and the flexural resistance of the wall about an axis parallel to the longitudinal axis is determined from the vertical reinforcement. Since the barrier wall varies for most profile shapes, it is convenient to divide the wall into sections for calculation purposes. Once the bending strengths are found for each section, the total moment strength of the wall about the vertical axis is the sum of the strengths. For the horizontal axis, a weighted average is used to find the total moment resistance.

Since TL-4 is the focus of this project, the values used to determine the yield line pattern for this case are displayed in Table 2.3

**Table 2.3. Test Level 4 design forces**

<b>Design forces and designations</b>	<b>TL-4</b>
$F_t$ Transverse (kips)	54.0
$F_L$ Longitudinal (kips)	18.0
$F_V$ Vertical (kips) Down	18.0
$L_t$ and $L_L$ (ft)	3.5
$L_V$ (ft)	18.0
$H$ (in.)	42.0

Source: AASHTO 2012



## **Experimental Evaluation**

Almost all roadside safety features are required to sustain some minimum structural capacity to assure that they can resist the applied load. Barriers must have sufficient structural capacity to resist lateral loads from an impacting vehicle. There are multiple types of test that can be done to demonstrate this in a laboratory setting on a newly developed barrier system. Laboratory testing can include, but is not limited to, a gravitational pendulum, a bogie test, a static test, or a vehicle crash test. The cost of these tests varies significantly and each test provides a valuable set of information.

An emerging trend in evaluating the impact performance of barrier rails is the use of surrogate test devices such as a bogie vehicle or a pendulum. The gravitational pendulum is characterized by a striking mass that swings in a circular arc suspended by cables or rigid arms from a main frame. The structure of the mass is designed to replicate the dynamic crush properties of a model test vehicle and is considered a low-speed test device. Due to height limitations, gravitational pendulums generally are used to test impact speeds of about 25 mph or less. As stated previously, the purpose of this study was to develop a barrier that can withstand an impact at Test Level 4 (TL 4). TL 4 passing impact speeds are 62 mph; therefore, a gravitational pendulum would not be the best option for this test.

A bogie vehicle is designed to replicate vehicular crush characteristics. It is a vehicle on four wheels with a mass equal to the selected test level vehicle. The vehicle is steered or guided to impact the test specimen. A push or tow vehicle can be used to get the bogie to the impact speed. Designing and calibrating the bogie to represent the selected passenger vehicle would be a long and expensive process.

Many transportation safety features, including the bridge barriers, are designed to meet the required ultimate capacity. Static testing can be used to load the structural system beyond the elastic limit until it experiences failure. This process could be used to evaluate and validate the safety of critical details and connections. Static testing can also help identify the force transfer paths and evaluate failure modes. Static testing is a simple and easy way to test and compare design details. For all these reasons, it was chosen to examine the precast concrete bridge barriers for this project.

After a barrier system has gone through the early stages of development and has been tested to reach its desired capacity, it may need to go through a final proof test through a vehicle crash test. Vehicle crash tests are the most direct tie to an actual highway collision. However, this type of testing is fairly expensive to perform and requires extensive facility capabilities.

## **Practice of State DOTs**

With help from the Iowa DOT, information on current practices from other state DOTs was sought via a survey distributed to various DOTs. The survey also inquired what is currently in use for precast barriers within the states. Responses were received from 22 states and eight of

them were currently using a form of precast barrier system. Table 2.4 displays the survey responses from the states for developing a precast barrier.

**Table 2.4. Summary of results obtained from eight states**

State	Precast barriers in use?	Profile	Barrier Length	Barrier Height	Connection	Testing	Desired Test Level
Alaska	Yes	F or NJ	12'-6"	32"	Pinned connection		TL-3
Nebraska	Yes	F	12'		Bolted	Full-Scale Crash Test	TL-4
New York	Yes	SS or NJ	20'	32" & 42"	Bolted or hooked	Static - Hydraulic ram, crash test	TL-4
Ohio	Yes	Temp. NJ	10' or 12'	32"	Anchor bolts	Full-Scale Crash Test	TL-3
Pennsylvania	Yes	F or Vertical	12'	42"	Integral with deck	No	
Rhode Island	Yes	NJ	10'-20'	33"	Thru bolt/epoxy adhesive	No	
Texas	Yes	Vertical	30'	32"	Through bolt	Full-Scale Crash Test	TL-3
Utah	Yes	SS	23'-6" – 25'	42"	Integral with deck	No	TL-4

Of the eight responses with experience with precast barriers, most of the uses were for temporary purposes. Other systems in use are built into the bridge deck instead of connecting to the bridge deck as a separate unit. Six of the eight responses had crash tested their precast barrier systems to either test level 3 or level 4. From these responses, a standard shape and length were determined for the purposes of this research. The shape chosen was a standard F-shape barrier 12 ft in length. This survey also demonstrated the need for more research in the area of permanent, precast, concrete, and bridge barriers.

### **Precast Barriers**

Precast barriers are generally categorized by the shape of their profile. The profile shapes are demonstrated in Figure 2.3.

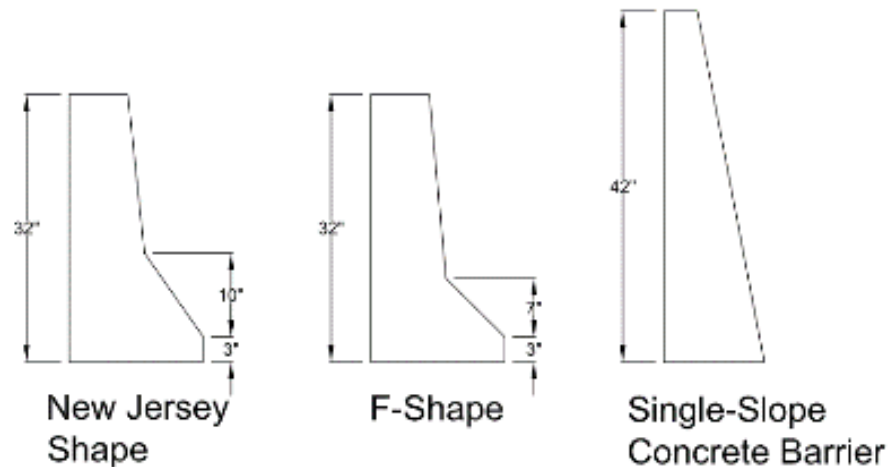


**Figure 2.3. Commonly used concrete bridge barrier profile shapes**

The New Jersey shape, the F-shape, and the single slope are the three most commonly used precast concrete barrier profiles in the US. The barrier shapes were designed to disperse the energy of the impact of the crash. The F-shape and the New Jersey shape have a 3-in. vertical face starting at the pavement. They then break into a sloped face and change to a nearly vertical face towards the top of the barrier. Some of the impact energy is dissipated from the climbing or lifting action that occurs when a vehicle collides with the barrier. Between the F-shape and the New Jersey shape, the only difference is the distance from the ground to the sloped face. The single slope barrier has a constant-sloped front face. Due to this vertical face, single slope barriers do not lift the vehicle and therefore do not disperse the energy quite like the F- or New Jersey shape. Following are some suggested details for using precast barriers.

#### *Florida DOT*

A few permanent precast concrete barriers have been developed with different anchoring methods. Common methods for anchoring precast concrete barriers to bridge decks include through-deck bolts and adhesive anchors. With the through-deck anchoring method, a hole is drilled through the entire bridge deck and a bolt is inserted through both the barrier and the deck. It is secured with heavy washers and nuts on both ends of the steel bolt. This concept, used by the Florida DOT (FDOT 2012), is called the Type K temporary concrete barrier system. It is used for median traffic barriers, but may also be used on concrete bridge decks. The shape of the median traffic barrier is similar to a New Jersey or an F-shape profile. Due to traffic on either side of the barrier, the sloped faces are on both sides instead of one side for a bridge barrier. One challenge with this design is getting access to the underside of the bridge deck to secure the nut. Another issue is weathering of the exposed connection. Figure 2.4 shows a typical anchoring detail for the through-deck configuration.

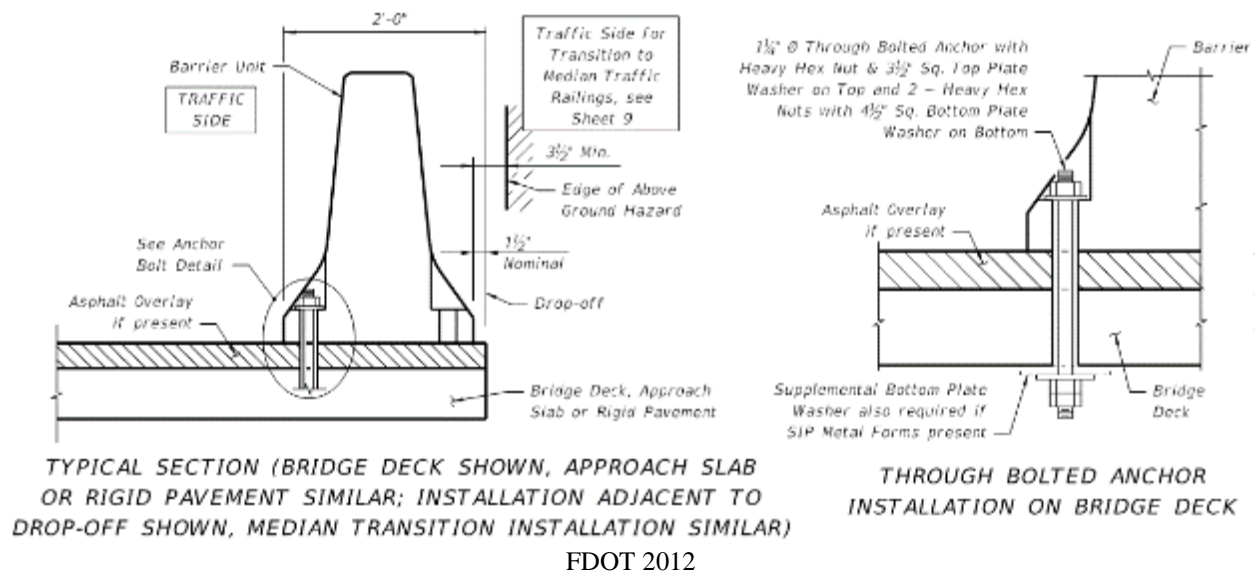


**Figure 2.4. Through-deck bolting detail developed by Florida DOT**

Another precast concrete barrier anchoring technique that is used by the Florida DOT is an adhesive-bonded anchor. This method involves drilling a hole into the bridge deck and then inserting a threaded bolt through the barrier and into the deck. The bolt is then secured with an adhesive. This method can be seen in Figure 2.5. This concept is used by the Florida DOT for median traffic barriers, but may also be used on concrete bridge decks. One issue with this anchoring method is the anchorage strength of the adhesive used.

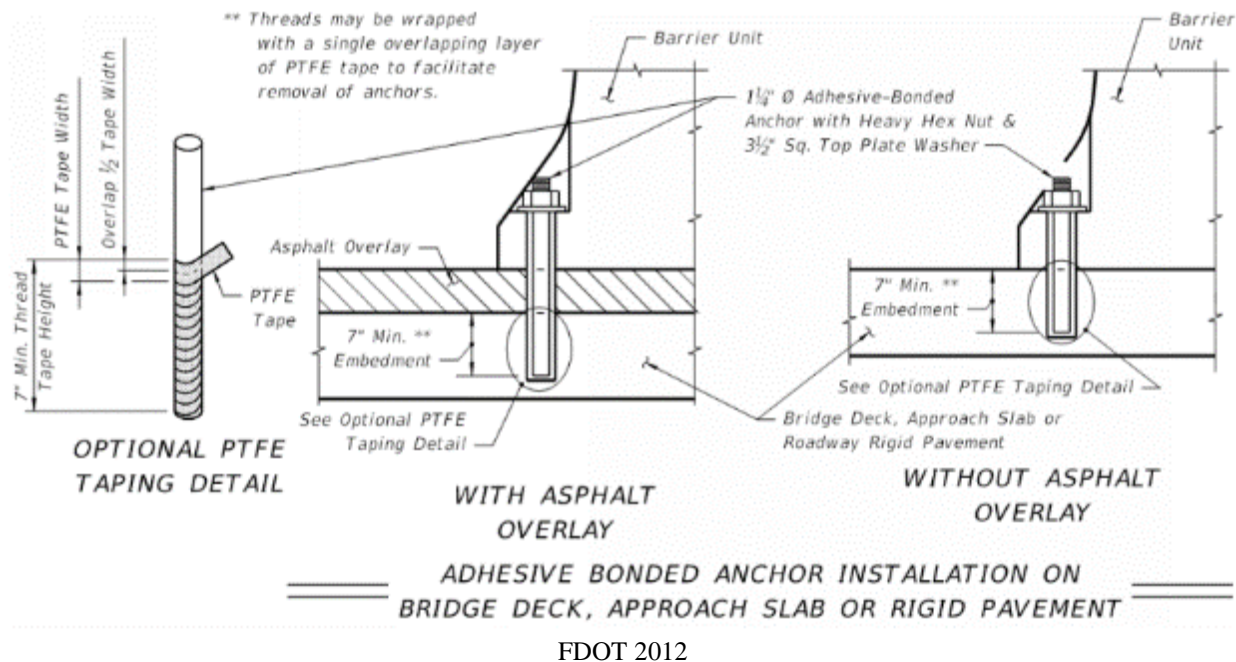
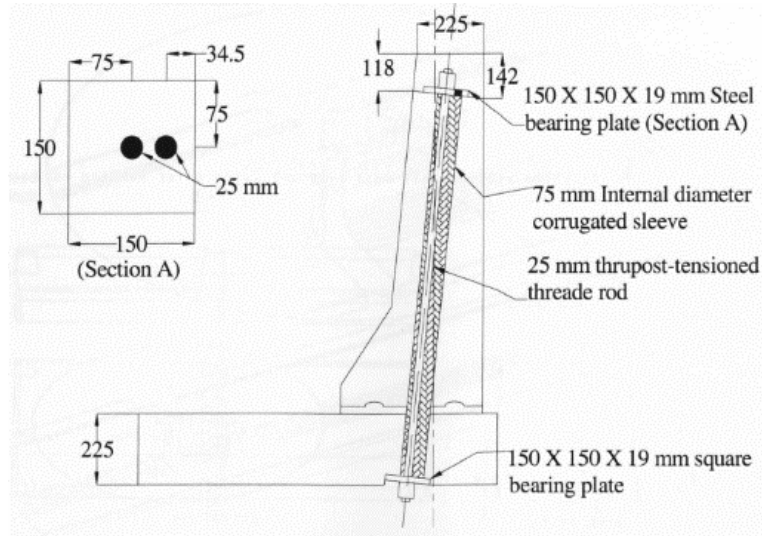


**Figure 2.5. Adhesive-bonded anchor detail**

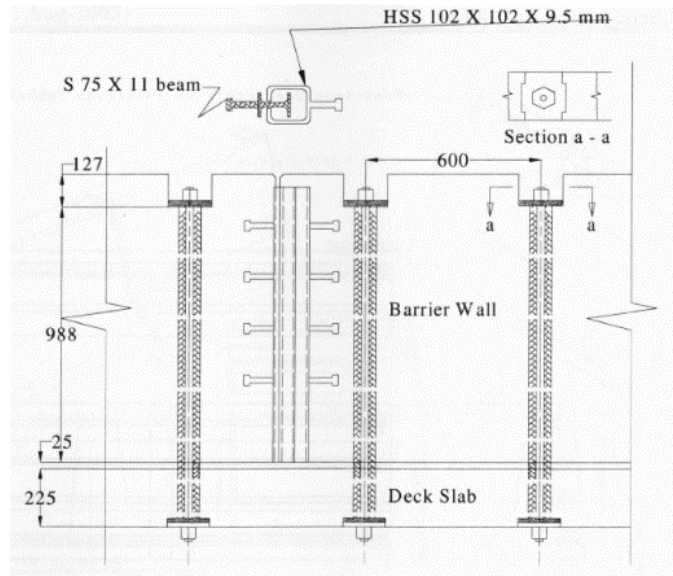
A different way of connecting a barrier with the through-deck method is by pre-tensioned rods that are inserted all the way through the wall and the deck slab. A study conducted by Ryerson University in Canada tested this method. The pre-tensioned rods were then anchored to the bridge deck by the end plates, washers, and nuts. Details of this system can be seen in Figure 2.6. As before, the challenges with this detail are gaining access to the bottom of the bridge deck and the corrosion of the exposed hardware.



All dimensions are in mm; 1 mm = 0.0394 in.  
Patel 2008

**Figure 2.6. Ryerson barrier-to-deck slab connection details**

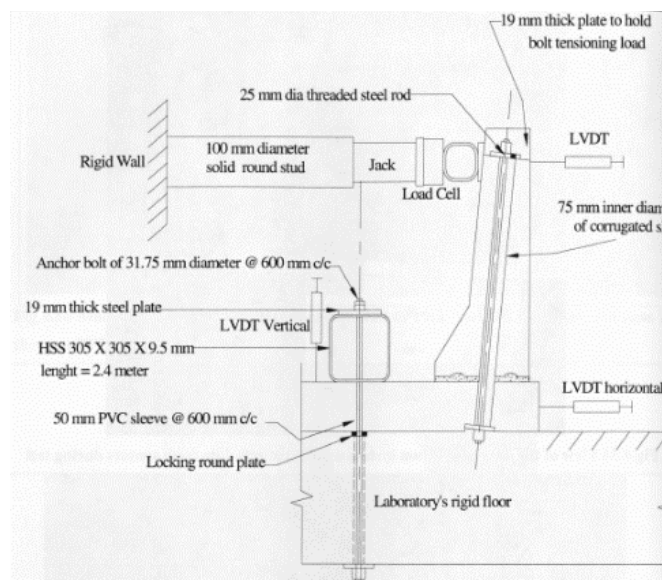
The vertical joint between the two barriers that was proposed by Ryerson University included a hollow structural steel (HSS) section with shear studs welded on to provide anchorage for one segment. The other segment would have an S-shaped steel beam projecting from it such that it would slide into the HSS in the other barrier. This connection detail is illustrated in Figure 2.7 but was not subjected to any structural testing.



Patel 2008

**Figure 2.7. Proposed barrier-to-barrier connection details by Ryerson University**

Four barrier segment units with the barrier-to-bridge-deck connection were made and tested with various loading patterns. One of the five model units was a cast-in-place detail used for comparison. The barriers were tested according to the Canadian Highway Bridge Design Code (CHBDC) at performance level 3 (PL-3), which is comparable to MASH TL 5. A hydraulic jack was used to apply a horizontal load to the barriers, as shown in Figure 2.8. Each specimen was quasi-statically loaded to collapse. All precast units with the barrier-to-deck connection proved to be adequate for the desired design loads.

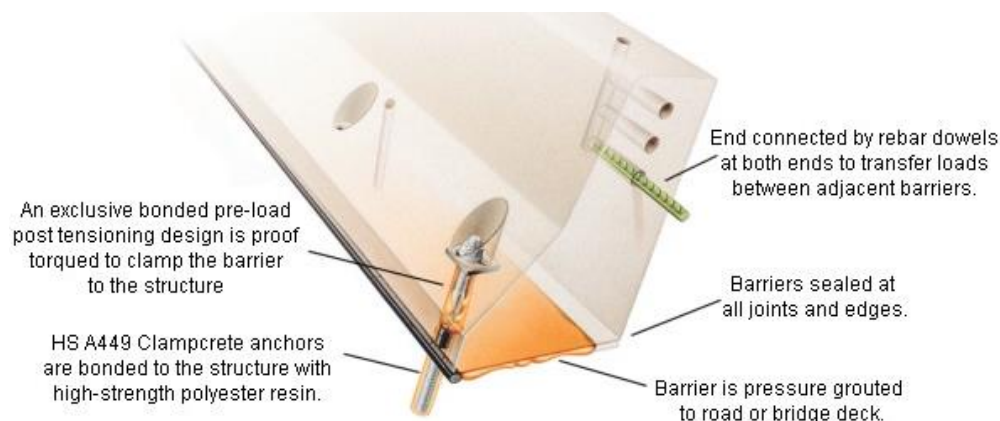


Patel 2008

**Figure 2.8. Barrier load application**

## *Clampcrete*

A precast barrier wall system similar to the adhesive-anchored connection was engineered and patented by Clampcrete. It was crash tested at TL-4 in accordance with AASHTO LRFD guidelines and approved for use by the FHWA in 1989. It is connected to the bridge deck by drilled-in polyester resin anchors. This system, shown in Figure 2.9, can be applied to any of the profile shapes in both permanent and temporary barriers. These barriers come in 20-ft-long segments with a height of either 32 in. or 34 in. The connections between the barriers consist of a minimum of three deformed reinforcement dowels as seen in Figure 2.9. The dowels are bonded into dowel holes in the adjacent barrier section.

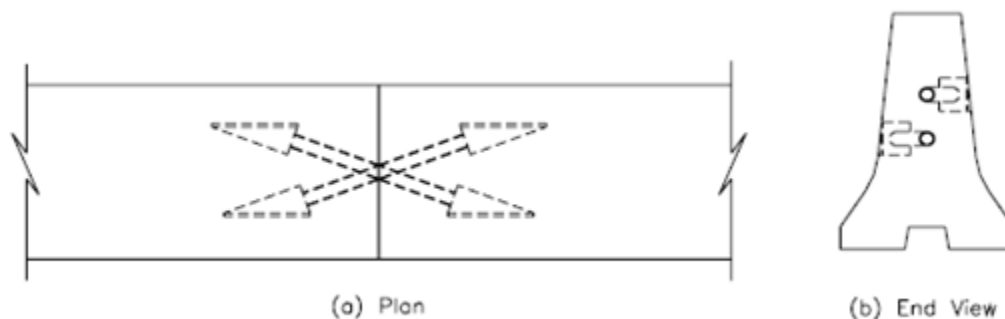


[www.clampcrete.com/html/featuresindex.htm](http://www.clampcrete.com/html/featuresindex.htm)

**Figure 2.9. Clampcrete barrier system**

## *Texas Transportation Institute*

A study done by the Texas Transportation Institute (Bligh et al. 2005a) used an X-bolt connection concept for a portable, temporary concrete barrier. A conceptual drawing of the connection design can be seen in Figure 2.10.



Bligh et al. 2005b

**Figure 2.10. X-bolt connection concept**

The purpose of the study was to design a portable concrete traffic barrier with the minimum dynamic deflection that could also be easily inspected and repaired. The connection was studied using full-scale crash tests (Bligh et al. 2005a). As seen in Figure 2.11, the connection uses two threaded rods across the joint.



Bligh et al. 2005a

**Figure 2.11. X-bolt test specimen**

The barriers had a standard F-shape profile and were 32 in. in height. The cross bolts used a 7/8-in. diameter threaded rod and were 25-1/4 in. and 29 in. in length. The cross-bolt barriers were tested under TL-3. There were two crash tests conducted. One test consisted of 20, 10-ft long concrete barrier sections for a total test installment length of about 200 ft. A 4,960 lb pickup truck was used for the crash test. The resulting damage is shown in Figure 2.12. Some permanent deformation of the connection bolts was noticed when disassembling the barrier. The barrier system experienced 27.0 in. of maximum deflection.



Bligh et al. 2005a

**Figure 2.12. Damage to 10-ft long prefabricated barrier with X-bolt connections**

The second test had the same barrier and connection details, but the test installment included seven 30-ft barrier segments for a total length of about 210 ft. The pickup truck used for this experiment was 4,531 lbs. The damage resulting from the vehicle impact is shown in Figure



2.13. After the test, the connection bolts could easily be removed and possibly reused. The maximum deflection experienced by the system was 19.0 in.



Bligh et al. 2005a

**Figure 2.13. Damage to 30-ft long precast barrier with X-bolt connections**

#### *Midwest Roadside Safety Facility*

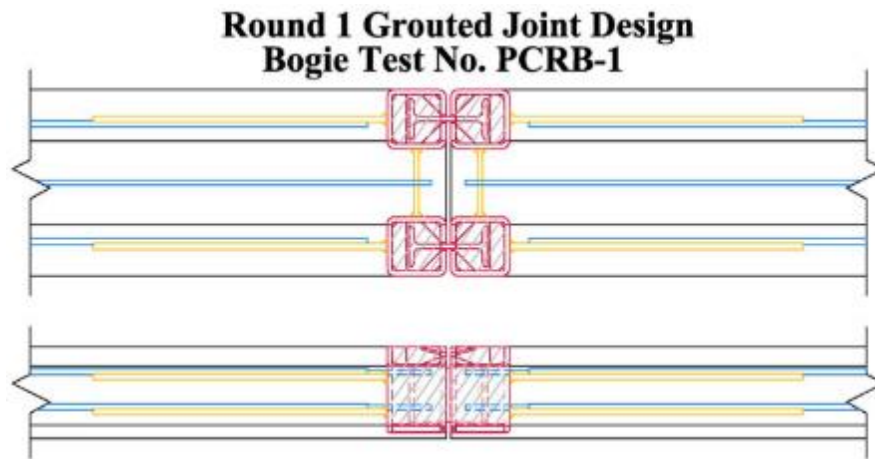
The Midwest Roadside Safety Facility (MwRSF) at the University of Nebraska-Lincoln conducted a study with an objective of developing an aesthetic precast concrete bridge rail. This study examined six different dry joint design details and three different grouted joint design methods. Two of the most promising details were selected to be tested using a dynamic impact bogie vehicle as shown in Figure 2.14.



Rosenbaugh et al. 2012

**Figure 2.14. Impact bogie vehicle**

The first tested connection used I-shaped steel segments to connect the rails. The I-shaped sections were placed inside steel pockets that were filled with grout. This is illustrated in Figure 2.15.



Rosenbaugh et al. 2012

**Figure 2.15. Plan view and elevation view of I-shaped rail connection between barriers**

During the test, the joint failed and the rail segments completely separated. The connection was able to resist a force of 143 kips, exceeding the design forces needed for TL-4. The test connection and the failure of the connection are shown in Figure 2.16 and Figure 2.17, respectively.



Rosenbaugh et al. 2012

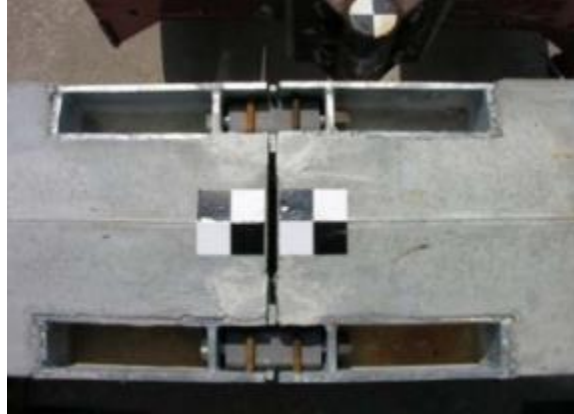
**Figure 2.16. A plan view of MWRSF I-shaped rail connection**



Rosenbaugh et al. 2012

**Figure 2.17. Failed MWRSF I-shaped rail connection**

The second tested connection used two bolts and two shear tubes to connect the adjacent rails. During this test, the rails stayed connected, but the joint was severely damaged. The concrete between the steel pockets completely broke apart. The connection was able to resist a force of 102 kips, exceeding the design force of 54 kips needed for TL-4. The test connection and the failure of the connection are shown in Figure 2.18 and Figure 2.19, respectively. After these experiments were conducted, the results were analyzed, and they were redesigned according to their failures.



Rosenbaugh et al. 2012

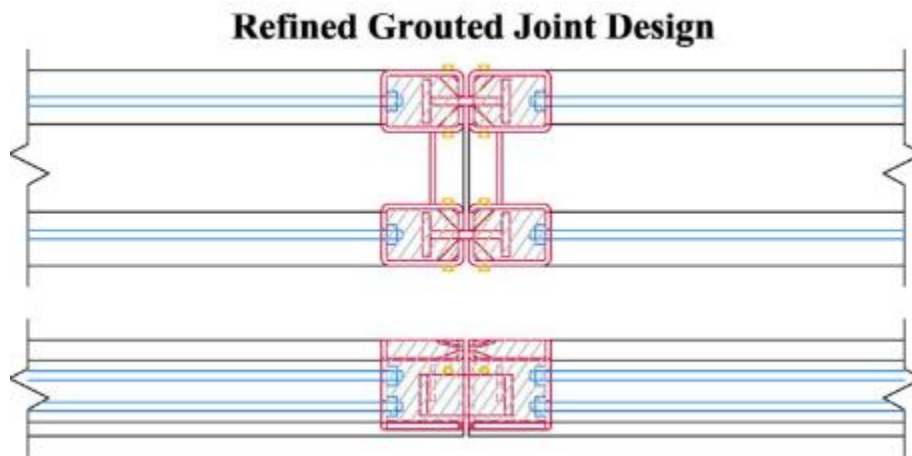
**Figure 2.18. Side bolts and shear tube connection prior to testing**



Rosenbaugh et al. 2012

**Figure 2.19. Side bolt and shear tube connection failure**

Redesign of the I-shaped steel connection included an increase in reinforcing steel bar sizes from no. 5 longitudinal reinforcing bar to no. 7 threaded reinforcing bar and the steel pockets were changed to steel tubes. The shear reinforcement was modified as well. To prevent the connection from prying open, shear bolts were added. This is detailed in Figure 2.20.



Rosenbaugh et al. 2012

**Figure 2.20. Plan view and elevation view of I-shaped rail connection improvements**

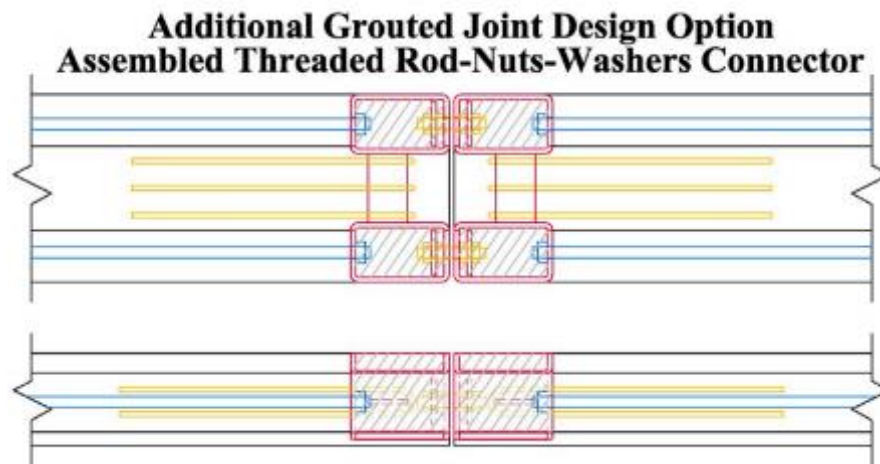
This joint held up to an approximate load of 100 kips, exceeding the design impact force of 62 kips. The joint also sustained minimal damage. The resulting damage is shown in Figure 2.21.



Rosenbaugh et al. 2012

**Figure 2.21. Redesign I-shaped rail connection after bogie testing**

During the initial improvements, another alternative to the I-shaped connection arose. Instead of a steel I-shaped connector, this joint utilized a threaded rod to connect the adjacent rail pockets. Similar to the first redesign, this detail also increased the rebar size to a single no. 8 bar with threaded ends. A shear plate was placed between the pockets with U-shaped bars wrapped around the plate and extending into the rail. This is detailed in Figure 2.22.



Rosenbaugh et al. 2012

**Figure 2.22. Plan view and elevation view of alternate modifications to the I-shaped rail connection**

This joint sustained a load that averaged over 100 kips and absorbed slightly more energy than the grouted I-shaped joint. However, the specimen suffered much more damage from concrete spalling and cracking. Damage after testing is illustrated in Figure 2.23.



Rosenbaugh et al. 2012

**Figure 2.23. Alternate redesign I-shaped rail connection failure**

The side bolt and shear tube connection were modified in a similar fashion. The longitudinal steel size was increased to a threaded no. 8 bar, the steel tubes were cut to form U-shaped pieces, the size of the joint pockets increased, and shear bolts were added. See Figure 2.24.



Rosenbaugh et al. 2012

**Figure 2.24. Side bolts and shear tube connection improvements**

The testing results of this joint proved that the connecting threaded rods were too weak and failed at a load just over 60 kips. Resulting damage is shown in Figure 2.25.



Rosenbaugh et al. 2012

**Figure 2.25. Side bolt and shear tube connection after testing**



## **EXPERIMENTAL PLAN**

### **Introduction**

Based on both the literature review that was conducted and discussion with academics, professionals, precasters, and members of the technical advisory committee (TAC), some guidelines had to be established when designing and testing the barrier segments. It was decided that the laboratory testing would include two connections between the barrier and the deck and one connection between the barriers and that it would simulate the load on a barrier away from the bridge end regions. The barrier segments chosen would be 12 ft in length with a 0.5-in. construction tolerance between them. From the national survey, the barrier profile shape selected was the standard 42 in. F-shape barrier. The deck, deck overhang, and barrier placement on the deck were designed in accordance to Iowa DOT standards.

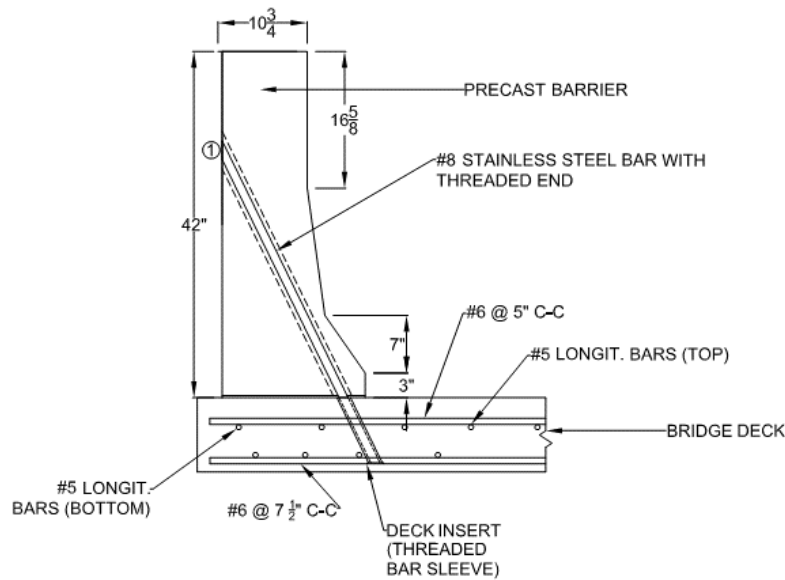
### **Guiding Parameters**

For this research, the design of the precast concrete barrier covered multiple parameters. Those parameters included the following: 1) ease of construction of the connections, 2) improved durability and lower maintenance cost, 3) easy repair of the damaged barrier, and 4) cost effectiveness. The laboratory testing also needed to demonstrate the safety of the barrier and how the loads are transferred upon impact at different locations. Two connections between the barrier and the bridge deck were designed for this project. One of the connections was designed to be durable, easily constructible, and replaceable if it experienced damage due to a vehicular collision. The other connection was designed to be cost effective and have a durable anchorage system, but not easily repairable.

### **Barrier-to-Deck Connections**

After evaluating the benefits and challenges of various connections concepts, the first precast barrier to be tested was designed with an inclined, #8 bar as the primary connection element between the barrier and deck. Five #8 bars were used to connect the barrier segment to the bridge deck with a maximum spacing of 30 in. between two adjacent bars. A schematic illustrating this detail is shown in Figure 3.1.





All dimensions are in in.

**Figure 3.1. Inclined bar connection between precast barrier and deck**

This first barrier-to-deck connection was designed to be easily constructed and repaired as well as durable. At the design force corresponding to TL-4, the inclined bars were designed to remain elastic. After inserting the bars through the barrier, they were anchored into the deck using a special threaded bar sleeve hardware and grouted. With this connection approach, there is no steel hardware exposed to the environment. The inclined rods could be stainless steel to help make them more durable. Since the main connection piece would already be in place in the bridge deck, the connection detail would be relatively simple to construct. Upon impact, this barrier system was designed to fail in the inclined rod at the barrier-to-deck connection interface, which would make for an easier repair. Only the damaged barrier segments would need to be removed and replaced versus the barrier and the deck. This is because the failure in the connecting rod would minimize the damage to the bridge deck. Due to the specially made hardware used within the deck and the choice of using stainless-steel rods, this connection may not be very cost effective.

The second connection that was designed includes a U-shaped reinforcing steel bar that was inserted under the bridge overhang, through the bridge deck and into the precast barrier, and grouted. A schematic showing this detail appears in Figure 3.2.

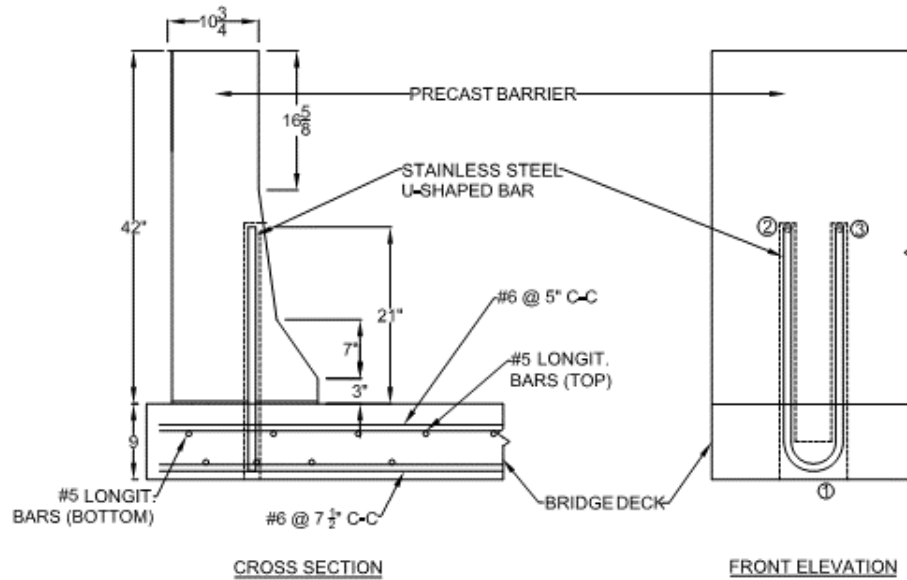


**Figure 3.2. U-bar connection between precast barrier and deck**

The second connection detail between the barrier and the bridge deck was designed based on minimizing the cost and ensuring durability. Through calculations this design was shown to resist the design load corresponding to TL-4. There was no exposed steel hardware in this connection and stainless steel was used for the U-shaped bars to help make the connection system more durable. Thanks to the use of simple steel hardware, this connection concept was considered more cost effective than the inclined bar connection. However, replacement of a barrier connected with U-bars will be more labor intensive and may require replacement of a portion of the deck. More details about grouting of the connection reinforcement and of the interface between the precast barrier and the deck are presented in the next section.

### Barrier-to-Barrier Connections

The only barrier-to-barrier connection chosen for testing included four double-headed ties between two adjacent barriers. In addition, transverse reinforcement was used to provide confinement in the direction perpendicular to the double-headed ties. A drawing of this detail is shown in Figure 3.3.

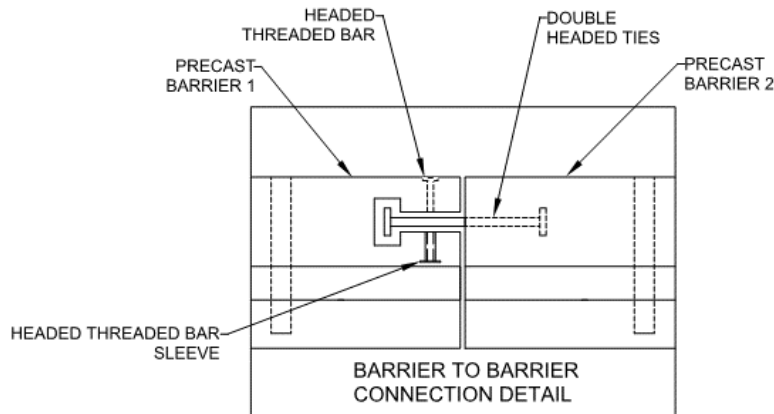


**Figure 3.3. Plan view of the barrier-to-barrier connection**

The connection between the barriers was designed to create continuity between barriers such that the load imposed on one barrier would be appropriately distributed to adjacent barriers, as would be the case in a slip form barrier. The connection regions need to be easily fabricated with the barrier, constructed, and installed. As with the other connections, this had no exposed reinforcing steel bar to affect its durability.

### **Deck Design**

The bridge deck was designed to meet the Iowa DOT standards and some of the reinforcement quantities were refined according to the expected loading conditions. The selected failure mechanism for the entire deck and barrier system was within the barrier connection reinforcing bars. To ensure this, the deck had to be able to withstand the loading applied to the barrier, and analysis of the deck reinforcement was done in SAP2000. According to Iowa DOT standards, typical AASHTO type decks use #6 reinforcing steel bar with 10-in. spacing. For this project, the main concern was the response of the barrier. To ensure that premature failure would not take place in the deck, additional deck reinforcement was added, and the corresponding strain demand was monitored. The top mat of the deck would experience the most tension during the tests. As a result, the reinforcement was adjusted to #6 bars with 5-in. spacing. The bottom mat was adjusted to #6 bars at 7.5 in. spacing. The force distribution from the application of the load to the barrier was assumed to be based on a 1:1 slope, which is consistent with the recommendation in AASHTO. This resulted in a 7-ft distribution length on the bottom of the barrier and edge of the deck and a 10.5-ft distribution length when the load was applied sufficiently away from the edge of the barrier. These values were used in the SAP2000 analyses to establish the respective moment-curvature responses. The analyzed profiles for the 7- and 10.5-ft sections are displayed in Figure 3.4 and Figure 3.5, respectively.

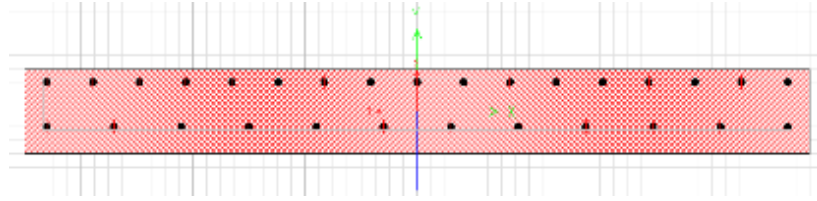


**Figure 3.4. End of bridge deck reinforcement (7-ft segment analysis)**

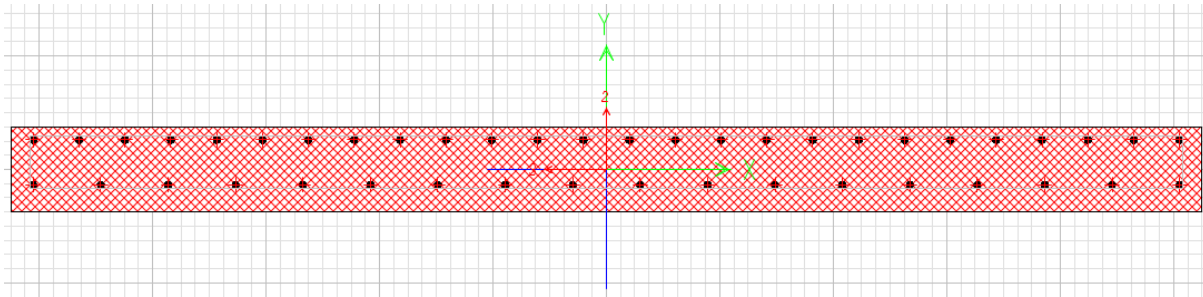


**Figure 3.5. Bridge deck reinforcement (10.5-ft segment analysis)**

Since the ends of the test barrier unit were not intended to simulate the details of the bridge ends, no additional reinforcement or modification was included.

The flexural behavior of the reinforced deck cross sections is displayed in Figure 3.6.

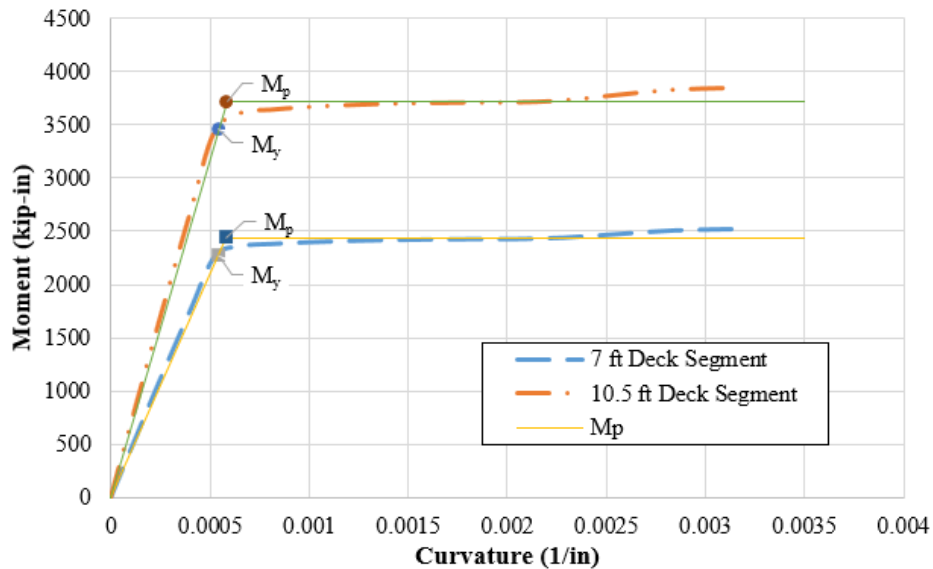


**Figure 3.6. Moment curvature responses of different deck segments**

For the 7-ft cross section, the predicted yield moment was 2282 kip-in. and the predicted plastic moment was 2437 kip-in. with an idealized yield curvature of 0.00058 1/in. The 10.5-ft section had a predicted yield moment of 3457 kip-in. and a predicted plastic moment of 3721 with a 0.00058 1/in. idealized yield curvature.

## CONSTRUCTION OF TEST UNIT

### Introduction

The testing of the concrete precast barrier rails was conducted in the Wallace W. and Julia B. Sanders Structural Laboratory at Iowa State University (ISU). Construction of the two precast barriers was completed at a precast facility and the supporting system, including the deck beams and deck, was fabricated in place in the laboratory. As previously described, two barrier-to-deck connections were tested: the inclined reinforcement connection, PBI, and the U-bar connection, PBU. Only one barrier-to-barrier connection was tested as planned. Testing was monitored by various instrumentation that included string potentiometers, linear variable differential transducers (LVDTs), strain gauges, and a three-dimensional (3D) Optotrak system with multiple displacement targets. The test unit assembly was completed with multiple materials that included special reinforcement and ultraflow grout.

### Precast Barrier Construction

The two precast barriers were built at a CoreSlab facility in Omaha, Nebraska, and delivered to the ISU laboratory. The barriers shown in Figure 4.1 were built with the standard F-shape barrier profile reinforcing, as previously shown in Figure 1.2.

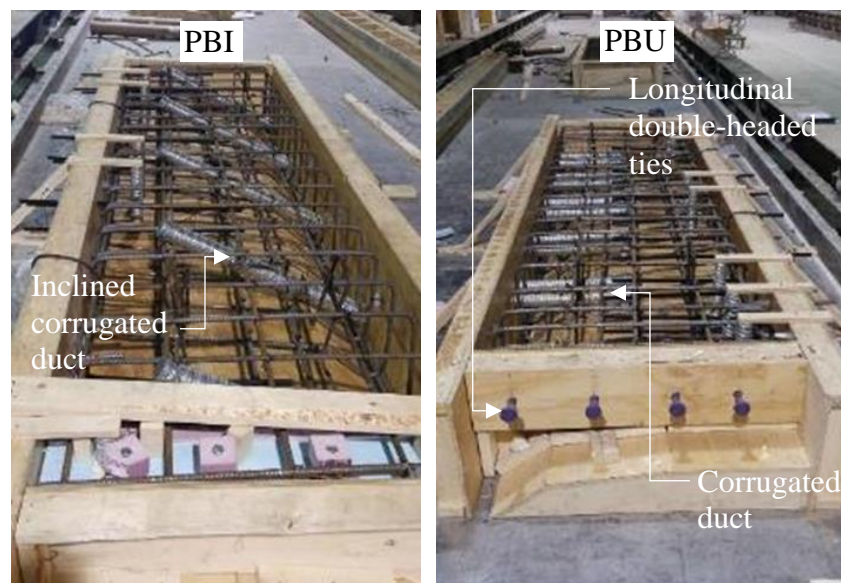


**Figure 4.1. PBI and PBU at the CoreSlab facility prior to the concrete pour**

The first precast barrier to be tested used an inclined bar connection to the bridge deck, which was designed with five #8 bars serving as the tension reinforcement at the connection interface. The inclined reinforcing bars were spaced at 30 in. as this was deemed to be the maximum spacing for practical use. To accommodate this reinforcement, the barrier was cast with 2.5-in.

diameter, inclined corrugated ducts. For this project, this barrier is known as precast barrier with inclined bars (PBI).

The second barrier included a U-shaped reinforcing steel bar connection. The U-bars are inserted from the underside of the bridge overhang, through the bridge deck, and into the precast barrier. For research purposes, one side of the barrier was designed to use #7 U-shaped bars. The other side included two bundled #5 U-shaped bars. The U-shaped barrier-to-deck connections were spaced at 24 in. As with the last connection detail, corrugated ducts are cast into the precast barrier for the U-bar placement. These ducts were kept vertical with a height of 21 in. For the #7 bars, ducts with 2-in. of inside diameter were used. For the bundled #5 U-bars, the inside diameter of the duct was increased to 2.5 in. For this project, this barrier is known as precast barrier with U-bars (PBU).

The only barrier-to-barrier connection that was chosen for testing included four double-headed ties along the barrier length. For this project, the longitudinal double-headed tie was cast into PBU. Figure 4.2 displays a photo of the longitudinal double-headed ties as used.



**Figure 4.2. Longitudinal double-headed ties used for barrier-to-barrier connection**

A receiving pocket was cast into PBI. To connect the two barrier segments, PBU is lifted and slid into the pocket on PBI. With the pocket running along the height of the barrier, there was minimal concrete near the barrier-to-barrier connection. Another set of #3 bars was added to confine the connection to the transverse direction. This detail consisted of a threaded, headed bar that was inserted into a steel, headed receiving piece as shown in Figure 4.3. The headed bars were inserted as part of the connection assembly prior to grouting.



**Figure 4.3. Transverse double-headed ties used for barrier-to-barrier connection**

The end region of the two precast barriers that are supposed to form the barrier-to-barrier connection is shown in Figure 4.4.

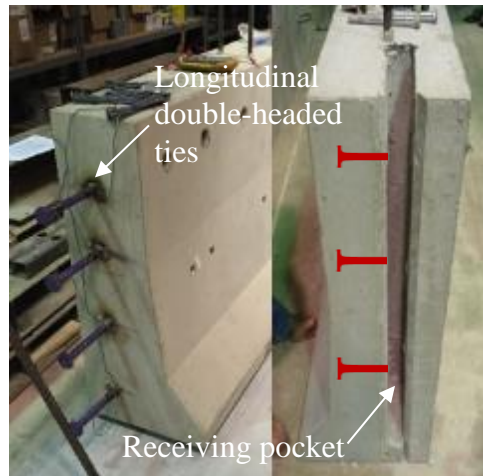


**Figure 4.4. End of precast barriers with longitudinal double-headed ties and receiving pocket**

The left side of the image is PBU and has the exposed longitudinal ties. The right side of the image shows the PBI side. This side has the receiving pocket that the longitudinal ties are slid into. The transverse ties are embedded in PBI on the right side of the image as indicated.

### **Bridge Deck Construction**

Bridge deck construction began with the bridge deck supporting beams. For this project, there were three beams beneath the deck cast to support the test specimen. Each beam had a cross-section of 12 in. (width) x 18 in. (height) and was placed to align with the tie-down holes of the laboratory strong floor. The beams were positioned 3 ft apart. Once the beams were situated and poured, the deck was fabricated on top of them with an overhang. The deck was 10 ft and 8 in. wide by 24 ft long. This allowed the deck to accommodate for an adequate length for the two 12-ft barrier segments as well as a 3.5-ft deck overhang for the barriers to be included. Figure 4.5 shows the formwork and the supporting beams.



**Figure 4.5. Bridge deck supporting beams with formwork**

As seen in this figure, the sleeves used for positioning the loading block are spaced 3 ft apart from each other in every direction.

With the bridge deck support beams in place, the deck slab was formed, and the inserts needed to establish the two barrier-to-deck connections were installed. The threaded bar sleeve used for the inclined PBI connection (Figure 4.6) was nailed to the deck formwork to keep the connection in place during the concrete pour (Figure 4.7).



**Figure 4.6. Inclined bar connection in deck**





**Figure 4.7. Connected inclined receiving end piece to the deck formwork**

As noted, the U-bars for the PBU connection were inserted from the underside of the overhang into pockets in the bridge deck. Cutouts were made, and proper blockage was established before pouring the deck concrete. The block outs of these access pockets are shown in Figure 4.8.



**Figure 4.8. Deck block outs to facilitate U-bar installation**

After the materials needed for the barrier-to-deck connections were installed, the bridge deck reinforcement was placed (Figure 4.9).



**Figure 4.9. Bridge deck reinforcement**

The bottom reinforcement mat was placed with 1-in. chairs and reinforcing ties were used at every intersection. The top reinforcement was then placed with 5-in. metal reinforcing steel bar chairs and tied at every longitudinal and transverse intersection.

Some of the deck reinforcement interfered with the barrier connection regions. On the PBI side, this reinforcement was shifted to avoid the inclined threaded bar sleeve (Figure 4.10).

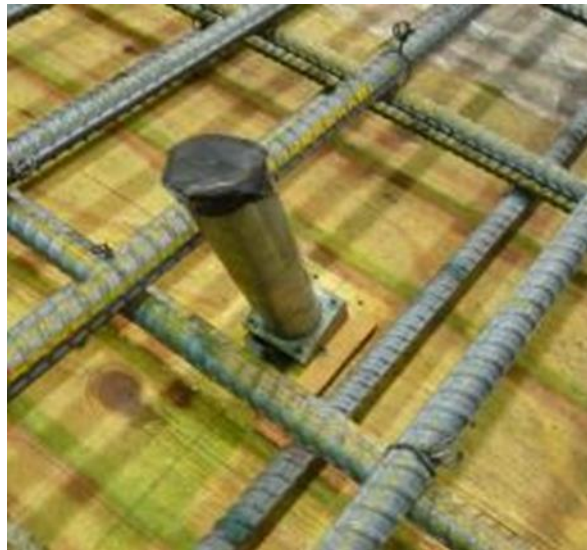


**Figure 4.10. Installed PBI connection sleeve with deck reinforcement**

On the PBU side, some of the bottom deck reinforcement interfered with the U-bar access pockets. These bars were terminated at the pocket. The top deck reinforcement that interfered

with the U-bar pockets was shifted so that at least two bars were within the U-shaped connection as seen in Figure 4.11.



**Figure 4.11. U-bar access blocks outs with terminated bottom deck steel and top deck steel positioned to be within a U-bar connection**

Following the reinforcing steel bar installation, the bridge deck concrete was poured (Figure 4.12).

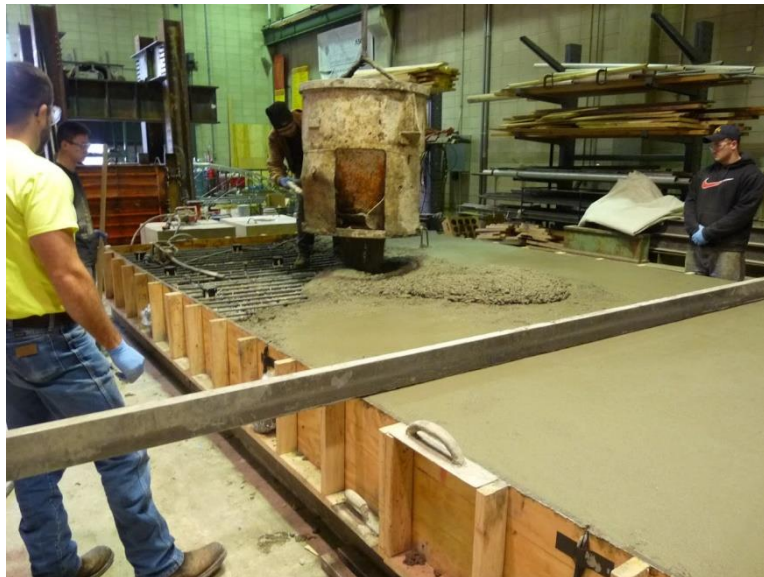


**Figure 4.12. Bridge deck concrete pour**

The deck was completed in two continuous pours. After the top of the concrete was leveled, the portion of the deck where the barriers were to be placed was finished with a wire brush to create a roughened surface.

## Assembly and Grouting

Once the deck was poured, the precast barrier was placed on the deck overhang. There were two options for connecting the inclined connection to the bridge deck. The first option was to place the barrier on the overhang deck and then insert the inclined, threaded reinforcing bars (Figure 4.13) from the backside of the barrier through the ducts, down to the deck where they are threaded into the hardware embedded in the bridge deck.



**Figure 4.13. Threaded end of inclined reinforcement**

Another option was to first connect the inclined reinforcement to the bridge deck and then lower the precast barrier onto the deck over the bars. The second option was used for this project. An image of the inclined bars connected to the bridge deck before the installation of the precast barrier is shown in Figure 4.14.



**Figure 4.14. Inclined reinforcing bars connected to bridge deck before placement of precast barrier**

Once PBI was in place, PBU was installed. PBU was lifted and lowered so that the exposed longitudinal double-headed ties slid into the receiving pocket cast into PBI. An overhead look at the barrier-to-barrier connection is shown in Figure 4.15.



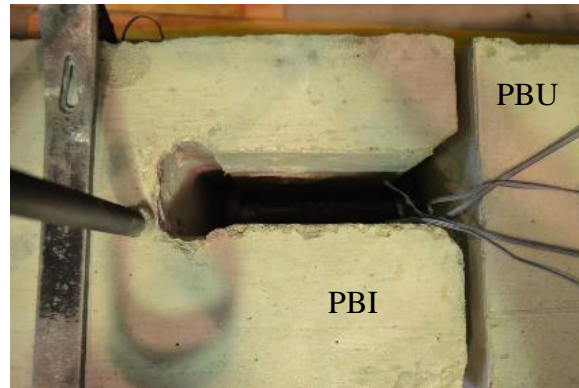


**Figure 4.15. Barrier-to-barrier connection**

With the two barriers in place on the deck. The final piece of the transverse barrier-to-barrier connection was installed. The threaded, headed transverse reinforcement was inserted into the pockets cast into the back of PBI and threaded into the receiving end cast into the front part of PBI. The pockets used for this installation are shown in Figure 4.16



**Figure 4.16. Pockets used to install transverse barrier-to-barrier connection**

During the assembly of the PBU's deck connection, proper cover for the U-shaped reinforcing steel bars was ensured by using two varying forms of reinforcing bar chairs. For the two bundled #5 bars, 1-in. clip-in chairs were used. This is shown in Figure 4.17.



**Figure 4.17. Reinforcing steel bar chairs for #5 bars**

For the #7 bars, a spacer wheel was used to obtain the 1-in. cover. This is demonstrated in Figure 4.18.



**Figure 4.18. Reinforcing steel bar chairs for #7 bars**

Then the U-bars were inserted (Figure 4.19), and the pockets were sealed for grouting (Figure 4.20).



**Figure 4.19. Insertion of U-bars**



**Figure 4.20. Sealed U-bar pocket for grouting**

After the bars were in place, the grout pad between the overhang and the barrier was poured. In this case, the grout pad had a depth of  $\frac{3}{4}$  in. Also, a foam pad was placed under the barrier  $\frac{3}{4}$  in. from the backside to limit the damage to the barrier during the push test, shown in Figure 4.21.



**Figure 4.21. Foam added to grout pad to minimize damage cover concrete**

The inclined corrugated ducts for the inclined reinforcing connection in PBI, also shown in Figure 4.21, were grouted as well. To improve the aesthetics, the exposed bars can be cut flush with the backside of the barrier.

The corrugated tubes in PBU were grouted through the inlet until grout filled the U-bar pocket and began to outflow through the outlet hole on the front face of the barrier (Figure 4.22).



**Figure 4.22. Grouting of U-bar pockets**

The finished underside of the U-bar pocket is shown in Figure 4.23.



**Figure 4.23. Finished U-bar grout pocket**

The completed barrier installation is shown in Figure 4.24.



**Figure 4.24. Completed barrier installation**



## Instrumentation

To measure the longitudinal strain in the steel reinforcing bars at critical locations, strain gauges were used. These gauges were attached to the deck reinforcing steel bar, the precast barrier reinforcing steel bar, and selected steel reinforcement used in the connections. Figures 4.25 and 4.26 show the location of these strain gauges. Since not all gauges were connected simultaneously to the data acquisition system (DAS), only the strain gauges within the 45-degree slope from the load application region were primarily monitored during each test.

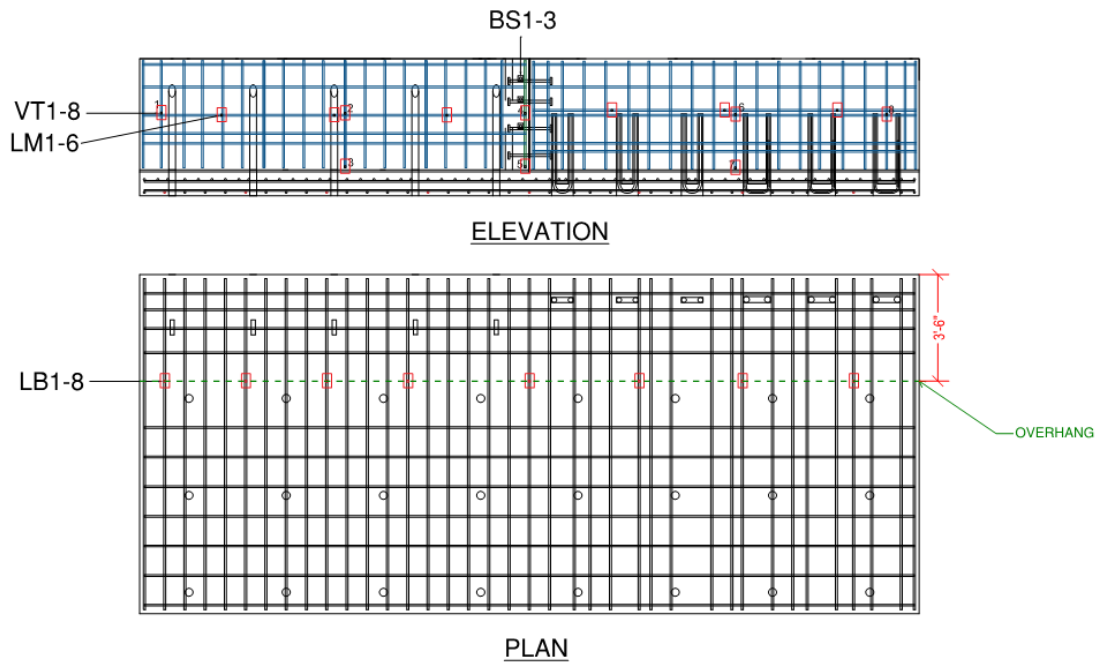


**Figure 4.25. Location of strain gauges in precast barrier reinforcement and bottom deck reinforcement**

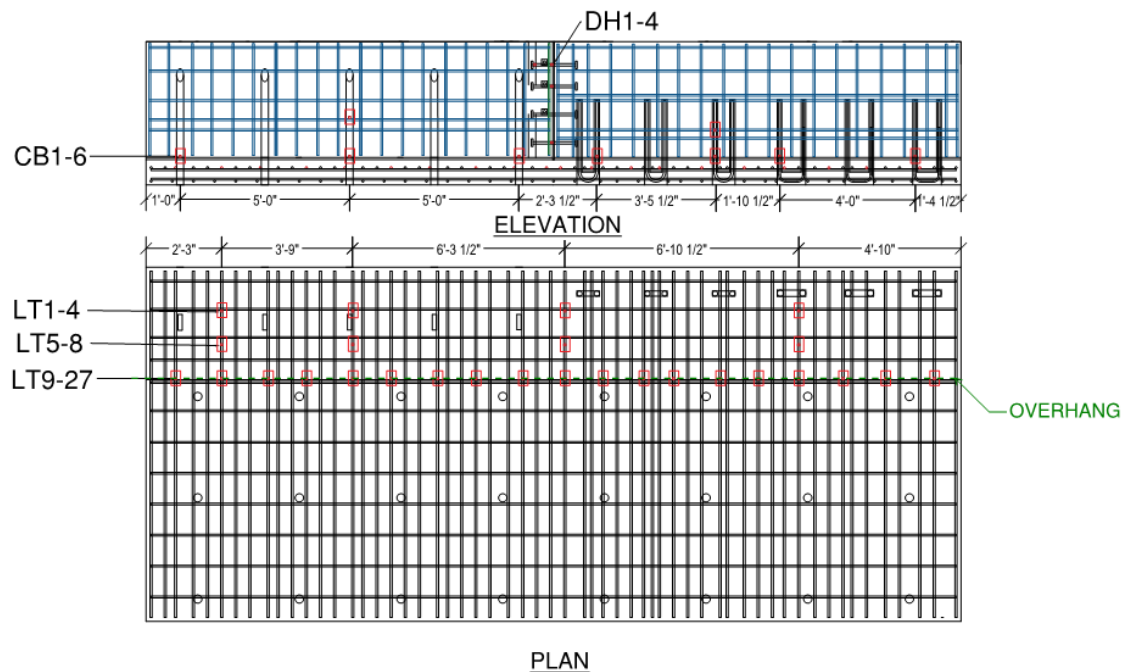
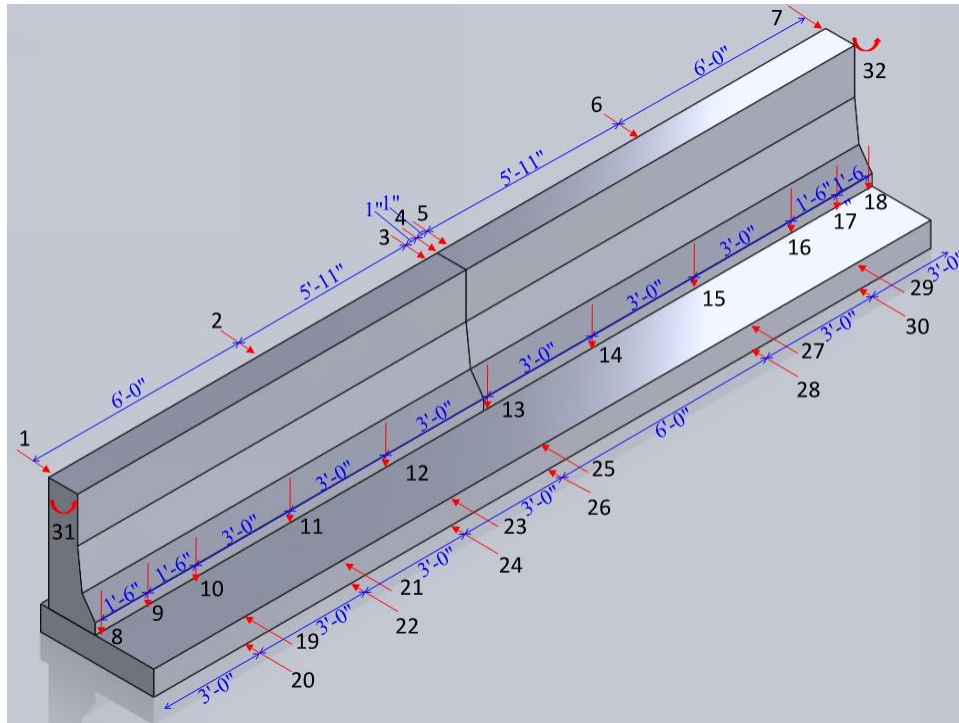


**Figure 4.26. Location of strain gauges in barrier connection reinforcement and top deck reinforcement**

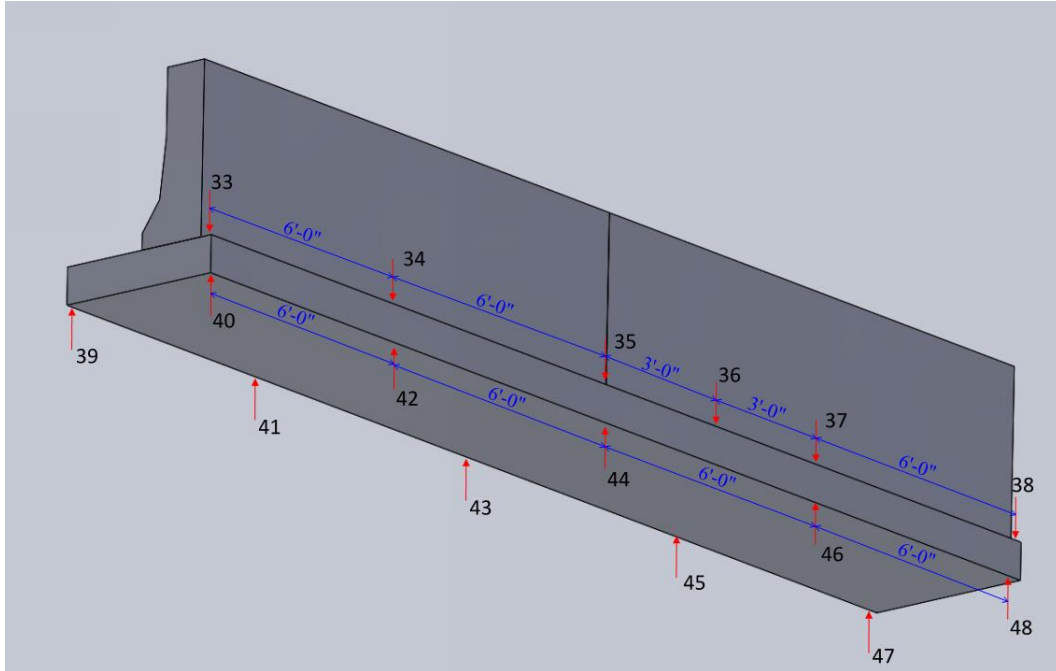
Figure 4.25 displays the locations of the strain gauges on the vertical barrier reinforcing (VT1-8), longitudinal barrier reinforcing (LM1-6), the transverse barrier-to-barrier bar splice (BS1-3), and the bottom deck reinforcing bars (LB1-8). The vertical barrier reinforcement strain gauges were placed in an attempt to coincide with the varying load application locations. VT1 is located within 1 ft of the end of PBI at mid-height of the barrier. VT2 and VT3 are near the center of PBI; VT2 at mid-height and VT3 near the barrier-deck interface. VT4 and VT5 are placed at the barrier-to-barrier interface; VT4 at mid-height of the barriers, and VT5 near the barrier-deck interface. VT6 and VT7 are near the center of PBU; VT6 at mid-height and VT7 near the barrier-deck interface. VT8 is located within the last foot of PBU. The strain gauges placed on the longitudinal reinforcement (LM1-6) were placed at 3- to 4-ft spacing. The gauges placed on the bottom deck reinforcement (LB1-8) were placed every four to five bars. There were three gauges placed on the three transverse bar splices (BS1-3). Gauges were placed near the center of the connection.

Figure 4.26 displays the locations of the strain gauges on the barrier-to-deck connections (CB1-6), the transverse double-headed bar between barriers (DH1-4), and the top deck reinforcing bars (LT1-27). The strain gauges were applied to the barrier-to-deck connections near where the load applications would occur. The dimensions to each gauge can be seen in Figure 4.26. There were four strain gauges placed on the double-headed transverse bars. DH1 was applied to the PBI side of the bar. DH2-DH4 were placed on the center of the bar at the barrier-to-barrier interface. There were three rows of gauges on the top deck reinforcing bars. Dimensions to LT1-8 are shown in Figure 4.26. LT9-LT27 were located at the beginning of the bridge deck overhang, roughly 42 in. from the edge of the deck slab. Gauges were attached every three to four reinforcing bars.

In order to measure the movements of the barrier and bridge deck overhang during testing, string potentiometers and LVDTs were used. String potentiometers were placed behind the barrier and underneath the bridge deck overhang to measure displacements. LVDTs were placed on the front and backside of the barrier to monitor the interface between the precast barrier and the deck. Additional LVDTs were placed on top of the bridge deck and underneath to characterize the critical curvature of the overhang. Figures 4.27 and 4.28 show the locations of all the devices used to measure the movements of the unit while testing. A rotational device was also attached to the outer face of the barriers to measure the rotation of the test unit during loading.



**Figure 4.27. Location of string pots and LVDTs on front side of testing unit**



**Figure 4.28. Location of string pots and LVDTs on backside of testing unit**

## Load Application

As described previously, a number of quasi-static tests were planned to be conducted on the precast barrier using a hydraulic actuator. There were six different load application areas identified, which required moving the location of the loading block and the actuator. The six load application areas are displayed in Figure 4.29.

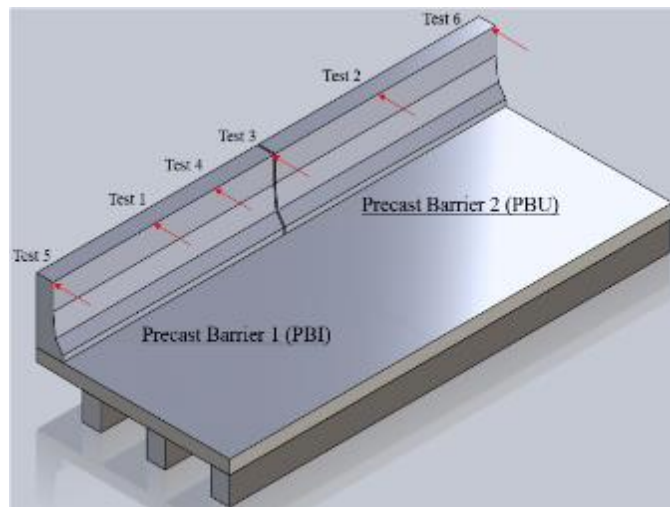


**Figure 4.29. 3D model of identifying the testing sequence and load application areas**

Each location had a differing testing purpose. The purpose of Test 1 was to examine the connection between the barrier and the bridge deck using an inclined rod before establishing the barrier-to-barrier connection. Similarly, Test 2 was conducted to inspect the barrier connection involving U-bars independently. After the connection between the two barriers was completed with additional reinforcement and grout, Test 3 was done to examine the connection between barriers. Test 4 was located slightly off to the side of the barrier-to-barrier connection on the PBI side to observe the force distribution across the barrier-to-barrier connection. The last two tests, Test 5 and Test 6, were located on the free ends of PBI and PBU. The purpose of these tests was to evaluate the connection performance at the free end of the barrier segments. Since neither the deck nor the connection reinforcement was strengthened to simulate the end condition of a bridge, these tests are required to provide 50 percent of the design strength.

For all tests, the actuator was made to react against a loading block that was rigidly secured to the strong floor of the laboratory through the bridge deck. The load block was positioned on the bridge deck away from deck overhang. For each test, the actuator was positioned such that the load could be applied at the top of the barrier, creating the maximum moment demand at the barrier-to-deck interface. With Test Level 4, the load is to be distributed over 3.5 ft, which was accomplished using an H-beam attached to the top of the barrier as shown in Figure 4.30.

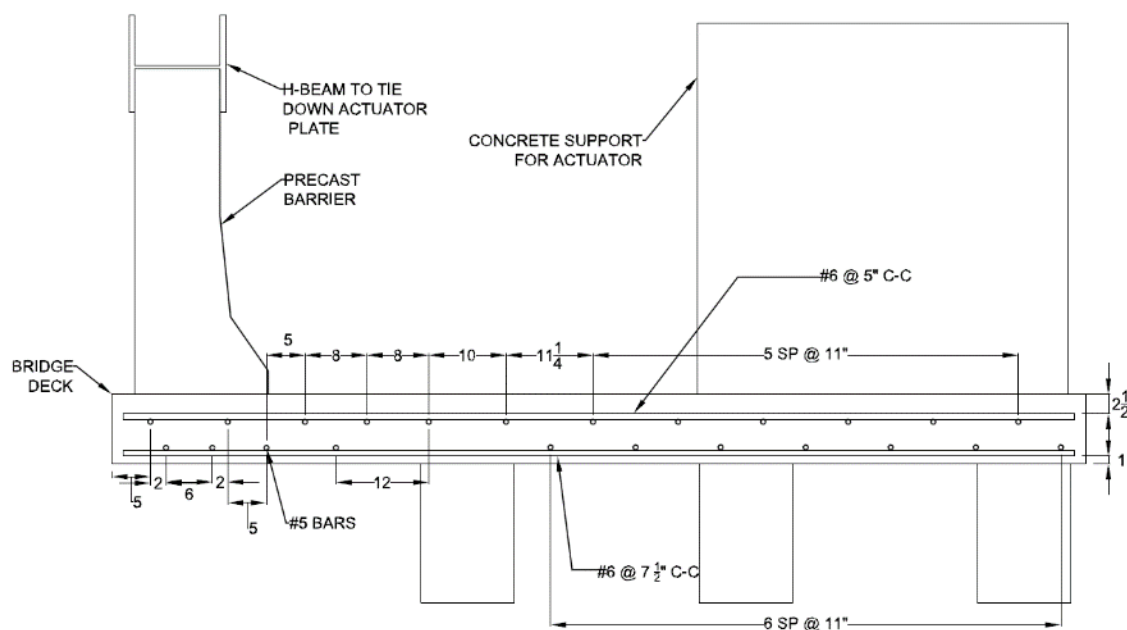


**Figure 4.30. Laboratory test set-up**

The loading block was anchored to the laboratory floor using post-tensioning applied vertically at four locations. The actual test set up for used for Test 1 is shown in Figure 4.31.

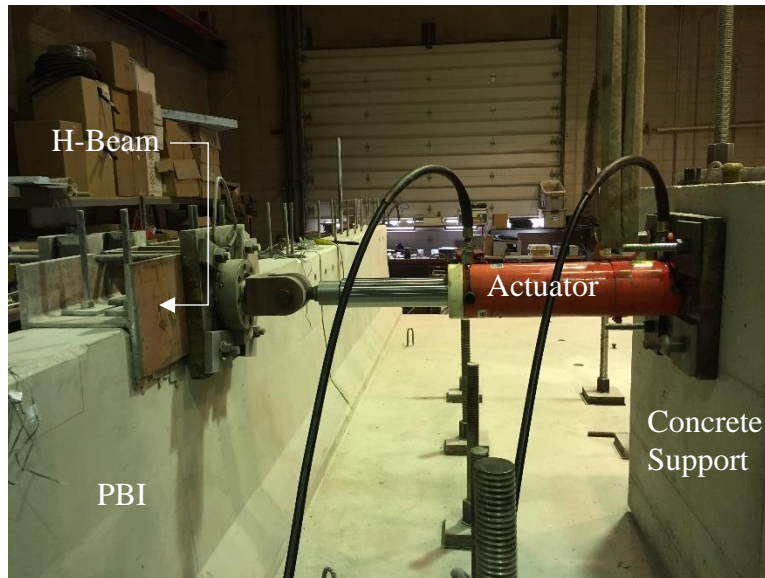


**Figure 4.31. Test set-up for Test 1**

## **Material Properties**

The concrete used for the bridge deck construction and the loading block had a specified concrete strength of 4 ksi. Both the bridge deck and the loading block were poured in two pours. Concrete cylinders were taken during the pours to establish the actual concrete strength. After seven days, the concrete had an average strength of 5.4 ksi for the two pours. The concrete continued to grow in strength until the day of the first test when the strength was measured to be 6.1 ksi.

The precast barriers were poured with high early strength 5 ksi concrete. The barriers were poured in a controlled setting at a precast plant. Concrete cylinders were included from the precast supplier. After 28 days, the barriers had reached an average strength of 7.4 ksi.

Grout used for the project was UltraFlow grout supplied by CTS Cement Manufacturing Corporation. This grout was used because it had a fluid consistency that allowed for an extended working time, but then gained strength quickly. The grout, which had a specified strength of 4 ksi strength after 8 hours, was used in the interface between the precast barriers and the bridge deck, as well as to fill each barrier-to-deck connection pocket. For PBI, the grout was poured from the back of the barrier into the corrugated tubes using a grout tube. For PBU, the grout was pumped into the pockets from the front face of the barrier. Grout was pumped from one side of the U-bar until it was seen flowing out of the second vent on the other side of the same U-bar. During the pour, grout cubes were cast to be used for strength testing. After 24 hours, the interface grout had an average strength of 7.3 ksi. After 7 days, the grout strength increased to 8.2 ksi. The connection grout had a strength of 7.7 ksi after 24 hours and a strength of 8.9 ksi after 7 days.

The reinforcement used in the bridge deck and precast barriers had a specified yield strength of 60 ksi. Testing of the deck reinforcing bar strength led to the measured yield strength of 72.0 ksi and the ultimate strength of 104.2 ksi. The reinforcing steel bar used for the U-bar connection in PBU was stainless steel with a specified yield strength of 75 ksi. The #5 reinforcing steel used for PBU had a measured yield strength of 70.2 ksi and ultimate strength of 114.3 ksi. The #7 stainless steel reinforcing steel used for PBU had a measured yield strength of 70.2 ksi and ultimate strength of 112.1 ksi. The steel used for the inclined connection in PBI was Grade 60 reinforcing steel. Testing of this #8 reinforcement produced a yield strength of 67.5 ksi and ultimate strength of 86.3 ksi.

## TESTING AND RESULTS

### Introduction

Since the precast barriers were designed for TL 4, they were required to sustain a maximum lateral load of 54 kips that is applied uniformly over 3.5 ft. During testing, the load was applied incrementally up to 54 kips. A load step of 6 kips was used and the test was paused at the end of each load step to observe any damage to the test unit. As planned, six different tests were conducted and a summary video of the tests is available at <https://youtu.be/up6sMEeqfaU>. For the first two tests performed, the barrier-to-barrier connection was left ungrouted and disconnected. Barrier PBI with an inclined bar connection was tested first. PBU with the U-bar connection was tested next before the barrier-to-barrier connection was established. This was accomplished by threading the transverse bar splicers and grouting the connection region. Once the connection between the two barrier segments was established, the third test was conducted directly at the center of the two barriers. For the fourth test, the load was applied 1.75 ft from the barrier-to-barrier connection. It was tested on the PBI side of the test specimen to ensure that the selected failure mechanism was achieved. The last two experiments included load application to the free ends of both PBI and PBU, where the load resistance was expected to be only 50 percent of those from Tests 1 and 2. The chart in Figure 5.1 illustrates the top of the barrier's deflection throughout the course of the first four tests. Even though the actuator was moved for each test, a single reference point was used at the center of the entire test specimen and was used to create the continuous plot to demonstrate the performance during different tests.

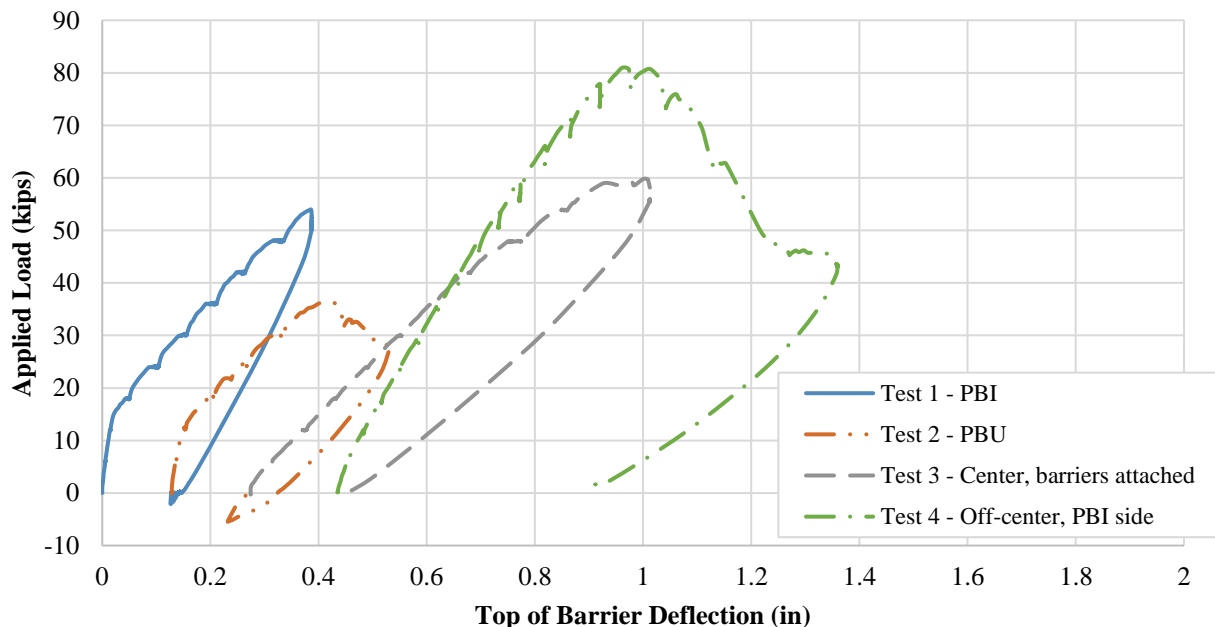


**Figure 5.1. Continuous test plot of top of barrier deflection for Tests 1–4**

PBI was subjected to the desired target force of 54 kips during Test 1. During Test 2, PBU experienced premature failure and thus the test was terminated after applying 36 kips. Test 3,



conducted at the center barrier-to-barrier connection, was tested to the desired target force of 54 kips, followed by an additional load step of 6 kips to further evaluate the connection performance. In order to avoid any more damage occurring to PBU during Test 4, which was conducted on the PBI side of the barrier-to-barrier connection, a brace beam was added to the test unit to limit the deflection of PBU (Figure 5.2). This explains the increased stiffness seen in Test 4 in Figure 5.1.



**Figure 5.2. Brace beam**

The top of barrier deflection observed during Tests 5 and 6 is displayed in Figure 5.3.

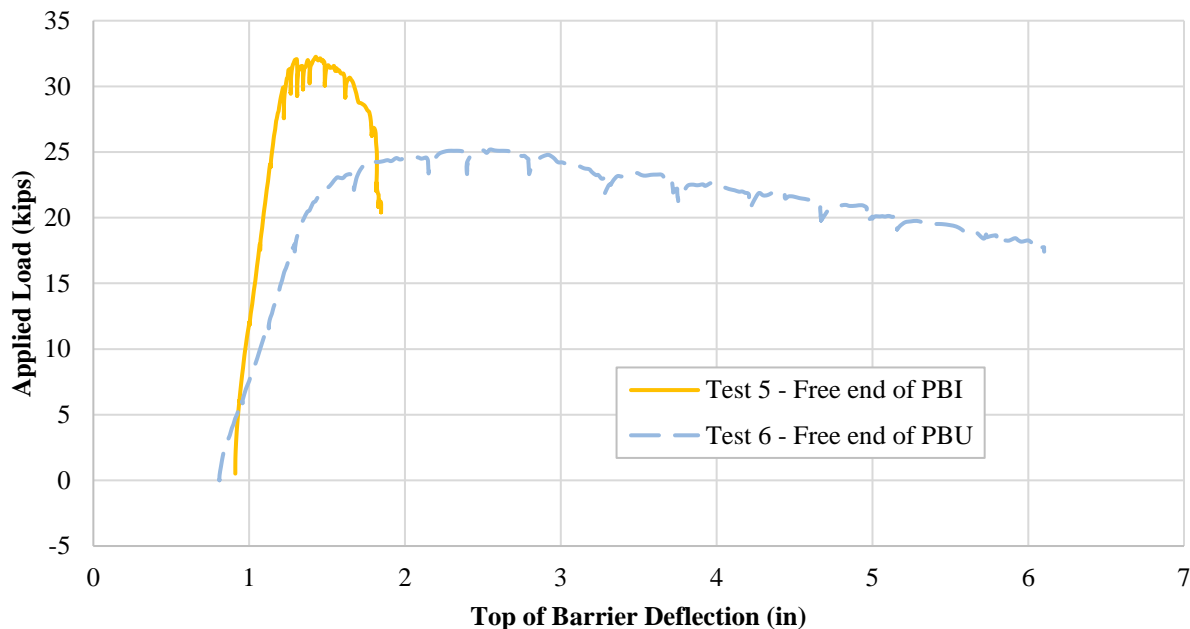


**Figure 5.3. Top of barrier deflection for Tests 5 and 6**

Test 5 was conducted on the free end of PBI in the push direction and was taken to failure. The brace beam was attached during Test 5. Test 6 was conducted on the free end of PBU in the push

direction and was taken to failure. The brace beam was disconnected during Test 6. In both tests, the barriers were pushed to deflect the extent of the hydraulic actuator used to apply the force. They were also pulled in the opposite direction to observe the damage. In comparison to Tests 1 and 2, lower resisting forces were obtained during Test 5 and 6. This is because the barrier ends were not designed to simulate the bridge end condition, producing 50 percent of the resistance at the barrier ends of the test unit rather than away from them.

### **Test 1 Observations: PBI Middle**

The loading block and actuator were set up to apply the load at the center of PBI at the top of the barrier over 3.5 ft length. The first two load increments produced no visible cracks on the test unit. The deck began to crack as the applied load approached 18 kips. The initial flexural cracks were noticed on the bridge deck overhang, as seen in Figure 5.4; three somewhat uniformly spaced flexural cracks formed on the deck overhang and they were visible along the entire length of PBI. The lateral deflection at the top of the barrier was 0.105 in. after applying 18 kips.



**Figure 5.4. Test 1: Formation of flexural cracks on the deck overhang**

As the load was increased, the flexural cracks extended along the overhang and over the side of the bridge deck. At 24 kips, cracks also began to develop along the grout pad that was placed between the barrier and the top of the deck. At 24 kips, the barrier deflection reached 0.215 in. When the load was increased to 30 kips, there were only minor crack extensions on the deck and on the side of the bridge deck. The measured deflection was 0.317 in. At 36 kips the cracks on the deck extended over to the other side where PBU was located. There was no crack extension on the side of the bridge deck, but a new crack developed behind PBU near the barrier-to-barrier interface. This crack was due to testing the barriers individually without connecting the two. At this point, lateral deflection of the barrier at the top was 0.426 in. The load was then increased to 42 kips, which led to small deck crack extensions and crack widening. The deflection corresponding to the 42-kip load was 0.536 in. It was not until the load reached 48 kips that diagonal, hairline cracks began to develop on the barrier near the barrier-to-barrier interface (Figure 5.5), at which point the deflection was 0.67 in.



**Figure 5.5. Test 1 (PBI middle) barrier cracks**

Finally, the load was increased to the full 54 kips. The crack on the back of the deck behind PBU widened and the cracks on the side of the deck had small extensions. No new cracks were seen on the barrier. The deflection of PBI at this point was 0.81 in., the majority of which was due to the deck rotation and the concentrated crack developed at the bottom of the barrier along the grout interface.

After the loading was complete, the crack widths were measured. The thickest cracks appeared on the backside of the bridge deck behind PBU (Figure 5.6).

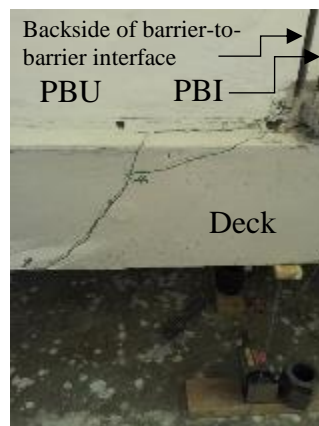


**Figure 5.6. Formation of crack on backside of test unit during Test 1**

The maximum width of this crack was 0.083 in. The widest crack measured on the bridge deck was 0.02 in. The cracks that developed within the grout between the deck and the barrier on the front side of the barrier reached 0.03 in. On the side of the deck, the maximum crack width was about 0.007 in.

Once all the testing and measuring was complete, PBI was unloaded. At zero load, PBI exhibited a residual displacement of 0.27 in. A small load was applied in the opposite direction and unloaded, but the residual displacement remained unchanged. No new cracks were seen during the pull direction loading. At this point, the test was terminated.

## Test 1 Results: PBI Middle

During testing, string potentiometers, DCDTs, LED sensors, and strain gauges were used to record data and measurements. A string pot was placed behind the barrier along the direction of the load application to measure the lateral deflection of PBI. This deflection was plotted against the applied load and can be seen in Figure 5.7, where the push direction of loading and displacements was taken as positive.

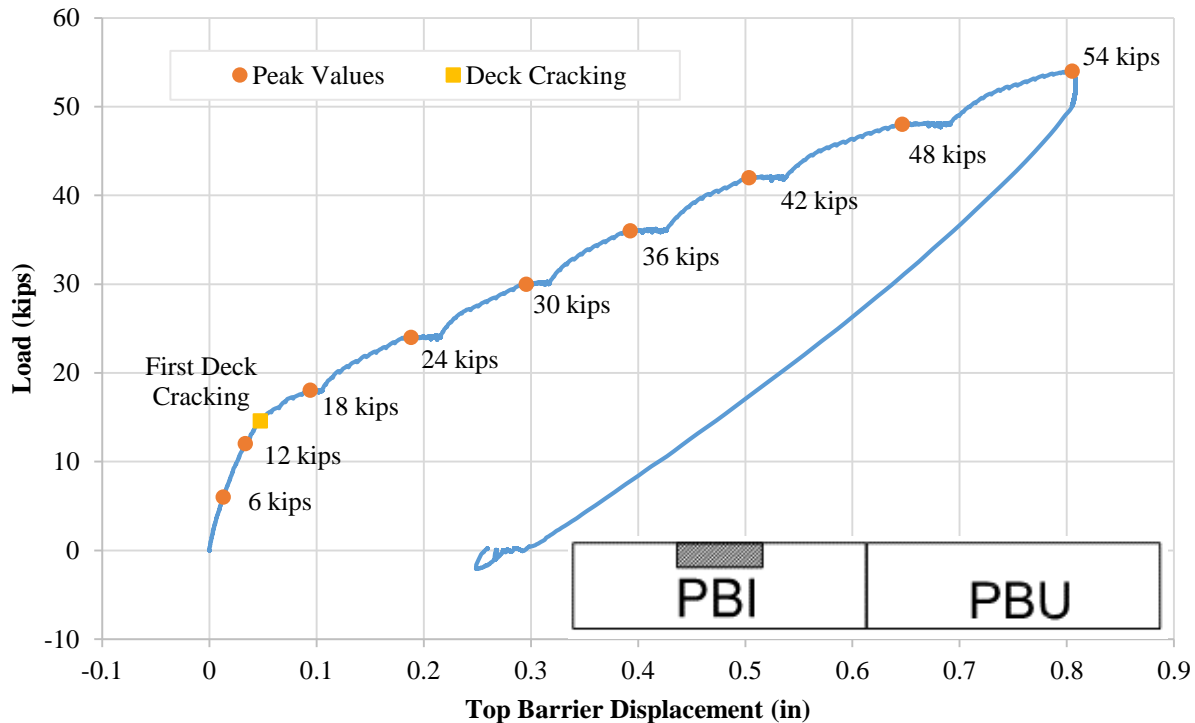


**Figure 5.7. Force displacement for Test 1 – PBI**

Within this figure, the testing location is also displayed. The barrier location denoted as zero is the center of the entire test specimen where the two barrier segments were eventually connected. At 14.6 kips the stiffness of the system was reduced, which corresponded with the formation of first cracks on the deck. (This is also shown in Figure 5.7.) Once the deck experienced cracking, the response followed a path reflecting the influence of cracked stiffness of the system and the deflection increased steadily with each load increment. There was no indication of yielding of the reinforcement. This is consistent with the design in that the barriers remained elastic for the design load of 54 kips.

Behind the barrier, along with the string potentiometers measuring the barrier deflection, were two other string potentiometers. They were placed 6 ft away from the center of the load application on both ends of the barrier. In Figure 5.8, the deflection of the entire length of PBI at each load increment is shown.

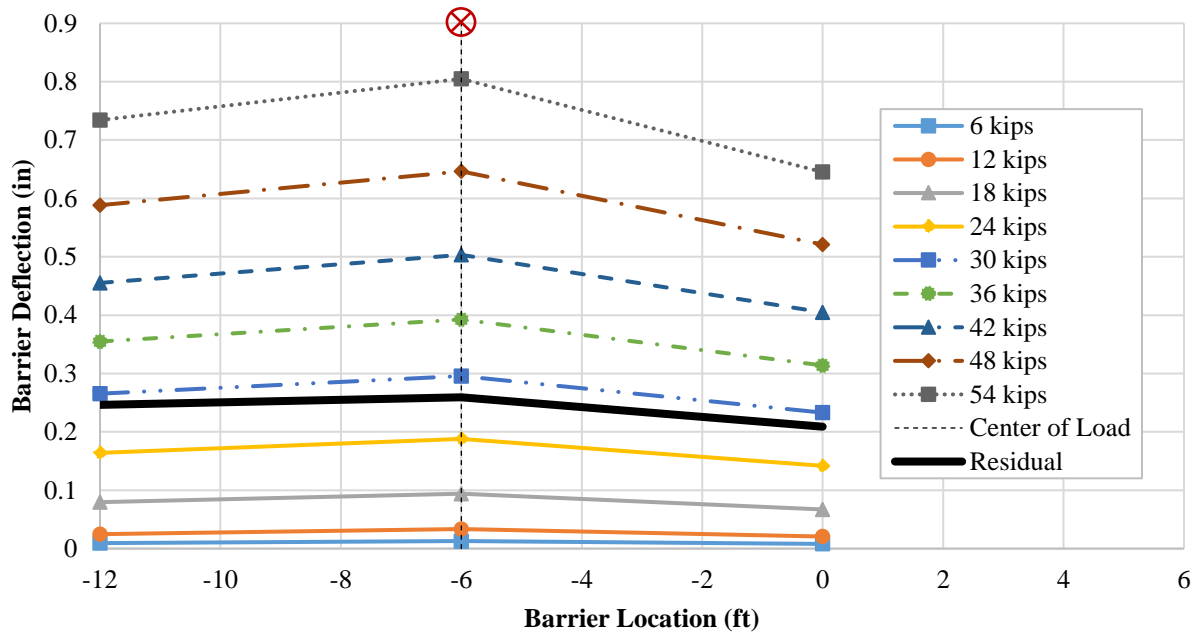


**Figure 5.8. Top barrier deflection profiles of PBI during Test 1**

Each end of the barrier experienced a similar deflection value while the center of the barrier deflected the most. The left end of PBI experienced a small increase in deflection versus the right end. This was due the deck being terminated below the left end whereas it was continuous below right end of PBI. As previously noted, after testing was complete, the barrier had a residual deflection of approximately 0.27 in.

During testing, the strains on the inclined reinforcing bars were also recorded. Strain gauges were placed on three of the five bars in the barrier. The bars on each end of the barrier and the bar in line with the center of the load were instrumented. Shown in Figure 5.9 are the profiles for the strains measured at the barrier-to-deck interface.

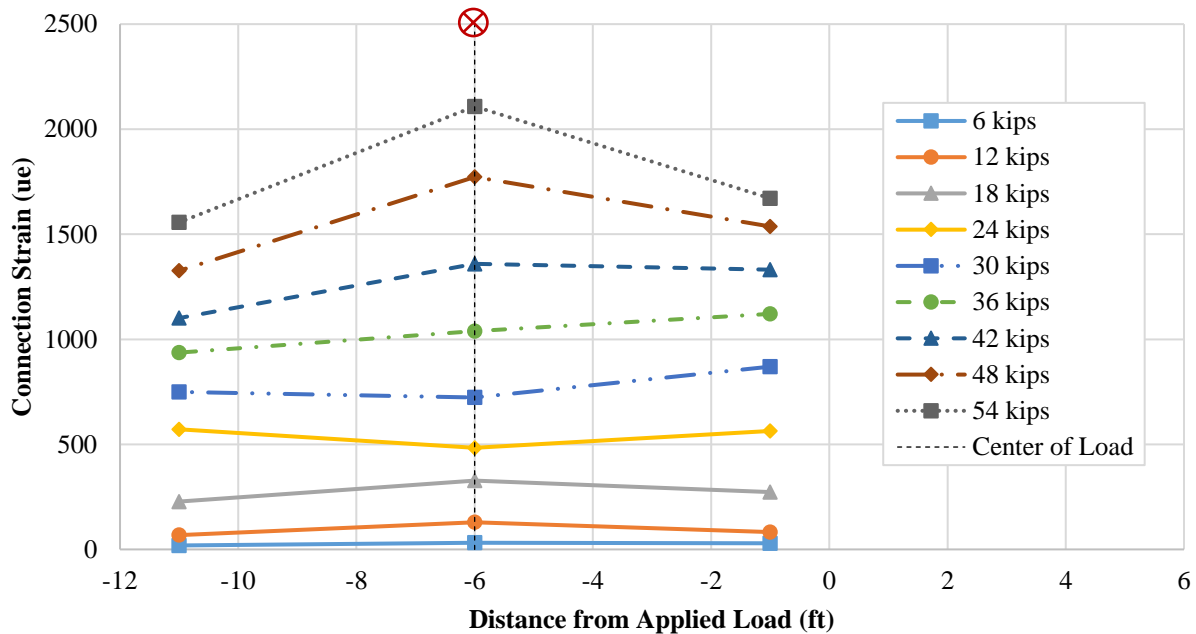


**Figure 5.9. Strain profiles of the inclined reinforcement barrier connection bars at the deck interface during Test 1**

As expected, the inclined connection reinforcement in line with the center of the load experienced the most strain and stayed just below yield when the maximum load was applied. Just before the load increment of 24 kips, it was noted that the first crack was seen along the length of the grout pad beneath the barrier. Figure 5.8 indicates that the cracking was initiated as the load was increased to 18 kips. From this point onward, strain demand on the connection reinforcing steel bar continued to increase. Both inclined reinforcement reinforcing steel bars near the ends of the barrier segment had similar strain values. On average, these strains were about 80 percent of that recorded at the center of the barrier at the design load. These inclined reinforcement bars were not expected to participate in resisting the moment according to AASHTO's expected force distribution of one-to-one slope from the load application (Figure 2.2). The deck reinforcement strain profiles are shown in Figure 5.10. The deck reinforcement in the free end of the PBI test unit experienced larger strain values than the restrained end of PBI.

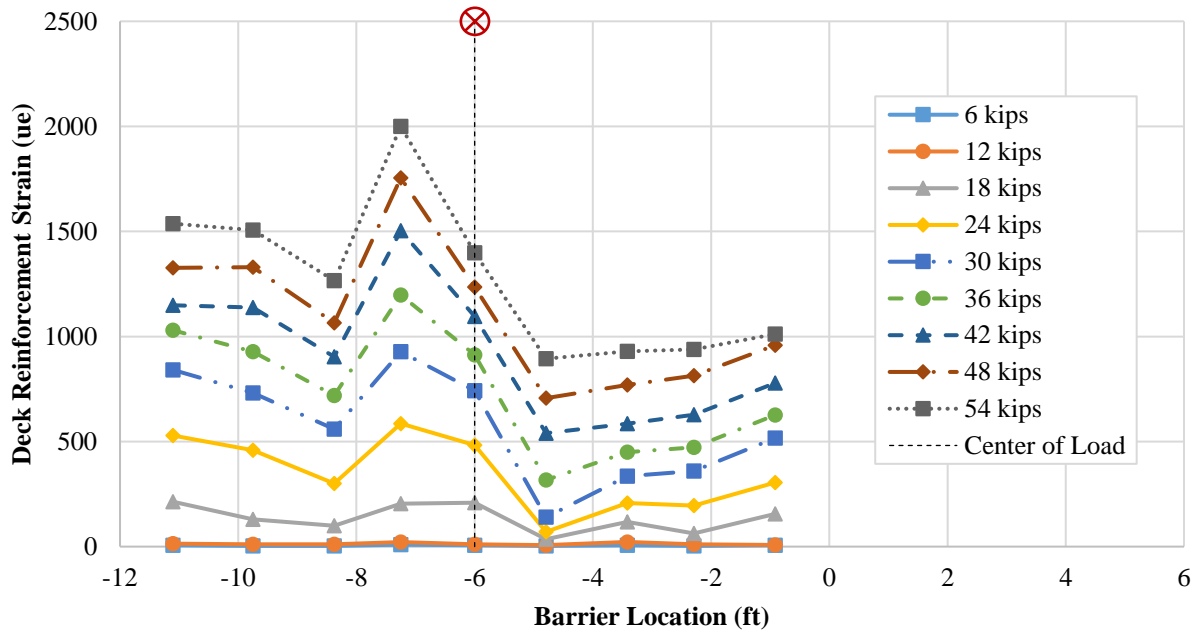


**Figure 5.10. Strain profiles of the deck reinforcement at the front barrier interface during Test 1**

The measured barrier displacement at the top, which reached a maximum value of 0.81 in. during Test 1, included the flexural deflection of the barrier at the deck interface and those due to the rotation of the barrier at the deck interface and the barrier deflection resulting from the rotation that the deck overhang experienced. As shown in Figure 5.11, the barrier's flexural deflection was only about 3.5 percent of the total deflection at 0.028 in. of the 0.81 in., and the deflection of the barrier due to formation of a crack at the barrier-to-deck interface accounted for 17.3 percent at 0.140 in.

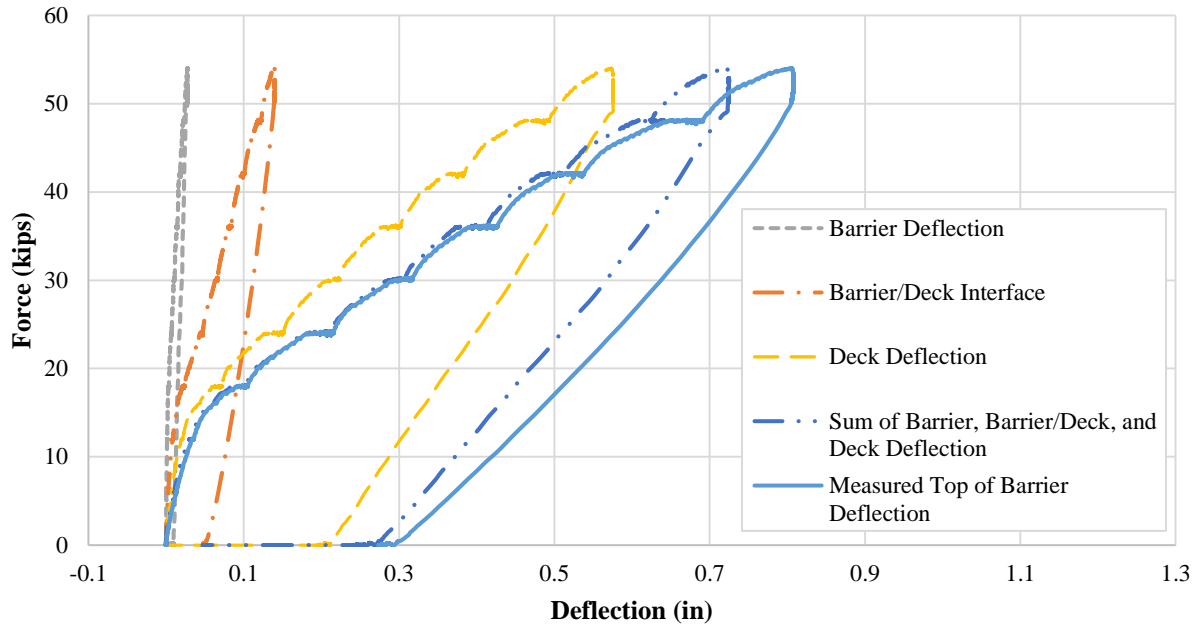


**Figure 5.11. Components of the measured PBI deflections**

This implies that the majority of the measured barrier deflection was largely due to the rotation of the deck. The deformation of the deck was somewhat amplified by a large deck crack that developed on the backside of the deck behind the PBI-PBU connection region (Figure 5.6). This crack developed because during Test 1, the barriers were not connected, and therefore not engaging PBU or the portion of the deck supporting PBU. This crack was the result of testing PBI in an isolated manner and the same results should not be expected when the barriers are connected together.

### **Test 2 Observations: PBU Middle**

The second test was conducted on PBU with the U-bar connections. The loading block and actuator were repositioned to apply loads in the center of PBU at a height of 3.5 ft above the deck. The purpose of this test was to examine the U-bar connection between the precast barrier and the bridge deck. It was planned to apply the loading up to 54 kips in 6-kip increments as completed for PBI. After PBU was loaded to 36 kips, it failed to sustain any further load without experiencing significant deflection and therefore the test unit was unloaded at this point.

The first three intervals, up to 18 kips, performed very similarly to the response of PBI in Test 1. New deck cracking began around 18 kips. At this point, the barrier was deflected 0.164 in. At 24 kips, a crack became visible along the entire length of the grout pad between the bottom of the barrier and the top of the bridge deck (Figure 5.12).





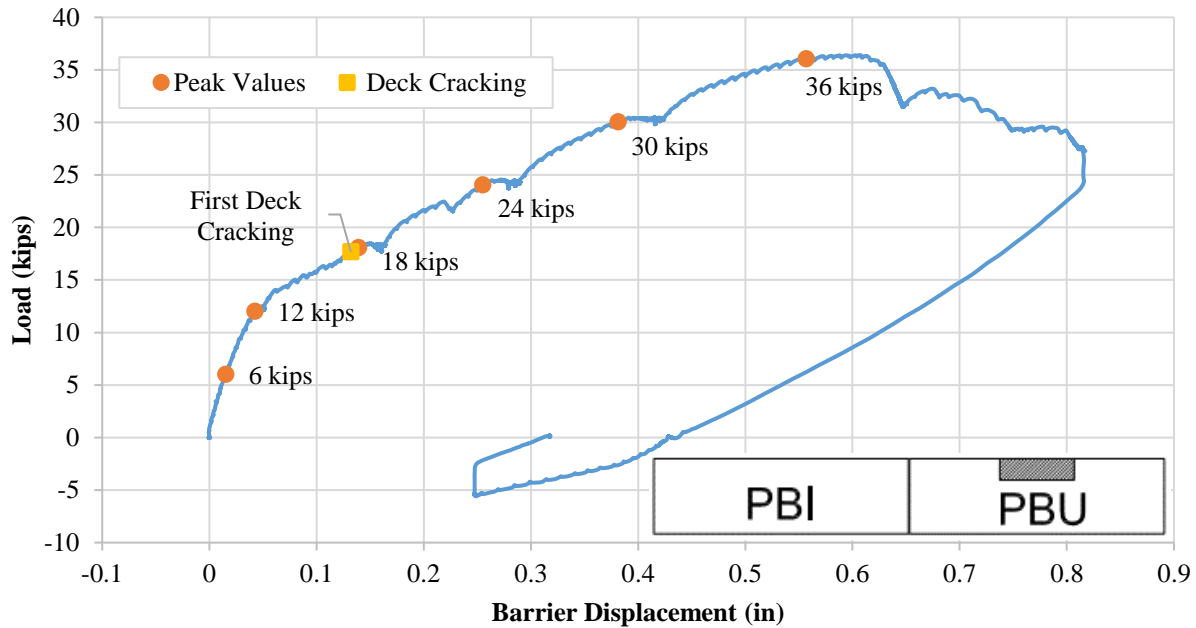
**Figure 5.12. Crack at the barrier-to-deck interface in PBU during Test 2**

The existing cracks continued to widen up until about 36 kips. Some softening in the system was observed when the load was about 36 kips and the barrier began to experience large displacements. The test was paused and unloaded after the barrier deflection reached 0.8 in.

After unloading from 36 kips, the barrier was subjected to 4 kips in the pull direction in an attempt to reposition the barrier to the residual displacement obtained from PBI. The final resting deflection of PBU after the pull direction loading and unloading was complete was 0.3 in.

#### **Test 2 Results: PBU Middle**

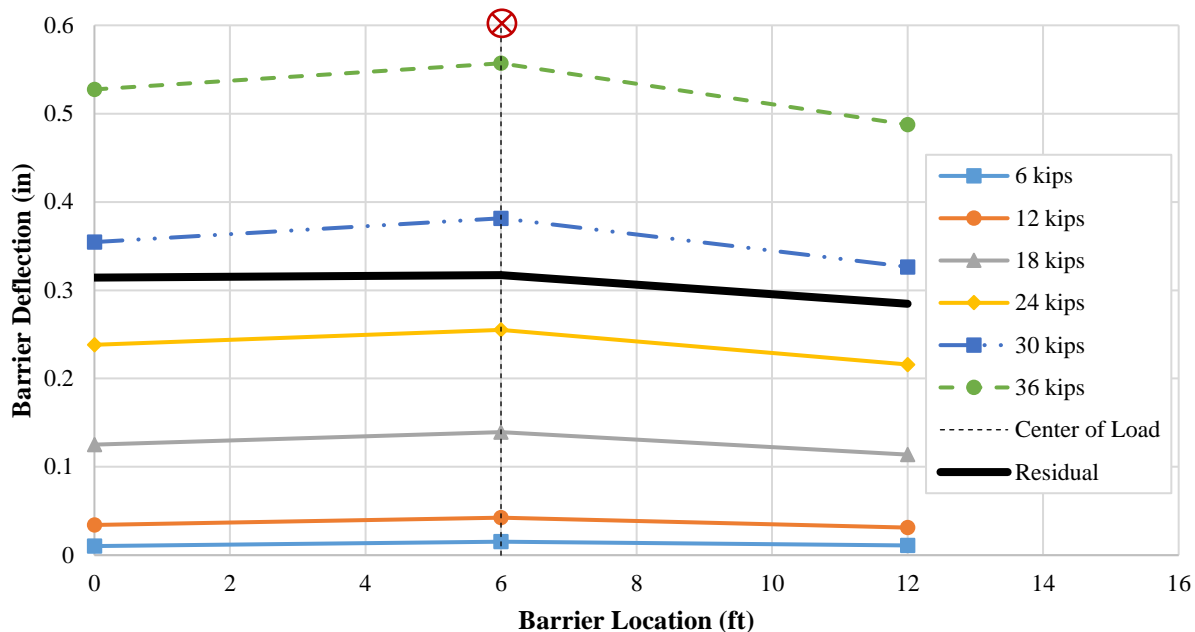
The applied force versus the barrier deflection obtained for PBU is shown in Figure 5.13, in which the positive values correspond to push direction loads and displacements.



**Figure 5.13. Lateral versus force displacement obtained for Test 2 – PBU**

Each load increment and the point when the deck crack was first observed are identified; the change in stiffness suggested that cracking probably developed when the applied load exceeded 12 kips. Although the initial response of PBU was similar to PBI, PBU experienced larger displacements than PBI for the same lateral load (see Figure 5.1). Beyond 36 kips, the lateral load resistance of PBU began to drop with increasing displacement.

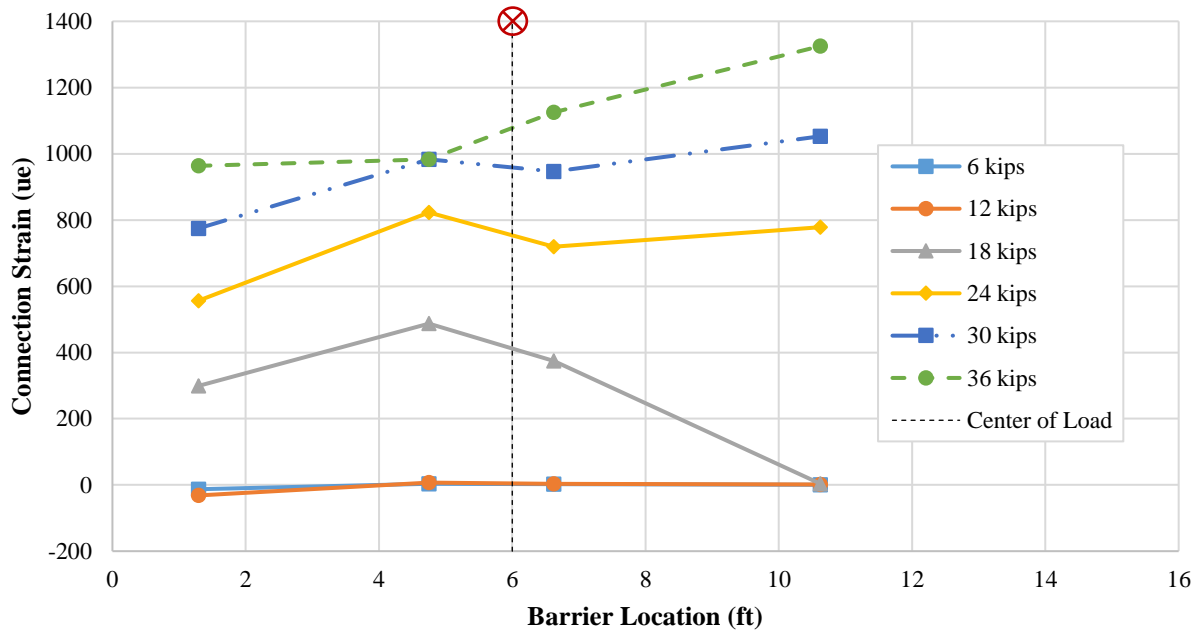
To monitor the movement of barrier PBU during testing, string potentiometers were placed behind the barrier at each end and in the center where the load was being applied as with the PBI testing. For each loading increment, the barrier deflection is shown in Figure 5.14.



**Figure 5.14. Lateral top deflection of PBU during Test 2**

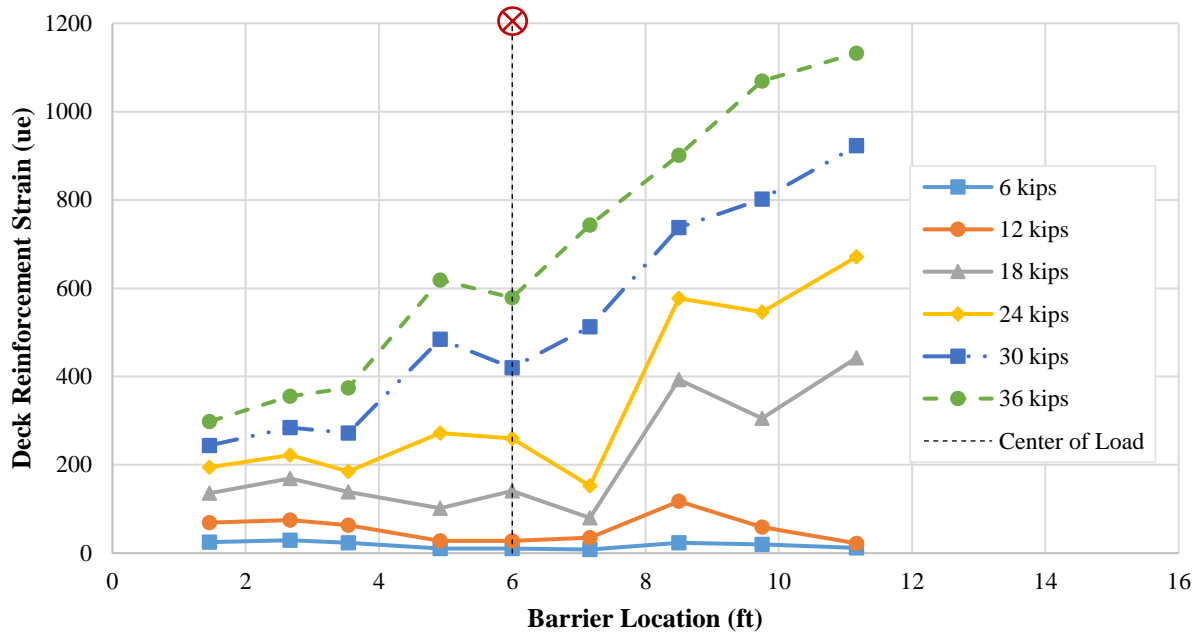
Behind the center of the force, the barrier deflected the most, as expected. The free end of the barrier where the deck was terminated in this figure was at  $x = 12$  ft. The end with the barrier-to-barrier connection where the deck was continuous is indicated with  $x = 0$ . As with PBI, the free end of PBU experienced a small increase in deflection versus the fixed end. However, the difference in barrier deflection between the free end and the fixed end was not as large as was observed for PBI.

Figure 5.15 shows the strain in the U-bar connection at the barrier-to-deck interface.



**Figure 5.15. Strain in the U-bar at the deck to barrier interface during Test 2**

The left side of the graph used a #7 reinforcement U-bar while the right side included a bundle of two #5 reinforcement bars at each connection location. The #7 U-bars were near the end of the barrier adjacent to the barrier-to-barrier connection and they experienced less strain than the bundled #5 U-bars, which were positioned on the other half closer to the free end of the test unit. Compared to Test 1 conducted on PBI, the strain values recorded in the connection reinforcement during Test 2 were similar up to the lateral load of 36 kips. The maximum recorded deck displacement was 0.28 in. at this point. The deck reinforcement strain profiles are shown in Figure 5.16. The deck reinforcement in the free end of the PBU test unit experienced larger strain values than the restrained end of PBU.



**Figure 5.16. Strain profiles of the deck reinforcement at the front barrier interface during Test 2**

The deflection of PBU recorded during Test 2 also included the flexural deflection of the barrier and the deflections due to the rotation of the barrier at the deck interface and the rotation that the deck overhang experienced. These components are depicted in Figure 5.17 along with the experimental value.

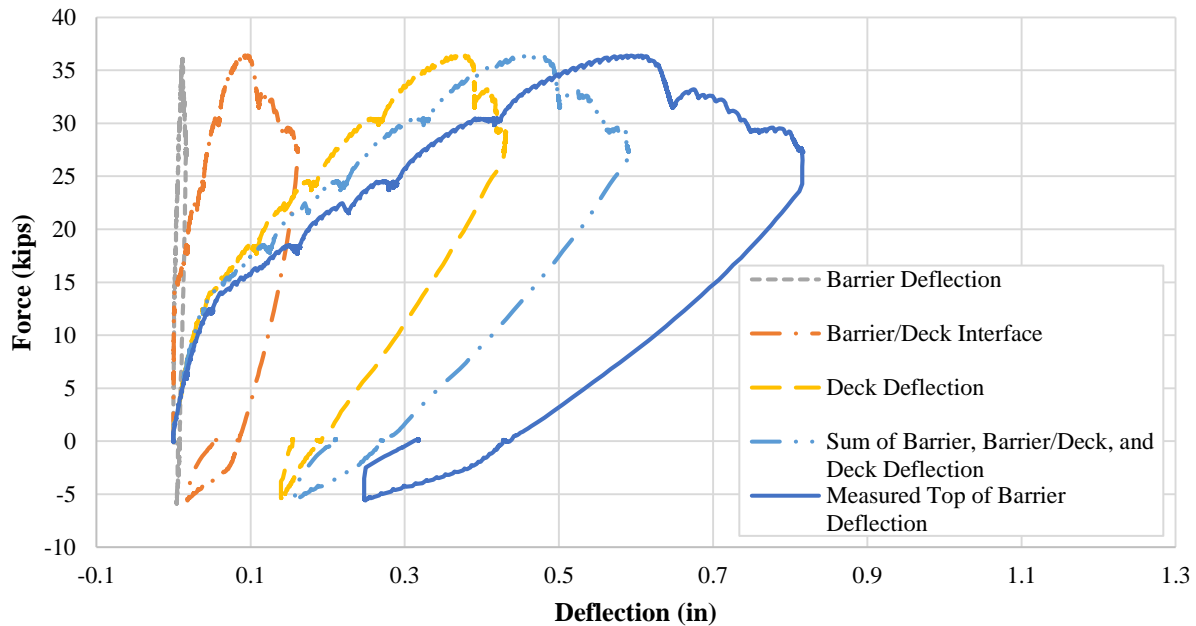


**Figure 5.17. Deflection of components**

Although the maximum measured lateral deflection of PBU was 0.8 in., the actual barrier's deflection accounted for 2.1 percent of the deflection at 0.017 in. and the deflection at the barrier and deck interface accounted for 20.3 percent at 0.162 in. As with Test 1, the majority of the measured barrier deflection was mainly due to the rotation of the deck overhang. The large deflection and rotation recorded were partly due to the damage that occurred to the deck behind the barrier as previously discussed.

### **Test 3 Observations: At Barrier-to-Barrier Connection**

After the connection between the two barriers was established, the third test was conducted on the precast barrier system between the two barriers, PBI and PBU. The loading block and actuator were set up to apply loads over a 3.5 ft length in the center of the entire test unit. The purpose of this test was to examine the connection between the precast barriers. In the early stages of testing, no new cracks developed, but old cracks began to open up. As the load approached 30 kips, a new crack appeared on the side of the bridge deck on the PBI side. It wasn't until 48 kips were reached that cracks began to appear on the PBI barrier itself. These were diagonal cracks running in the opposite direction to the ones formed during Test 1 (see Figure 5.18).

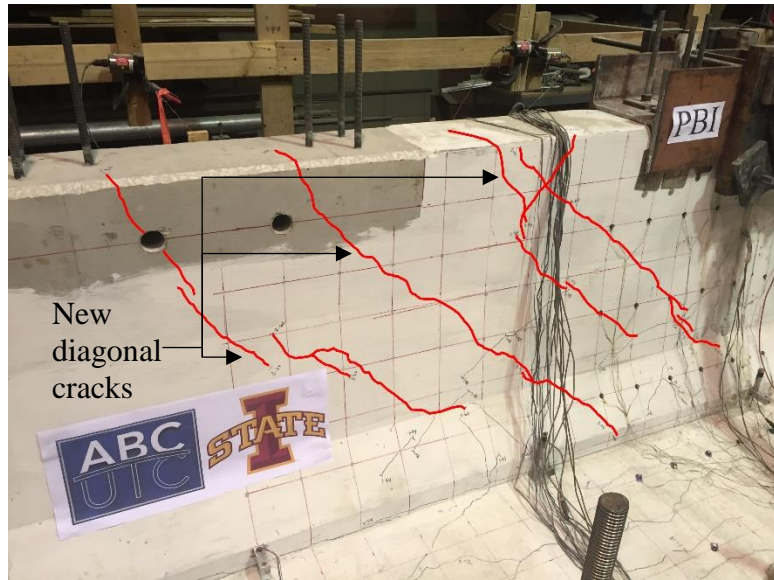


**Figure 5.18. Diagonal cracks developed on PBI during Test 3**

The barriers were able to withstand a maximum load of 60 kips prior to experiencing a change in stiffness, indicating a softer response. At this point, the load was released. The cracks along the grout between the barriers and the deck remained open after the actuator load reached a zero value. The crack on the PBI side of the grout pad was measured at a width of 0.005 in. The PBU side was measured at a width of 0.07 in. The majority of the residual cracks appeared on the PBI side, while most cracks that developed on PBU were closed. Due to PBU's weakened state, the bulk of the load was most likely transferred to PBI.

### **Test 3 Results: At Barrier-to-Barrier Connection**

The force-displacement plot established from Test 3 is presented in Figure 5.19, where the positive directions corresponded to the push direction loading. For each 6-kip load increment, the peak values were identified up to the maximum applied load of 60 kips. When the load was released, a residual displacement of 0.2 in. was registered.

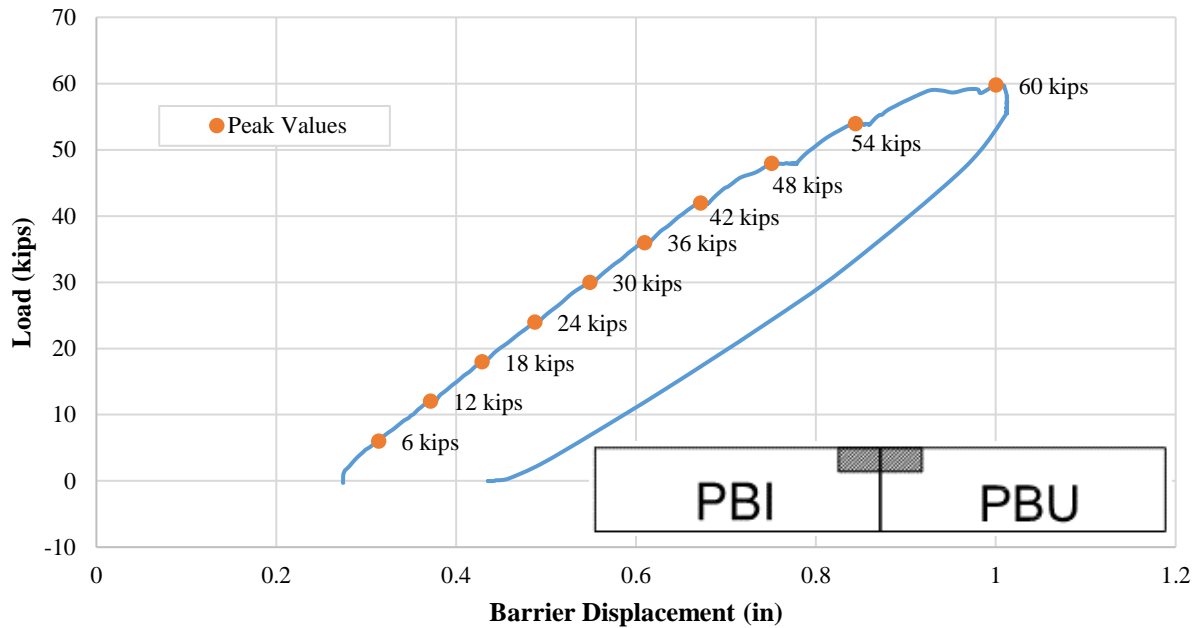


**Figure 5.19. Force-displacement response obtained for Test 3**

Figure 5.20 displays the deflection profiles established for the connected precast barriers.

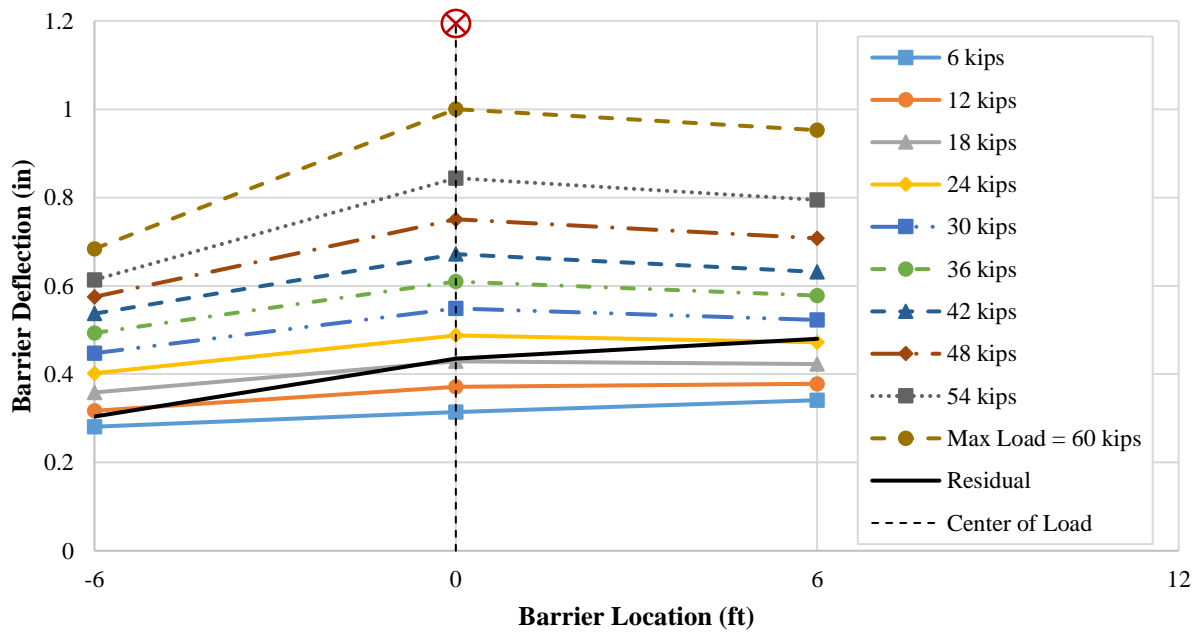


**Figure 5.20. Top barrier deflection profiles established from Test 3 data**

The applied load was centered directly between the two barriers and this is where the maximum deflections occurred. During the early stages of testing, the two barriers deflected similar



amounts at 6 ft away from the connection (i.e., at the center of each barrier). As the loading approached 48 kips, PBU began to experience larger lateral deflections and these were closer to the values recorded at the barrier-to-barrier connection, implying that the entire PBU was rotating at the base as the load was applied. The maximum deflection recorded during this test was 0.73 in. The residual deflections shown in this figure show 0.4 in. at the barrier-to-barrier connection and 0.4 in. at the PBU. This reported value at the barrier-to-barrier center is higher than that which can be inferred from Figure 5.19 because Figure 5.20 reports the absolute values from the beginning of the test. The higher residual displacement obtained at the center of PBU compared with that obtained at the center of the barrier-to-barrier connection was another indication that U-bars anchored into deck were failing.

The strain recorded in the connection reinforcement at the deck interface is shown in Figure 5.21.

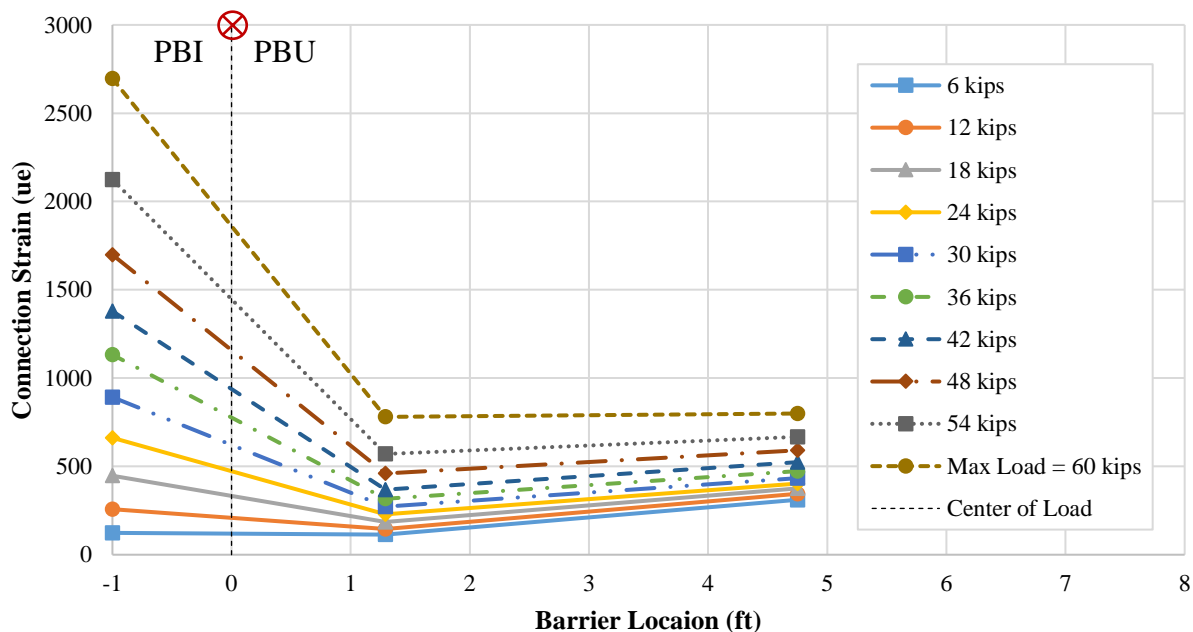


**Figure 5.21. Strain in barrier-to-deck connection interface during Test 3**

It is seen that the inclined reinforcing bars in PBI experienced significantly more strain than the U-bar reinforcement in PBU. This confirms the theory that the majority of the load that was applied at the center of the test unit was resisted by PBI and transferred to the deck, mainly in the left half of the specimen.

The strain recorded on the longitudinal, double-headed ties connecting the two precast barriers is shown in Figure 5.22.

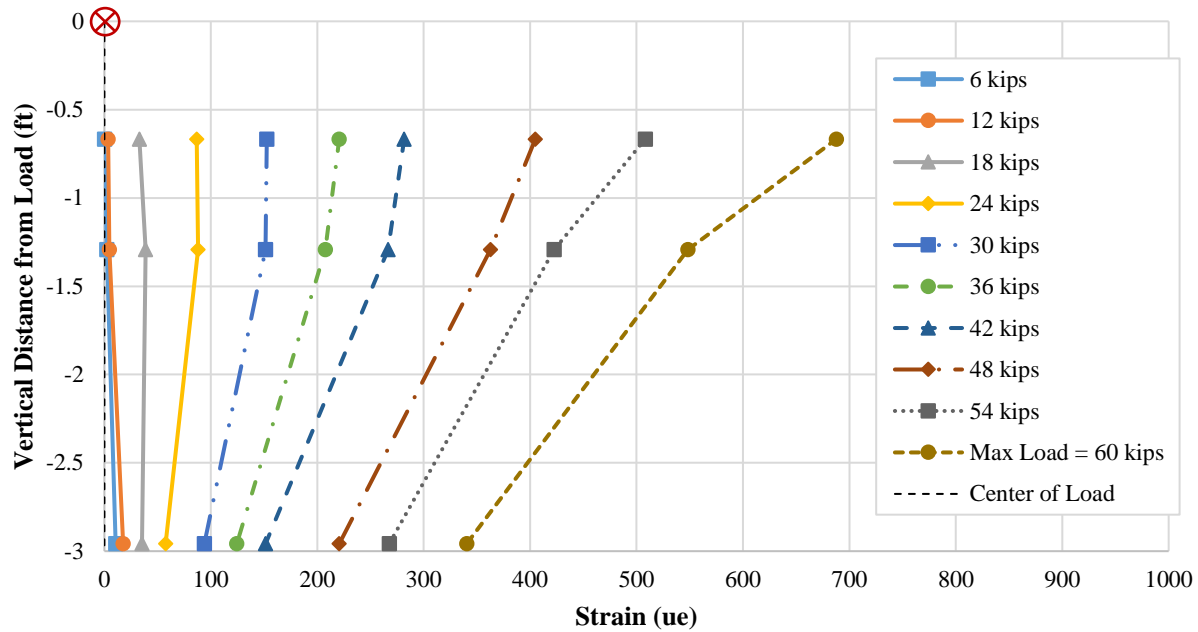


**Figure 5.22. Strain in the center of the longitudinal double-headed ties in barrier-to-barrier connection during Test 3**

Strain gauges were placed on the center of the double-headed tie at the barrier-to-barrier interface. As the distance from the load increased, the strain values decreased. The top double-headed tie was closer to the applied load and therefore had the highest strain readings—about twice those recorded closer to the deck interface. The strain demand on the ties was generally low because the beam used to distribute the load assisted in transferring the loads to the barriers.

The strain in the transverse double-headed ties used in the barrier-to-barrier connection is shown in Figure 5.23. As with the longitudinal ties, the transverse ties decreased in strain as the distance from the applied load increased. The magnitude of strains was very small.

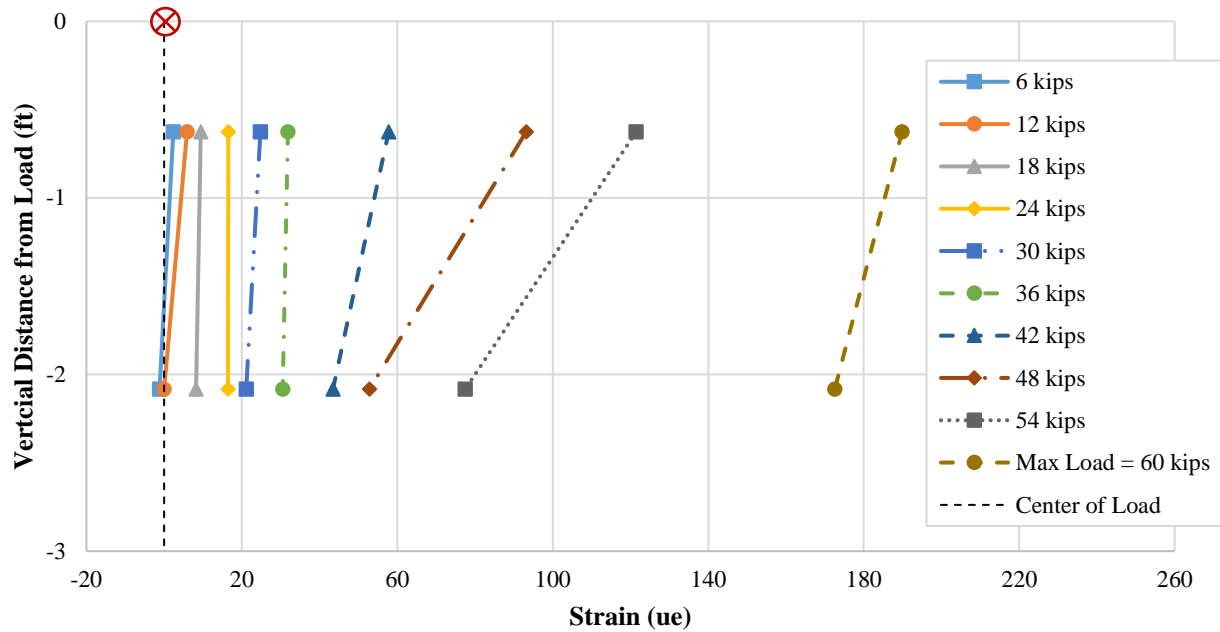


**Figure 5.23. Strain in transverse double-headed ties placed near the barrier-to-barrier connection during Test 3**

#### **Test 4 Observations: Off-Center, PBI Side**

For Test 4, the loading beam was placed to the PBI side of the barrier-to-barrier connection. The center of the load was 3 ft from the barrier-to-barrier connection. The purpose of the test was to observe the force transfer through the barrier-to-barrier connection and to evaluate the capacity of the center connection. Before this test was performed, a beam was placed on the PBU side to brace the barrier and keep it from deflecting. This brace beam can be seen in Figure 5.24.



**Figure 5.24. Beam used to brace PBU with respect to the deck during Test 4**

New hairline cracks didn't form on the grout between the barriers until 24 kips of load was applied. Other previous cracks just opened and extended. At 48 kips, a vertical crack developed

on the front face of the grout between the barriers, while another vertical crack formed on the back of the barrier-to-barrier grout at 54 kips. This crack started at the bottom of the barrier. As the loads were increased, cracks continued to extend vertically. At 72 kips, new cracks developed on the top of the barrier-to-barrier grout. The load was increased up to 81 kips before it started dropping. The test continued until the deflection of 1.75 in. was recorded. A large crack developed along the barrier under the loading beam (Figure 5.25), and the barrier-to-barrier grout broke all the way along the top to the back (Figure 5.26).

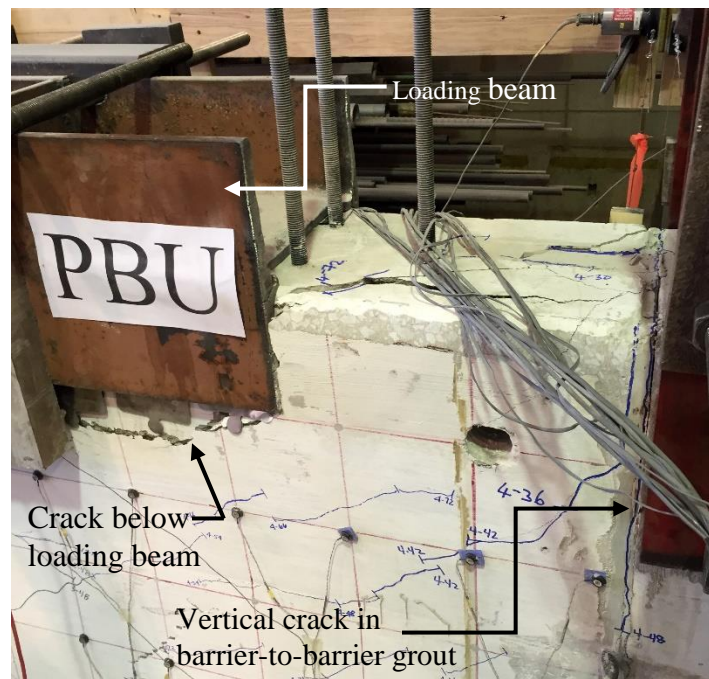


**Figure 5.25. Cracking under the loading beam on PBI during Test 4**

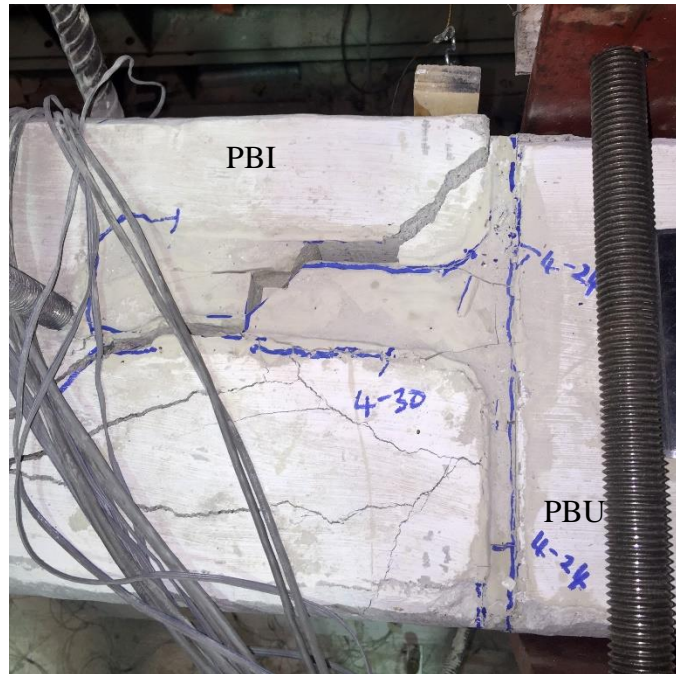


**Figure 5.26. Failure pattern of barrier-to-barrier connection at the end of Test 4**

#### **Test 4 Results: Off-Center, PBI Side**

The force-displacement response obtained for Test 4 is displayed in Figure 5.27.

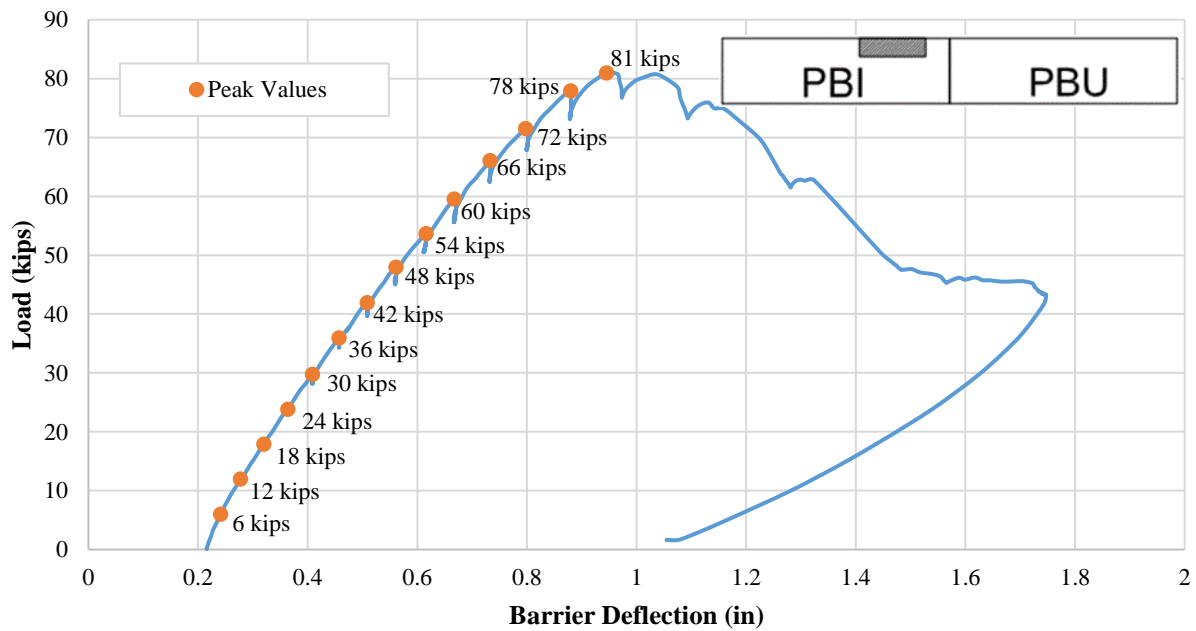


**Figure 5.27. Force-displacement response obtained for Test 4**

The peak value corresponding to each loading increment is identified in the figure. Following the maximum load of 81 kips, the load dropped to 43 kips as the displacement was increased. From this point, the load was released, exhibiting a residual displacement of 1.06 in.

The top deflection of the barrier system is shown in Figure 5.28.

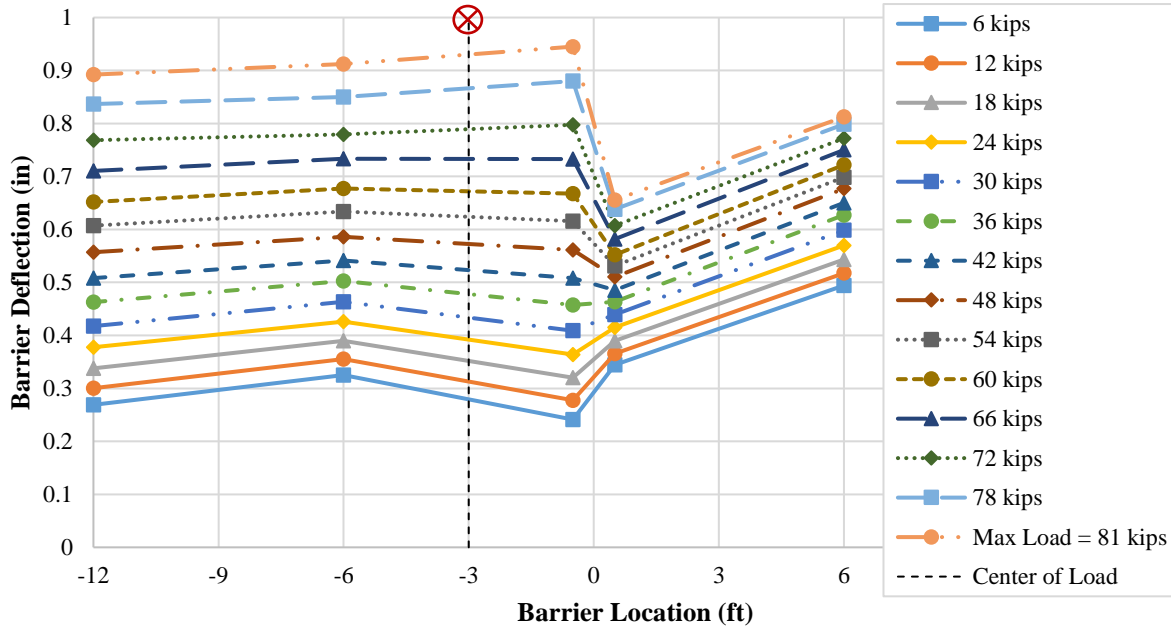


**Figure 5.28. Top lateral deflection of barrier during Test 4**

Recall that before starting Test 4, a beam was used to brace PBU to limit its movement. The brace location was near 0 ft in Figure 5.28. The data points to the left of zero are the deflection readings from PBI. The data points to the right of zero barrier location are the deflection readings from PBU. As the lateral load was increased, the deflection of PBI became uniform along the length, indicating the participation of the entire barrier in resisting the load. According to this figure, PBU recorded a lateral deflection in excess of 6 in., a majority of which came from the deck deflection. The difference in movement between PBI and PBU toward the end of the test is shown in Figure 5.29.



**Figure 5.29. Difference in barrier movement at barrier-to-barrier connection at the maximum load during Test 4**

The strain in the barrier-to-deck connections during Test 4 is shown in Figure 5.30.

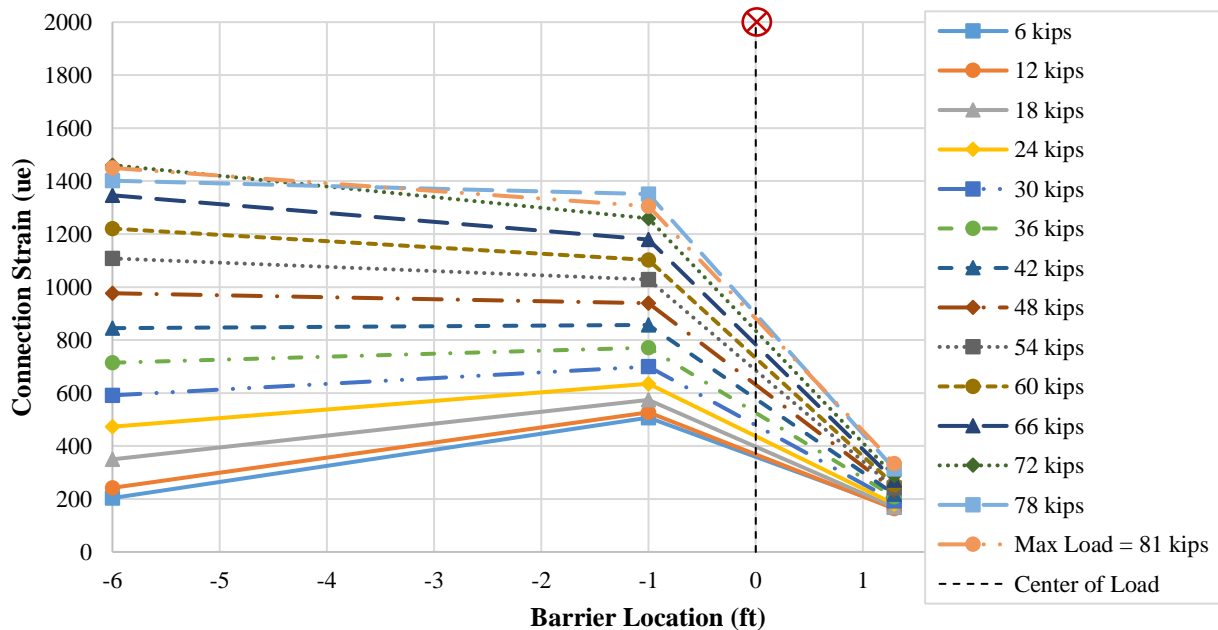


**Figure 5.30. Strain in barrier connection reinforcement at the deck interface during Test 4**

The inclined reinforcing steel in PBI experienced similar strains throughout the length of PBI while the U-bar connection in PBU experienced noticeably lower strain values. This image also demonstrates that the force is dispersed at an angle lower than the expected 45°, meaning more connection reinforcement and a longer deck length would participate in resisting loads compared to that stipulated from the current code recommendation.

The strain recorded on the longitudinal, double-headed ties connecting the two precast barriers is shown in Figure 5.31.

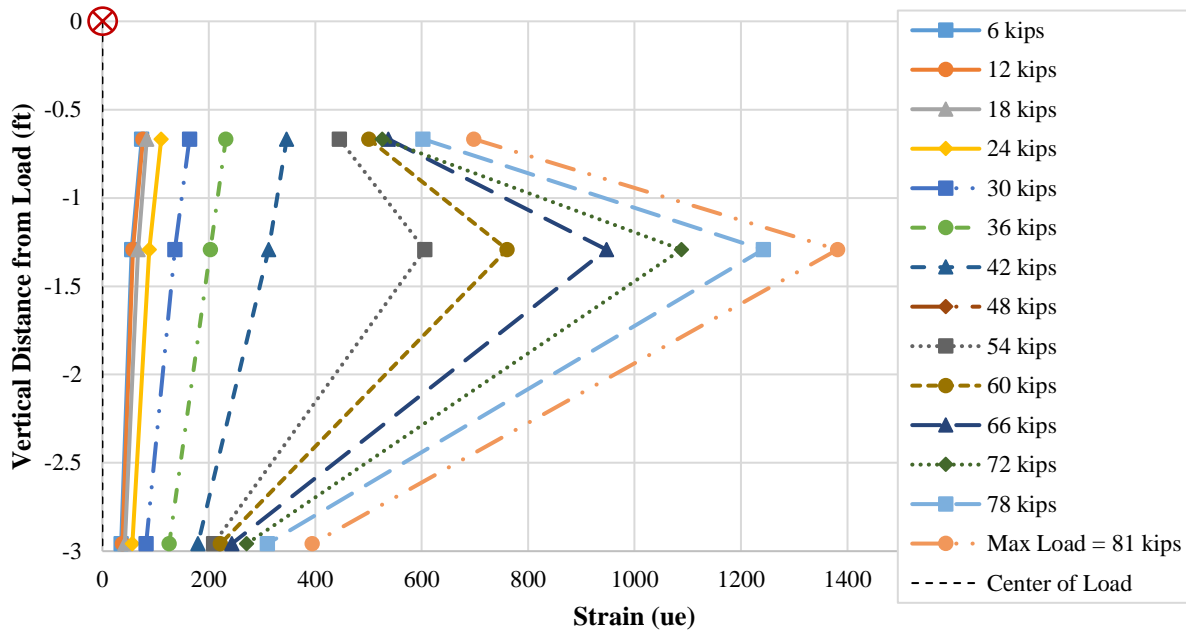


**Figure 5.31. Strain in longitudinal double-headed ties in barrier-to-barrier connection during Test 4**

Strain was recorded at the center and is shown as a function of vertical distance from the top of the barrier where the load was applied. Test 4 was intended to test the barrier-to-barrier connection to failure. As the load approached 48 kips, cracks within the barrier-to-barrier grout were observed. The longitudinal ties became more engaged in the load transfer as the load was increased, with the maximum demand in the tie that was 1.3 ft from the top of the barrier.

The recorded strain in the transverse double-headed ties used in the barrier-to-barrier connection in the transverse direction is shown in Figure 5.32. As with the longitudinal ties, once the cracking was observed in the barrier-to-barrier interface grout, the transverse ties farther away from the load became more engaged.



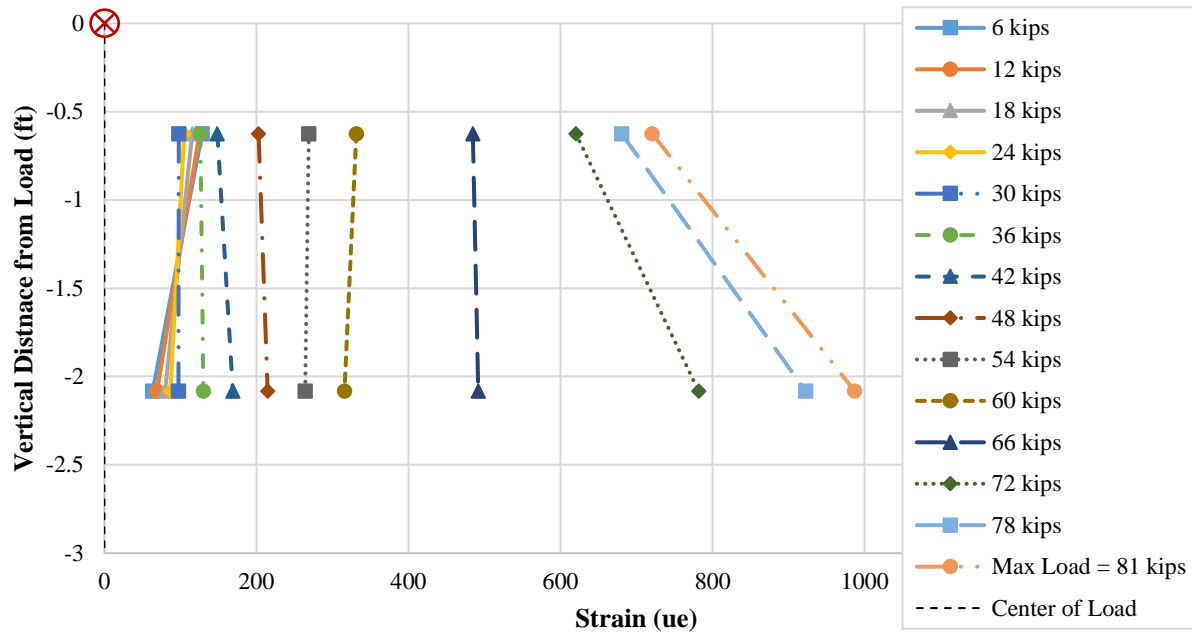


**Figure 5.32. Strain in transverse double-headed ties during Test 4**

### Test 5 Observations: End of PBI

For Test 5, the loading beam was moved to the free end of PBI. The brace beam was kept in place for this test. The purpose of the test was to observe the failure of PBI with loading at the free end of the barrier and evaluate the connection performance that included the inclined reinforcement to connect the barrier to the deck. Recall that this free end was not designed to simulate the end of the barrier condition.

As loading was applied to the barrier, the cracks that developed earlier on the barrier and deck began to open and widen. When the load increment approached 30 kips, the barrier began to fail to endure any further loading. This is consistent with the expectation that the end region as designed should support 50 percent of the design load. Testing was continued under displacement control. During this phase of testing, the crack along the barrier-to-deck grout interface was visible along a length of up to 9 ft from the free end of the barrier. The inclined cracks on the barrier were widespread on the entire barrier. Loading continued from 1.25-in. deflection to 4.85 in. when the actuator stroke was at its maximum, shown in Figure 5.33.



**Figure 5.33. Final barrier deflection and cracking in bridge deck during push direction loading in Test 5**

In this figure, the widening of the bridge deck cracks may also be observed. Splitting cracks formed throughout the overhang between the top and bottom deck reinforcement mats. The diagonal cracks along the front and rear face of the barrier also continued to extend. Loading was then released, and a pull direction load was applied to the barrier, which began to open up the backside of the barrier-to-deck interface.

The pull load applied to the barrier reached a maximum of 22 kips. The resulting barrier profile is displayed in Figure 5.34.



**Figure 5.34. Damage to barrier and deck after Test 5 pull test**

During the pull direction loading, the front of the barrier experienced minimal damage while the connection between the barriers experienced significant damage and failure (Figure 5.35).

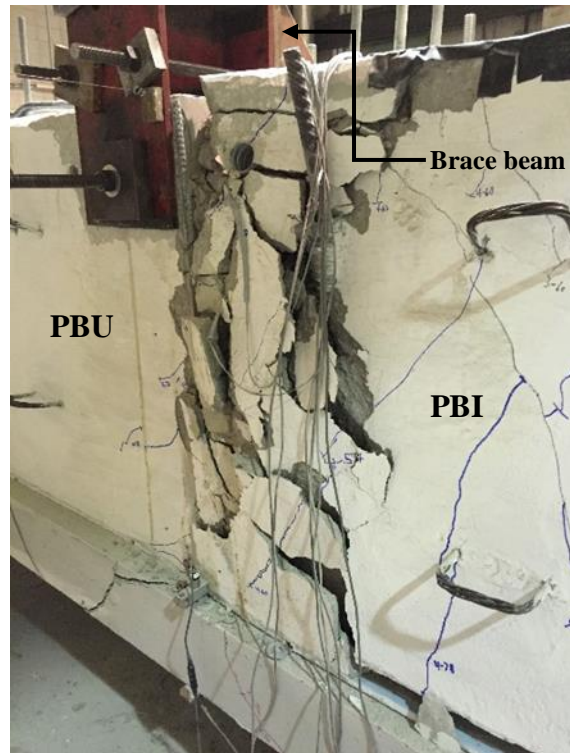


**Figure 5.35. Damage to barrier-barrier interface after Test 5**

As a result of the pull test, the front side of the barrier at the deck interface began to spall. This spalling exposed the sleeve and connection of the inclined reinforcement (Figure 5.36). It can be seen that the barrier-to-deck connection was still intact and undamaged.



**Figure 5.36. Concrete spalling on front of PBI at deck interface and barrier-to-deck connection**

### Test 5 Results: End of PBI

The force-displacement response obtained from Test 5 is displayed in Figure 5.37, where the reported displacement reflects the absolute values from the beginning of Test 1.

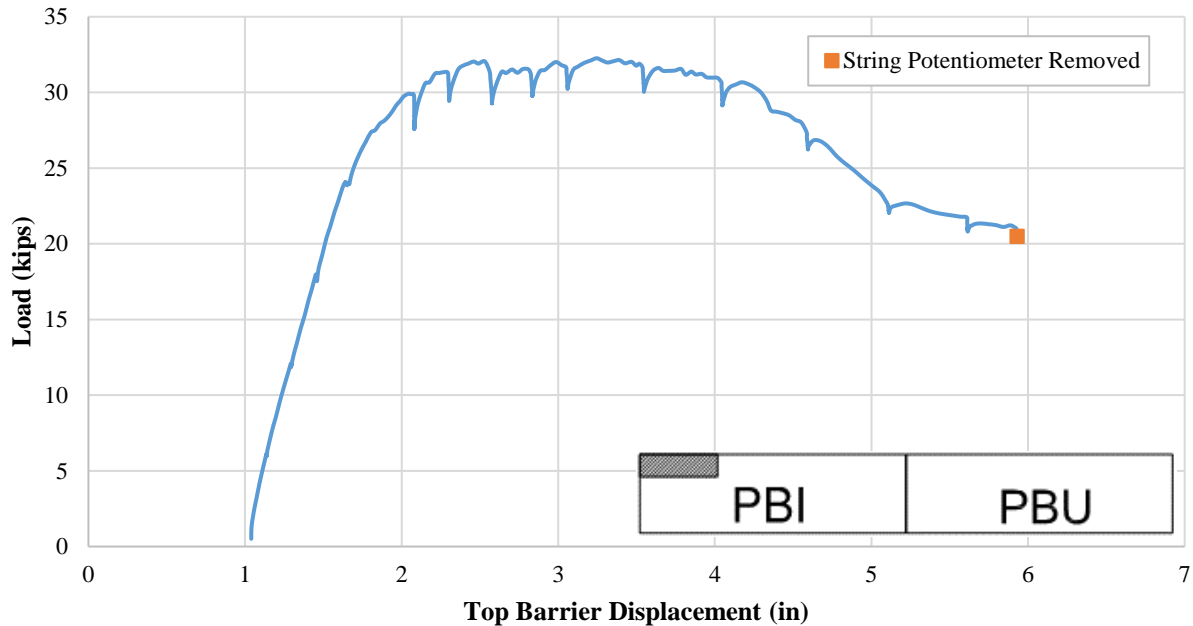


**Figure 5.37. Recorded force-displacement response during Test 5**

The maximum applied load in excess of 30 kips was sustained until the displacement reached close to 6 in., demonstrating sufficient toughness for the connection. After that, the barrier progressively failed. The test was continued until the barrier experienced a deflection in excess of 6 in.

The deflection at the top of PBI during Test 5 is shown in Figure 5.38.

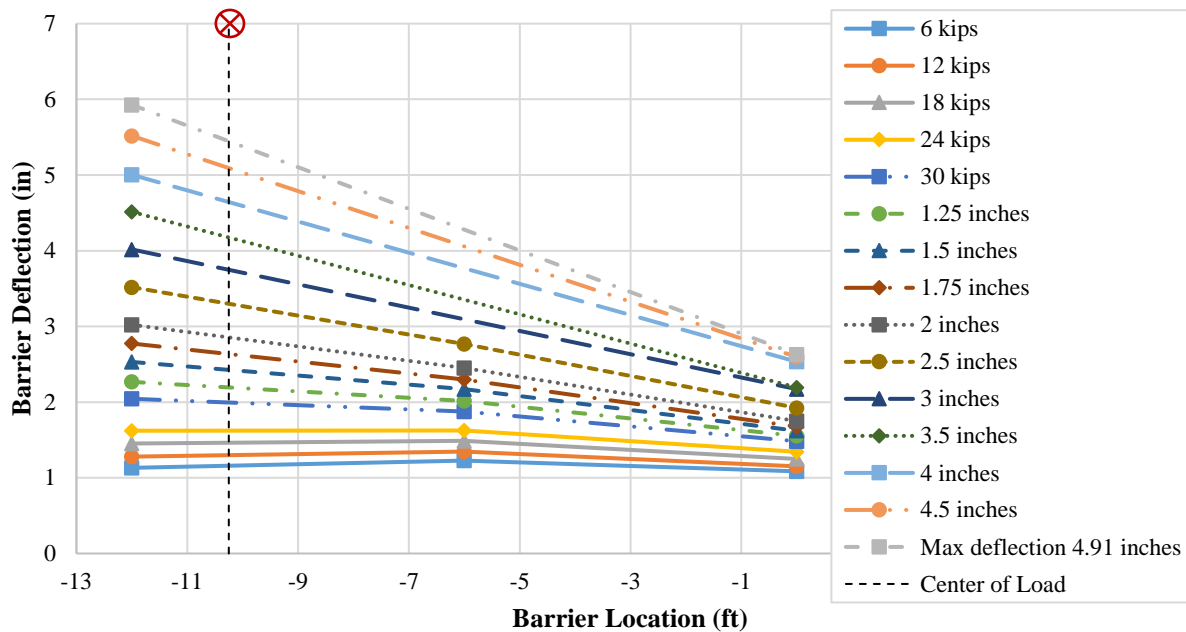


**Figure 5.38. Deflection at the top of the barrier during Test 5**

The reported displacement of this figure reflects the absolute displacement from the beginning of Test 1, while the values in the legend reflect the relative target displacement from the beginning of Test 5. The placement of the brace beam limited the amount of deflection at the barrier-to-barrier interface, which was located at  $x = 0$  feet in this figure. The free end of PBI, where the load was applied, experienced the most lateral deflection. During testing, instrumentation was removed at various stages to protect it from damage. The first testing instruments were removed after the top of barrier deflection was at 2.5 in.

The strain in the barrier-to-deck connections during Test 5 is shown in Figure 5.39.



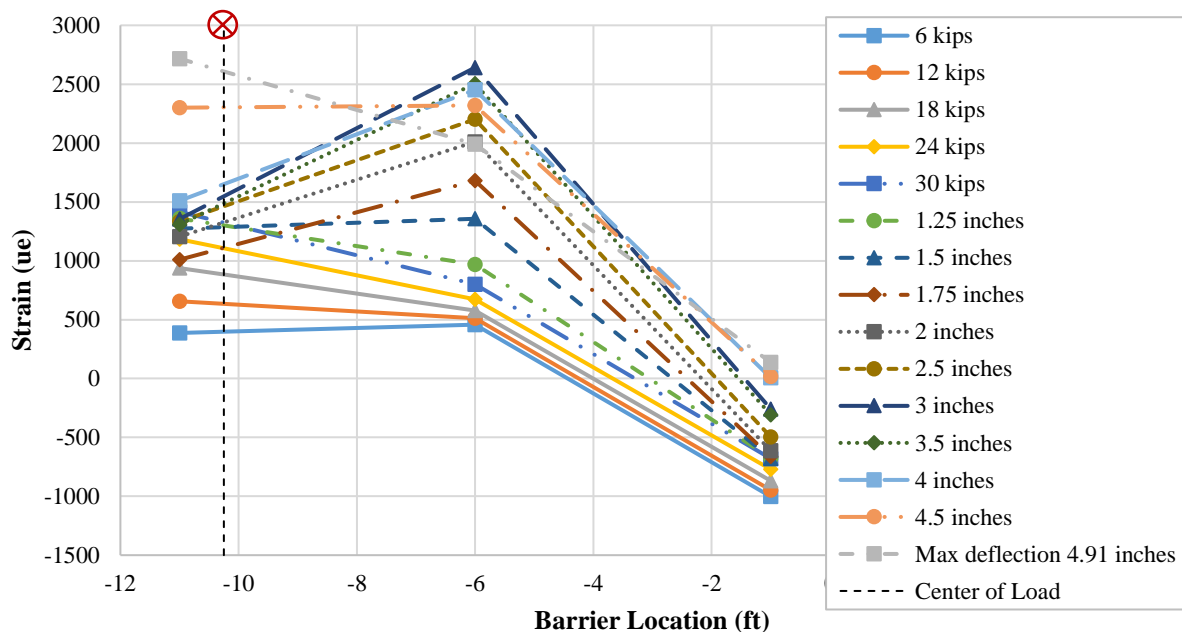


**Figure 5.39. Strains in PBI at the barrier-to-deck connection interface during Test 5**

The inclined reinforcing steel nearest to the barrier-to-barrier interface showed no significant strain demand. This is believed to be due to that region of the barrier experiencing damage during Test 4. The longitudinal, double-headed ties and the transverse double-headed ties connecting the two precast barriers also sustained further damage during Test 5. As such, usable data was obtained during this phase of testing.

### Test 6 Observations: End of PBU

For the final test, Test 6, the loading beam was moved to the free end of PBU. The brace beam near the barrier-to-barrier connection was removed for this test. The purpose of the test was to observe the failure of the U-bar barrier-to-deck connection.

The applied load to the barrier was taken to about 24 kips under force control before switching to a deflection-based loading. As the PBI was loaded, the crack between the deck and the barrier interface opened and continued to widen. At 1-in. of lateral deflection, the crack was visible along the entire length of PBU. When the deflection reached around 3 in., the cover concrete under the deck overhang started to spall. The barrier appeared to start slipping horizontally in the direction of loading when testing to 4.5-in. of deflection. In total, it slipped about 0.75 in. back from its starting position when the lateral deflection of 4.5 in. was reached. As the testing continued and the barrier deflection reached about 6 in., the sliding measured about 1 in. Figure 5.40 shows PBU at the final resting position after the push test was completed.



**Figure 5.40. Final barrier deflection and the corresponding damage to the bridge deck during Test 5**

The load was then completely released, and the pull direction loading was started. The pull test was continuous until the barrier and/or its connections experienced failure. As the testing continued, the top cover concrete of the deck behind the barrier completely separated and fell off. The barrier and bridge deck opened sufficiently behind the barrier to expose the top reinforcement in the deck with the U-bars connecting the barrier to deck being responsible for causing the split between the top and bottom mat reinforcement of the deck (Figure 5.41).



**Figure 5.41. Top mat of the bridge deck reinforcement after the Test 6 pull test**

In order to prevent this phenomenon, the top and bottom mat reinforcement need to be tied where the connection bars are anchored. Though the same damage was not suspected during testing of PBI, this failure mode was visible to some extent during inspection following the completion of all the tests. Therefore, it would be prudent to place vertical-headed ties or hairpin type reinforcement near the connection reinforcement to avoid splitting failure developing between the top and bottom mat reinforcement. Alternately, the connection reinforcement could



be locked in place with the bottom mat reinforcement, which may pose constructability challenges.

### Test 6 Results: End of PBU

The force-displacement response obtained for Test 6 is displayed in Figure 5.42.

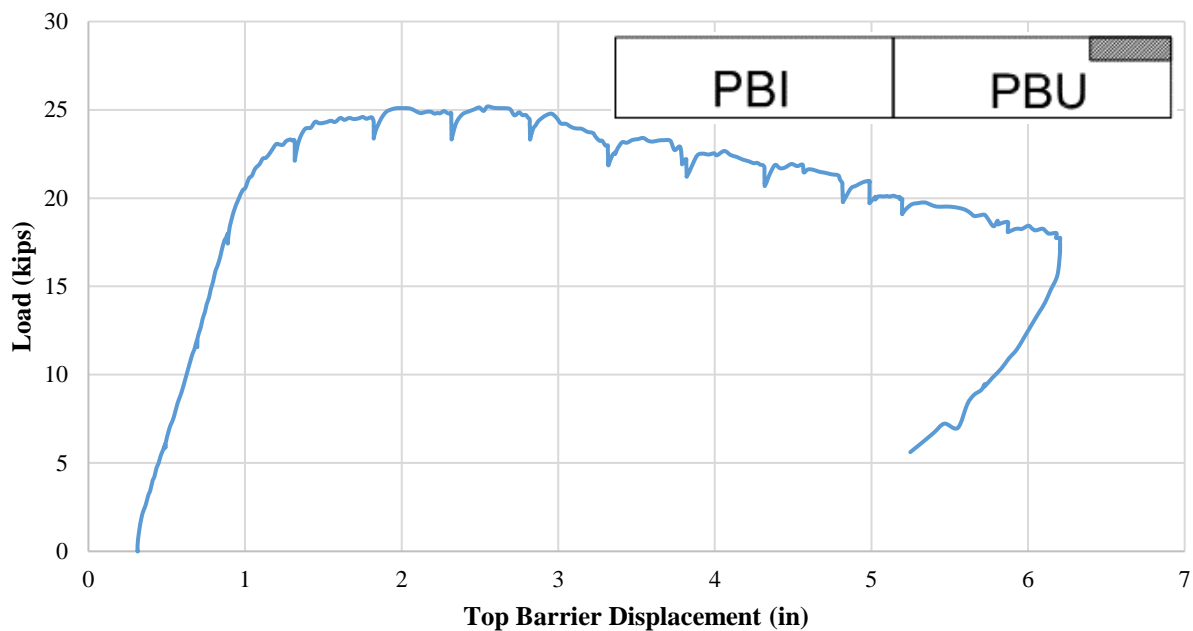


**Figure 5.42. Recorded force-displacement response for push direction loading in Test 6**

The maximum applied load to PBI was 25 kips. This value is more than 50 percent of the resistance observed in Test 2, which is not due to limiting the lateral deformation of the barrier. As can be seen, after experiencing about 3-in. lateral displacement, the barrier resistance continued to soften. To test the barrier connections to failure, the test was continued until the lateral deflection exceeded 6 in.

The deflection at the top of PBU during the push direction loading of Test 6 is shown in Figure 5.43.

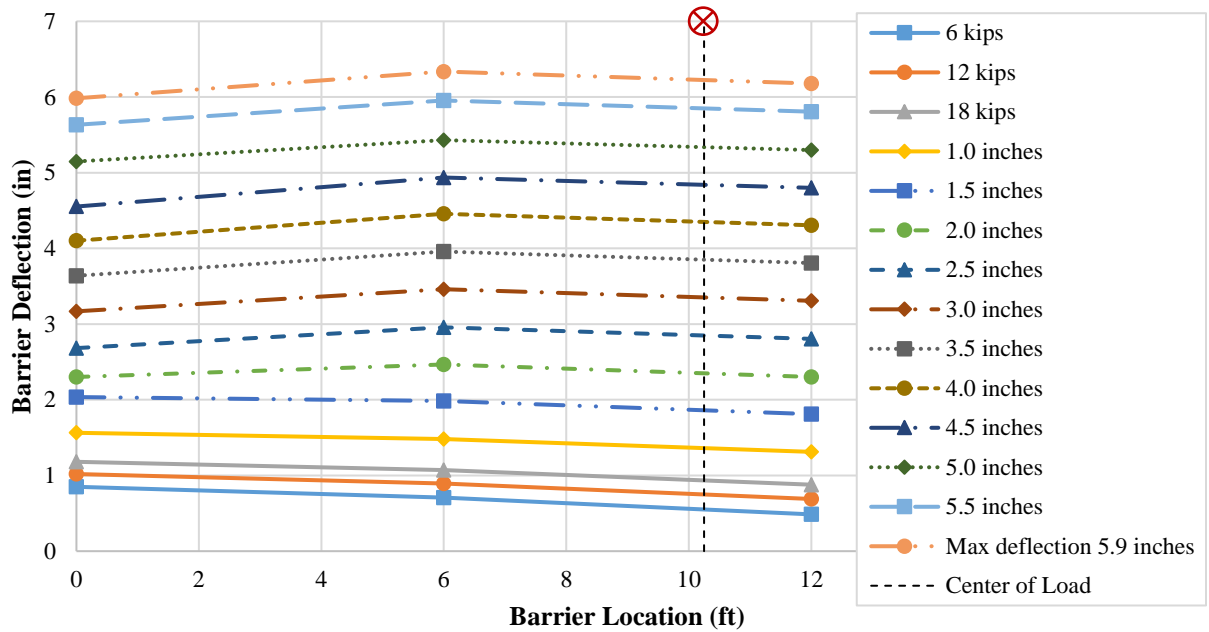


**Figure 5.43. Top barrier deflection during push direction loading of Test 6**

The entire length of PBU deflected at a similar rate through all increments of the test. This was believed to be due to the failure of the barrier-deck connection experienced during Test 2 and the insufficient anchorage of the U-bars with respect to the bottom mat reinforcement of the deck.

The strain in the barrier-to-deck connections during the push direction loading of Test 6 is shown in Figure 5.44.

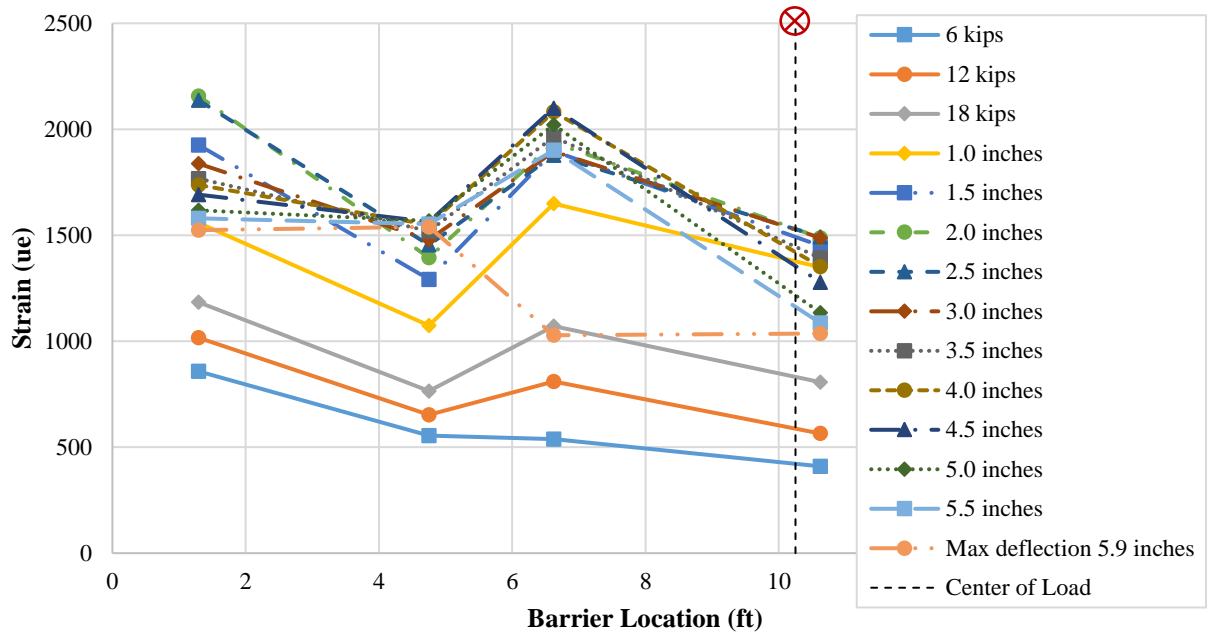


**Figure 5.44. Strain in barrier-to-deck connection interface in PBU during push direction loading in Test 6**

The left side of the graph is near the barrier-to-barrier interface and includes the #7 U-bar reinforcement. The right side of the graph is the free, unconnected end of PBU and includes the bundled #5 U-bars. It is seen that the strain increase in the U-bars after reaching a lateral deflection of 1.5 in. is relatively small, which is consistent with the force resistance as shown in Figure 5.42.

## SUMMARY AND CONCLUSIONS

### Summary

This report has summarized an investigation of the structural behavior of a developed precast barrier system that included durable connection details. In order to gain a better understanding of the design and performance of prefabricated concrete bridge barriers, a literature review was performed and was used to establish the basis for this study. Two barrier-to-deck connections and one barrier-to-barrier connection were designed and tested according to Test Level 4 from the Federal Highway Administration. The loading of 54 kips associated with Test Level 4 was used as the design load for the connections. The first barrier system included inclined reinforcing steel connecting the barrier to the bridge deck and was identified as PBI. The second barrier system included a U-shaped, stainless steel reinforcing bar connecting the barrier to the bridge deck and was identified as PBU. The connection details were designed to accommodate various parameters including ease of construction, maintenance and repair, durability, and cost effectiveness. The precast barrier systems were constructed and tested under different loading conditions to examine the structural performance, the load carrying capacity, and the force distribution.

### Conclusions

A total of six tests were conducted. Conclusions drawn from this study were as follows. The two precast barrier systems did not experience any construction challenges during fabrication. The barrier system connections were assembled as planned without any difficulties. The construction of PBI required minimal access to install the connection reinforcement. PBU required access from under the bridge overhang to install the U-shaped connection reinforcement. A summary of the loading and deflection of the barrier for each test is provided in Table 6.1.

**Table 6.1. Summary of various tests conducted on the barrier**

Test	Maximum load	Maximum lateral displacement for each test
<b>PBI Middle (Test 1)</b> Target = 54 kips	Push = 54 kips Pull = 2 kips	0.81 in. Residual displacement = 0.27 in.
<b>PBU Middle (Test 2)</b> Target = 54 kips	Push = 36 kips Pull = 4 kips	0.80 in. Final resting position = 0.30 in.
<b>Center - Attached (Test 3)</b> Target = 54 kips	Push = 60 kips	0.73 in. Final resting position = 0.17 in.
<b>Off Center, PBI (Test 4)</b> Target = Failure	Push = 81 kips	Loaded until 1.75 in.
<b>End of PBI (Test 5)</b> Target = Failure	Push = 30 kips Pull = 22 kips	4.9 in.
<b>End of PBU (Test 6)</b> Target = Failure	Push = 24.8 kips Pull = 27 kips	Relative displacement = 6.0 in.

When an isolated unit of PBI was subjected to Test Level 4 loading, it performed satisfactorily, which was expected. The barrier, deck, and barrier-to-deck connection performed well with no elastic strains developing in the deck reinforcement. The deck began to crack as the loading approached 18 kips. Hairline diagonal cracks were witnessed on PBI as the loading reached 48 kips. The cracking that developed on the deck was uniform and extended beyond the expected 45° force dispersion, suggesting that more length of the deck was participating in resisting the applied loads. As the applied load reached 54 kips, the top of the barrier experienced a total top lateral displacement of 0.81 in. with only 3.5 percent of the displacement coming from the barrier itself and the largest contribution stemming from the flexural deformation of the deck overhang.

During the isolated testing of PBU, Test 2, the barrier was able to resist 36 kips without experiencing significant rotations at the base. Larger rotation occurred from this point onward with localized deformation concentrated at the bottom of the barrier. This was suspected to be due to the U-bars not being adequately tied to the bottom deck reinforcement in the deck and the associated deformation of the top deck reinforcement.

The test conducted on the barrier-to-barrier connection, Test 3, also performed as expected. The barrier system was loaded up to 60 kips with PBI supporting the majority of the load. The strain developed in the PBI deck connection reinforcement was significantly more than the strain experienced in the PBU deck connection reinforcement. Test 4 included loading on the PBI side of the barrier-to-barrier connection and demonstrated the force distribution near the barrier-to-barrier connection and the failure pattern of the connection.

Testing at the ends of the barriers (i.e., Tests 5 and 6) produced lower resisting forces than Tests 1 and 2. This is because the barrier ends did not simulate conditions expected at the bridge ends, making them produce 50 percent of the resistance in comparison to the resistance expected when testing away from the ends. For both connections in Tests 5 and 6, the failure initially appeared within the deck. The premature failure was also due to the extent of damage from the previous tests. To increase the force resistance at the ends of the barriers when used at the bridge ends or where the deck is joined, it is recommended that the bridge deck be designed to resist a higher moment demand. It is also recommended that the vertical, inclined bars be spaced closer together. To double the load resistance to deal with an impact at the end of the bridge, it is suggested that all spacing be reduced by 50 percent (Figure 6.1).

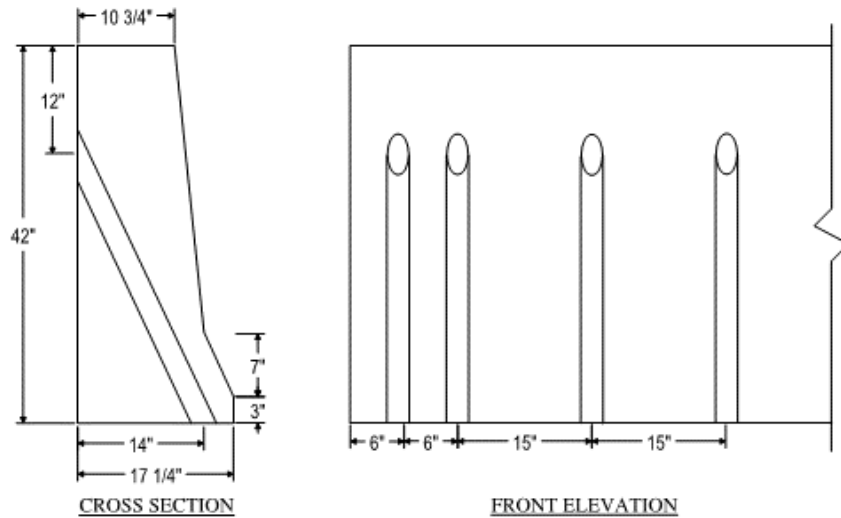


**Figure 6.1. Recommended spacing for inclined bar connection at a bridge end**

Due to the design of the U-bar barrier-to-deck connection, the bottom deck reinforcing bars had to be terminated where they interfered with the U-bar deck pockets. This resulted in a greater demand on the top deck reinforcement, causing a splitting crack to develop between the top and bottom mat reinforcements. This led the bridge deck overhang to fail.

In the design process, the impact force was assumed to disperse in the barrier at a  $45^\circ$  angle from the region where the load was applied. Results from this experiment demonstrated that the actual distribution angle was lower than  $45^\circ$ . Therefore, it appeared that more of the barrier and bridge deck were engaged in resisting the load. The deck cracking pattern observed during testing showed that engagement of the deck reinforcement was more extensive than the expected result. The strain experienced by the deck reinforcement was fairly uniform along the  $45^\circ$  dispersion, indicating that reinforcement in this area can be reduced by at least 30 percent.

The inclined reinforcement connection proved to be sufficient for a Test Level 4 barrier system. In light of the observed failure, it is recommended that when precast barriers are connected to the deck, it would be valuable to provide local reinforcement around the connection bars so that they engage both the top and bottom deck reinforcement simultaneously. This can be accomplished using vertical double-headed bars or hairpin type bars running horizontally.

## REFERENCES

- AASHTO. 2018. *AASHTO LRFD Bridge Design Specifications, Customary U.S. Units*. Eighth Edition. American Association of State Highway and Transportation Officials, Washington, DC.
- . 2012. *AASHTO LRFD Bridge Design Specifications, Customary U.S. Units*. Sixth Edition. American Association of State Highway and Transportation Officials, Washington, DC.
- . 2009. *Manual for Assessing Safety Hardware*. First Edition. American Association of State Highway and Transportation Officials, Washington, DC.
- Bligh, R. P., N. M. Sheikh, W. L. Menges, and R. R. Haug. 2005a. *Development of Low-Deflection Precast Concrete Barrier*. Texas Transportation Institute, Texas A&M University System, College Station, TX.  
<https://static.tti.tamu.edu/tti.tamu.edu/documents/0-4162-3.pdf>.
- Bligh, R. P., N. M. Sheikh, D. C. Alberson, and A. Y. Abu-Odeh. 2005b. *Low-Deflection Portable Concrete Barrier*. Texas Transportation Institute, Texas A&M University System, College Station, TX.  
[http://www.wsdot.wa.gov/publications/fulltext/design/RoadsideSafety/TxDOT\\_2.pdf](http://www.wsdot.wa.gov/publications/fulltext/design/RoadsideSafety/TxDOT_2.pdf).
- Buth, C. E., T. J. Hirsch, and W. L. Menges. 1997. *Testing of New Bridge Rail and Transition Designs Volume I: Technical Report*. FHWA-RD-93-058. Federal Highway Administration Office of Safety and Traffic Operations Research and Development, McLean VA.  
[ftp://ftp.odot.state.or.us/Bridge/BDDM/BDDM\\_Links/Rail%20Crash%20Testing/BR200CrashTestReport.pdf](ftp://ftp.odot.state.or.us/Bridge/BDDM/BDDM_Links/Rail%20Crash%20Testing/BR200CrashTestReport.pdf).
- FDOT. 2012. *Florida DOT Design Standards 414*. Florida Department of Transportation, Tallahassee, FL. <http://www.fdot.gov/design/standardplans/DS.shtm>.
- FHWA. 2018. Accelerated Bridge Construction. [www.fhwa.dot.gov/bridge/abc/](http://www.fhwa.dot.gov/bridge/abc/).
- Patel, G. 2008. Development of Precast Barrier Wall System for Bridge Decks. MS thesis. Ryerson University, Toronto, Ontario.
- Ross, H. E., Jr., D. L. Sicking, R. A. Zimmer, and J. D. Miche. 1993. *NCHRP Report 350: Recommended Procedures for the Safety Performance Evaluation of Highway Features*. National Cooperative Highway Research Program, Washington, DC.
- Rosenbaugh, S. K., R. K. Faller, R. W. Bielenberg, D. L. Sicking, and J. D. Reid. 2012. *Phase I Development of an Aesthetic, Precast Concrete Bridge Rail*. Mid-America Transportation Center, Nebraska Transportation Center, University of Nebraska-Lincoln, NE.
- Verrastro, R., R. Corsa, B. Rose, and R. Powell. 2014. Accelerated Bridge Construction Case Study: Design Build Replacement of Rock Ridge Road Bridge. Presented at the 2014 Design Training Expo, June 10–12, Tallahassee, FL.  
<http://www.fdot.gov/design/training/designexpo/2014/presentations/VerrastroRalph-AcceleratedBridgeConstructionCaseStudyDesignBuildReplacementofRockRidgeRoadBridge.pdf>.